ENERGY ABSORBER DESIGN AND ANALYSIS FOR MILITARY UTILITY HELICOPTER TROOP SEATS

ASKERİ GENEL MAKSAT HELİKOPTERİ MÜRETTABAT KOLTUKLARI İÇİN ENERJİ SÖNÜMLEYİCİ TASARIMI VE ANALİZİ

MUSTAFA DEMİRCAN

Asst. Prof. ÖZGÜR ÜNVER

Supervisor

Submitted to Graduate School of Science and Engineering of Hacettepe University

as a Partial Fulfillment to the Requirements

for the Award of the Degree of Master of Sciences

in Mechanical Engineering

2020

Atam'a…

ABSTRACT

ENERGY ABSORBER DESIGN AND ANALYSIS FOR MILITARY UTILITY HELICOPTER TROOP SEATS

Mustafa DEMİRCAN

Master of Science, Department of Mechanical Engineering

Supervisor: Asst. Prof. Özgür ÜNVER

November 2020, 73 Pages

In most of the helicopter platforms, usage of vertical or sideward ejection seats are not preferred since it is not practical considering the existence of the rotating main rotor blades on top and the spinning action caused by the main rotor which could yield uncontrolled behavior during jettisoning. In addition, it is not possible to provide ejection seats for each and every occupant on board. Therefore, to increase the chance of survivability of occupants, helicopter platforms and their components such as landing gear, fuselage and seats shall be designed crashworthy especially in vertical direction. Considering the importance of the seat for crashworthiness assessment, it becomes critical to investigate on seat energy absorption in a comprehensive way. According to regulations or military design standards, helicopter seats shall absorb some fraction of crash energy via plastic deformation mechanisms to save the life of the passengers during a crash. Accordingly, helicopter seats shall be qualified and shall be dynamically tested with the test scenarios provided in the applicable design standard. In this thesis study, a tube-stud type energy absorption system is designed and integrated into a simplified troop seat to verify its performance in dynamic test conditions specified by

MIL-S-85510. In order to absorb the crash energy and to decrease the load transferred to the occupants to the acceptable levels, the studs plastically deform the tube and decrease its diameter. The energy absorber concept is analyzed with dynamic explicit workbench of ABAQUS® and then tested in METU Central Lab Mechanical Testing Laboratories. After the correlation of the analyses and the test results, the energy absorber system is integrated into a simplified military troop seat and then analyzed to simulate the crash test scenario. The crash pulse provided in the MIL-S-85510 is applied and the results are evaluated.

Keywords: Crashworthiness, Military Helicopter Seats, Crash Analysis

ÖZ

ASKERİ GENEL MAKSAT HELİKOPTERİ MÜRETTEBAT KOLTUKLARI İÇİN ENERJİ SÖNÜMLEYİCİ TASARIMI VE ANALİZİ

Mustafa DEMİRCAN

Yüksek Lisans, Makina Mühendisliği Bölümü

Tez Danışmanı: Dr. Öğr. Üyesi Özgür ÜNVER

Kasım 2020, 73 Sayfa

Helikopter platformlarının çoğunda, dikey ve yatay fırlatma koltuklarının kullanımı, üstte yer alan ana rotor pali varlığı ve ana rotor palinin dönme hareketinin neden olabileceği kontrolsüz fırlatma durumları gerekçesiyle tercih edilmemektedir. Ek olarak, hava aracında yer alan her bir yolcu için fırlatma koltuğu sağlamak mümkün değildir. Bu sebeple, yolcuların hayatta kalma ihtimalini arttırmak için helikopter platformları ve iniş takımı, gövde ve koltuk gibi bileşenleri özellikle dikey yönlü kaza dayanımı özellikli olacak şekilde tasarlanmalıdır. Koltukların, kaza dayanımı değerlendirmesi konusundaki önemini düşünecek olursak, koltuk enerji sönümleme sistemlerini etraflıca incelemek önem arz etmektedir. Regülasyonlar veya askeri tasarım standartlarına göre, helikopter koltukları yolcuların hayatlarını korumak için kaza esnasında enerjinin bır kısmını plastik deformasyon mekanizması ile sönümlemelidir. Dolayısı ile, helicopter koltukları geçerli standartlarda sağlanan test senaryolarına uygun şekilde kalifiye edilmeli ve dinamik olarak test edilmelidir.

Bu çalışmada boru ve saplama tipi enerji sönümleme sistemi tasarlanmış ve MIL-S-85510 ile belirtilen test durumlarındaki performansını doğrulamak için basit askeri mürettebat koltuğuna entegre edilmiştir. Kaza enerjisini sönümlemek ve yolculara

iletilen yükleri kabul edilebilir seviyelere indirmek için silindirler boruyu plastik olarak deforme eder ve çapını daraltır. Konsept enerji sönümleyici, ABAQUS® Workbench ile analiz edilmiş ve sonrasında ODTÜ Merkezi Test Laboratuvarı'nda test edilmiştir. Analiz ve test sonuçları doğrulama faaliyeti sonrasında, enerji sönümleyici basit askeri mürettebat koltuğuna entegre edilmiş ve kaza test senaryolarını simule etmek amacıyla analiz edilmiştir. MIL-S-85510'da verilen yükler uygulanmış ve çıkan sonuçlar değerlendirilmiştir.

Anahtar Kelimeler: Kaza Dayanımı, Askeri Helikopter Koltukları, Kaza Analizi

ACKOWLEDGEMENTS

First, I would like to express my appreciation to my supervisor Dr. Özgür Ünver for his supports during the study. I would like to thank him for everything he has done.

I would like to thank my wife Cansu Karataş Demircan for her support. This long-term study is completed with her kindness toward my study. This study could not be finalized without her encouragement. She helped me in the hardest times.

I am appreciative to my mother Huriye Demircan, my father Alaattin Demircan and my elder sister Canan Demircan for their effort through my childhood, and education period.

Lastly, I am grateful to my company Turkish Aerospace for providing me chance to complete my study.

TABLE OF CONTENTS

LIST OF FIGURES

LIST OF TABLES

SYMBOLS AND ABBREVIATIONS

Symbols

ft	Feet
sec	Second
g	Gravitational acceleration
lbs	Pound
G_L	Limit load in terms of gravitational acceleration
L_L	Limit load
G_{min}	Minimum acceleration in terms of gravitational acceleration
G_{max}	Maximum acceleration in terms of gravitational acceleration
W_{eff}	Effective weight

Abbreviations

EASA:	European Aviation Safety Agency
FAA:	Federal Aviation Administration
AvCIR:	Aviation Crash Injury Research
CS:	Certification Specifications
AVSCOM:	U.S. Army Aviation Research & Technology Activity
ATD:	Anthropomorphic test dummy
HIC:	Head injury criteria
COTS:	Commercial off the self
RP:	Reference Point
CAD:	Computer Aided Drawing
OD:	Outer diameter
MPC:	Multi-point constraint

1. INTRODUCTION

1.1. Definition of Crash and Crashworthiness

Crash is called as high-speed impact of two or more objects, often making a loud noise and/or causing damage. In this study, crash means helicopter accidents which yield high g-loads to the fuselage structures and which cause occupants to get serious injuries.

Crashworthiness is the ability of a plane or a helicopter to absorb crash energy, with minimum structural contraction, in order to prevent occupants from experiencing serious injuries in the case of potentially survivable accident [1, 2]. Crashworthiness ensures structural integrity, adequate space for survivability and decreased load levels transferred to the occupants by using suitable restraining systems.

The term crashworthiness is used in the aerospace industries around 1950's [1]. For rotorcraft applications, crashworthiness is to significantly absorb crash energy via inelastic deformations using external or internal subsystems. External subsystems, for instance airbags, shall be easily deployable and storable without hindering the normal operation of the rotorcrafts. Internal systems, such as energy absorber seats, landing gears and deformable subfloor, are in use although they do not affect the normal operation of the aircrafts [3].

1.2. Crashworthiness of Helicopters

Compared to the aircrafts, crashworthy design concept is much more critical for helicopters since the accident rates per flying hour of helicopters are much greater by a ratio of 2 to 1 [4]. The purpose of crash resistance in helicopter design is to prevent fatalities and injuries in mild impact condition [5]. The main ideas for crashworthiness are intended to provide adequate safe volume for passengers during crash and to lessen the vertical impact load to an acceptable level, which can be tolerated by the human body. For these reasons, landing gears, helicopter fuselage and floor section shall be designed in a way that advances the crashworthiness performance of helicopter in harsh landing and crash conditions [6]. In addition to the energy absorbing landing gears and fuselage, it is required by authorities, European Aviation Safety Agency (EASA) or Federal Aviation Administration (FAA), that cockpit and cabin seat shall be designed crashworthy and that they shall absorb some portion of the crash energy.

In most of the helicopter crashes, vertical velocity component of the fuselage is much critical than the longitudinal velocity component. During the impact stage, while occupant and helicopter velocity decrease in a very short duration, human body experiences high g-loads, especially in vertical direction. Because of the sudden velocity changes and high g-loads, human body parts move relatively and different body parts face with different relative accelerations. These relative accelerations yield forces in body part connection segments. Injuries emerge if these load levels exceed the allowable limits. Considering that the change in the helicopter vertical velocity is higher in a crash condition and that the human body is delicate along the spinal axis, the most of the injuries are vertebral column injuries [7].

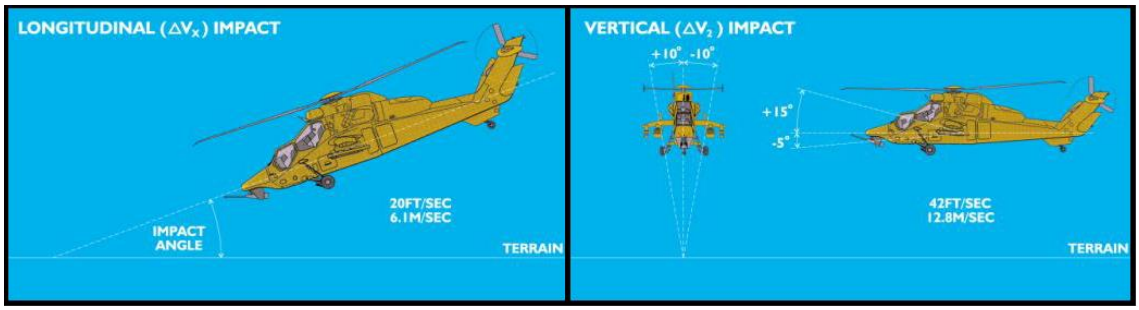

Figure 1.1. Helicopter crash velocities in longitudinal and vertical direction [8]

In order to increase the occupant survivability as much as possible, a system perspective to crash evaluation should be established. The system approach requires that landing gear, fuselage and crashworthy seat work together in a harmony to slow down the occupants and to decrease the load transferred to the occupants at safe levels [5].

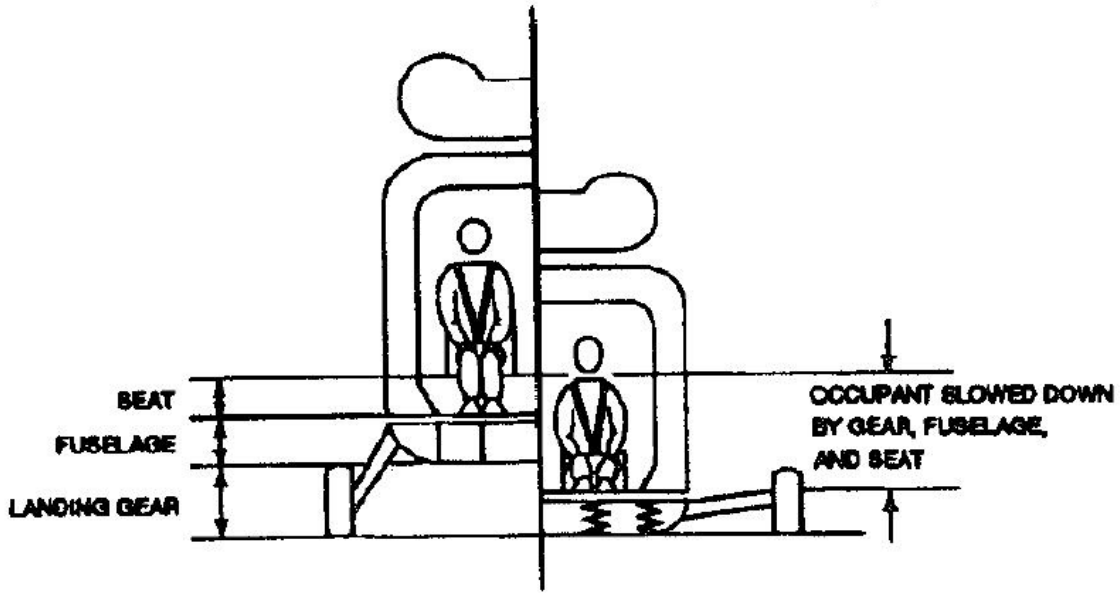

Figure 1.2. Energy absorber subcomponents of a helicopter [5]

1.3. Helicopter Seats

Crashworthy helicopter seats shall consist of safety belt, seat pan, seat-to-aircraft attachments and energy absorbing devices that connect the seat pan to the fixed structure of the helicopter or to the fixed structure of the seat via a translational joint. Crashworthy helicopter seats are designed to stroke downward relative to the helicopter floor as in Figure 1.3 to mitigate vertical crash loads. Compared to the fuselage and landing gears, energy absorbing seat systems are much more effective for crash energy absorption [9]. Considering that the seat systems are less delicate to the impact effects and that the seats are not severely deformed in the initial phase of the impact, it becomes possible to have a controlled energy absorption on seat systems.

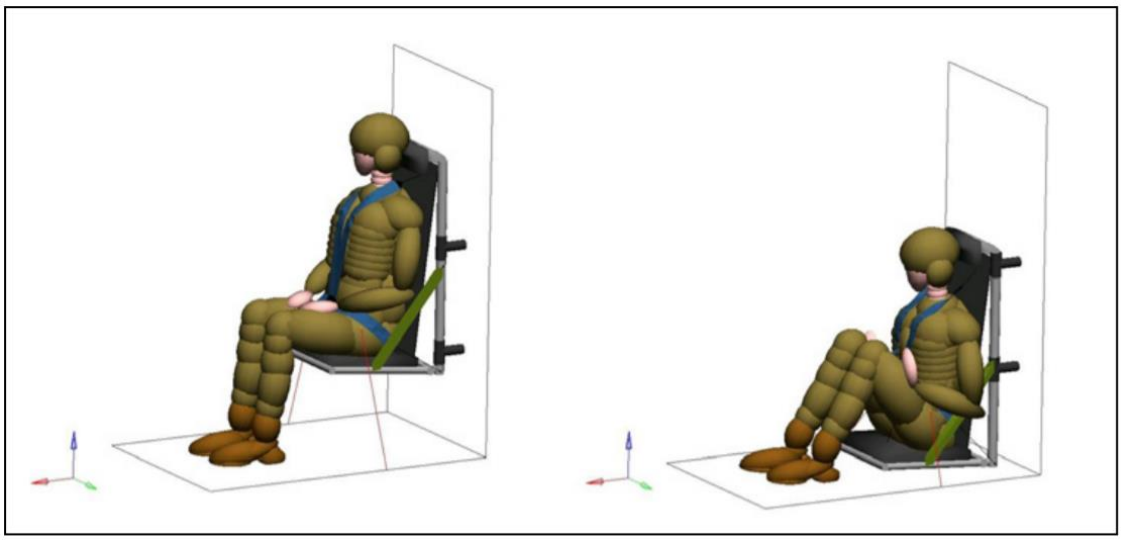

Figure 1.3. Troop seat downward stroking [10]

Helicopter seats are divided into two main categories as cockpit and cabin seats. The cockpit seats are named as pilot and copilot seats whereas cabin seats are named as passenger seats. Also depending on the type of the platforms, these seats could be subdivided as military and civilian seats. For civilian helicopters, passenger seats should be certified according to the civilian regulations. However, for military helicopters, passenger seats, which are called as troop seats, should be qualified according to the military standards.

Civilian passenger seats are certified according to the civilian regulations, which are provided by certification authorities such as EASA and FAA. This type of seats generally consists of four-point safety belts, padded headrest, non-foldable seat pan, L-shaped seat legs and seat floor attachments as seen in Figure 1.4.

Figure 1.4. A sample passenger (civilian) seat [11]

Military troop seats are qualified according to the military standards and the customer needs. These types of seats are generally simpler than civilian passenger seats. Troop seats consist of two main seat poles, fabric headrest, foldable seat pan, five-point safety belt, ceiling and floor attachments as seen in Figure 1.5.

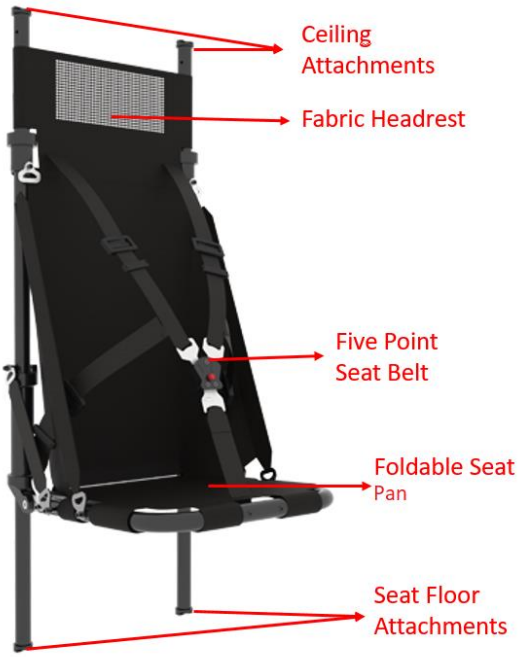

Figure 1.5. A sample troop (military) seat [12]

1.4. Motivation of the Study

Crashworthy seat development requires a series of laboratory tests in order to evaluate the crashworthiness performance of the seat energy absorber and the whole seat assembly. A minor change in the design requires retesting and investigation about possible effects on the crashworthiness feature of the design. This repetitive and iterative test sequence is time and money consuming. In addition, it becomes hard to implement and evaluate minor changes. However, finite element analysis could provide a way to implement the changes easily and to decrease the number of tests during the iterative development process. Therefore, motivation of the study is to design an energy absorber system via finite element analysis tool and to implement it to a simplified troop seat system after the energy absorber system is verified by tensile tests.

1.5. Objective of the Study

Design and manufacturing of subsystems for aerospace industry, which is emerged and developed recently in our country, is critical for evolution and sustainability of national defense industry. However, most of the systems and subsystem components are designed and manufactured by foreign companies abroad. Main objectives of this thesis study are to create a start-up for aerospace subsystem component design and development, to gather information, create knowledge about crashworthiness and perform a demonstration on a subcomponent design and optimization considering a tube-stud type energy absorber mechanism according to the requirements given by MIL-S-85510 [13] using ABAQUS® Workbench and dynamic finite element methods. The concept energy absorber is considered to be plastically deformable and provides a fixed load value during this deformation. Design of the absorber is done according to the finite element analyses results, which are evaluated for the selection of the material and the dimensions. Optimized energy absorber is manufactured at Turkish Aerospace and tested at Middle East Technical University Central Laboratories to check the load deformation results. Then, the optimized energy absorber is implemented into a simplified troop seat system to observe overall performance using dynamic explicit finite element analyses. The dynamic nonlinear finite element analyses enable us to predict whether absorber concept system protects occupants in a crash condition, and help to choose correct material and dimension combination for the absorber. In order to check the capability of the energy absorber system, the g-loads obtained from the seat

pan during explicit finite element analyses are evaluated in accordance with the criteria prepared by Department of Defense of US by Crash Protection Handbook for crew members [14].

1.6. Scope of Study

The main chapters of the thesis study as follows:

1) Introduction
2) Literature Review and Theoretical Background
3) Experiments and Analyses
4) Results and Discussion
5) Comments and Future Works

In Chapter 1 - Introduction, definitions of crash and crashworthiness are briefly given. Afterwards, the external and internal subsystems, which could be used on crashworthy platforms, are mentioned. Furthermore, common features of helicopter crashes, the needs for crashworthy helicopter seats are listed. Finally, motivation, objective and scope of the thesis are underlined.

In Chapter 2 - Literature Review and Theoretical Background, related civilian and military regulations including dynamic test conditions and injury criteria are mentioned. Information about seat energy absorber mechanisms are provided.

In Chapter 3 - Experiments and Analyses, stand-alone design, analyses and testing steps of the absorber are performed. Afterwards, integration of the energy absorber to a basic troop seat and dynamic explicit analyses are performed.

In Chapter 4 - Results and Discussion Section, dynamic test results of the explicit analysis are evaluated. Acceleration, velocity and displacement results are compared with the similar studies. Acceleration graphs are evaluated according to the acceptance criteria.

In Chapter 5 - Comments, information and experiences gained throughout the study and possible future works are summarized.

References which are used in this study are provided in the final section.

2. LITERATURE REVIEW AND THEORETICAL BACKGROUND

2.1. Regulations for Seat Crashworthiness

The occupant safety in rotorcraft and aircraft throughout any survivable mishap has been a major concern for a long time [15]. In addition to the crashworthy helicopter structure studies, the need for energy absorbing seats has been prepared by the Aviation Crash Injury Research (AvCIR) Division of Flight Safety Foundation during 1950s [16]. In 1970s, U.S. Army Aviation Research & Technology Activity (AVSCOM) sponsored the establishment of the design and testing methodologies. The Aircraft Crash Survivable Design Guide was established as Technical Report and subsequent revisions published as Technical Report 70-22 and as Technical Report 71-22 and 79-22 [5]. Then, the criterions established by the activities of AvCIR and AVSCOM incorporated into latest EASA and FAR regulations for civilian platforms. Certification Specification Documents (CS's) are technical standards accepted by EASA to provide necessary requirements for applicable platform and its subsystems such as seats. For example, CS-29 contains requirements for Large Rotorcraft and its subsystems whereas CS-27 contains requirement for Small Rotorcrafts [17,18].

2.1.1. Military Regulations

Military helicopter seats are generally classified as cockpit seats and cabin seats. For the cockpit seats, requirements are given by MIL-S-58095 Military Specification Seat System: Crash-Resistant, Non-Ejection, Aircrew, General Specification For Standard [19]. For military troop seats, which are installed to cabin section requirements, are provided by MIL-S-85510 Seats, Helicopter Cabin, Crashworthy, General Specification for Standard [13]. Considering the testing conditions of cockpit seats and cabin seats, it is possible to infer that the change in velocity is similar, which is 50 ft/sec for both. However, g levels for the cockpit seats are higher than the ones for the cabin seats, as indicated in Table 2.1.

Since military troop seats are installed in the cabin section of the helicopters, we will consider MIL-S-85510 standard in the following sections.

Dynamic Test Conditions:

In order to show crashworthiness performance of helicopter seats, authorities and standards require two main dynamic tests. The first test (Test 1 in Table 2.1) is combined vertical dynamic test and the second test (Test 2 in Table 2.1) is forward dynamic test.

In Test 1, which is combined vertical dynamic test, the main objective is to evaluate the energy absorption performance of helicopter seats in a vertical crash condition. In order to simulate real helicopter crash condition, the test setup is angled upward 60° and rolled 10° degrees as in Figure 2.1.

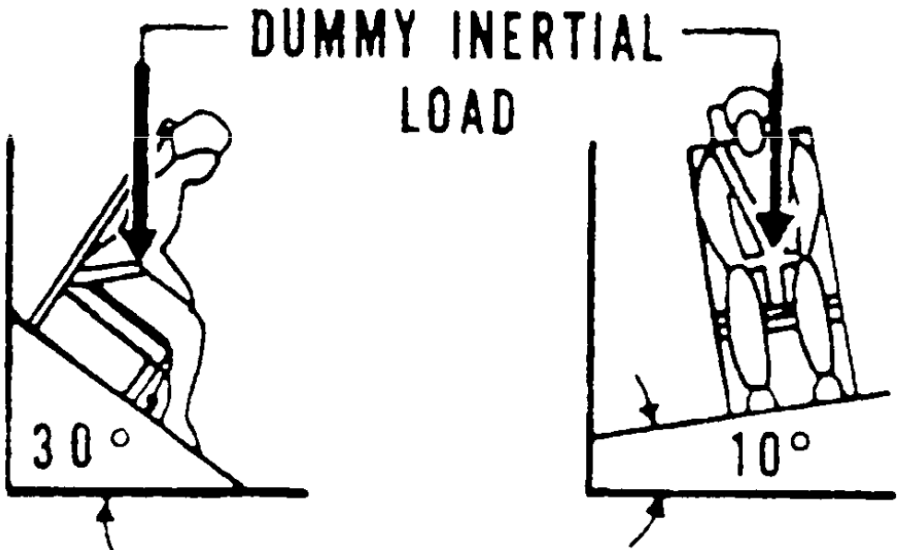

Figure 2.1. Combined vertical dynamic test setup alignment [13]

In Test 1, a triangular acceleration impulse that is similar to Figure 2.2 should be applied to the seat test setup. Time to reach to the maximum g-load is limited by t_1 and t_2, which are 0.059 and 0.087 secs. In addition, maximum acceptable g-load is limited by G_{min} and G_{max}, which are 32 g's and 37 g's. For this test scenario, the calculated change in the velocity should be 50 ft/sec.

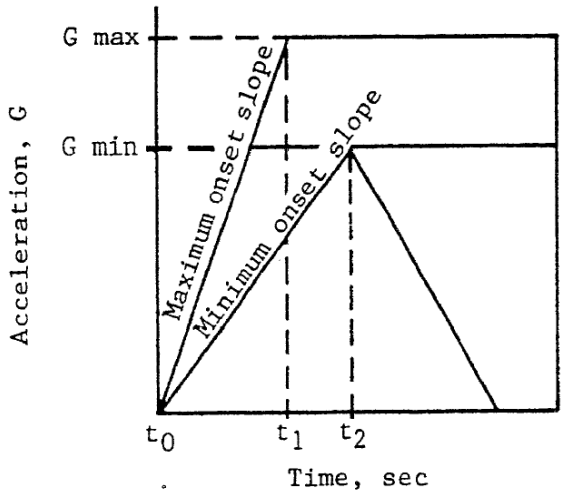

Figure 2.2. Triangular acceleration pulse for seat setup [13]

In Test 2, which is forward dynamic test, the main objective is to evaluate the performance of safety harness and the occupant motion in forward crash condition. During the test, the setup is yawed with an angle of 30° to the helicopter longitudinal velocity vector as in Figure 2.3.

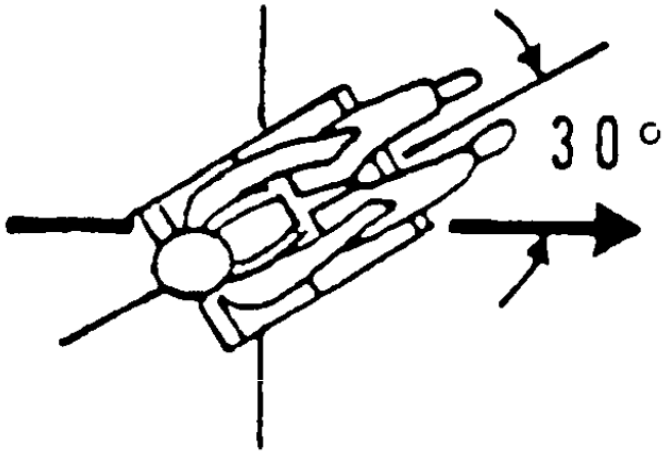

Figure 2.3. Forward dynamic test setup alignment [13]

In Test 2, a triangular acceleration impulse that is similar to Figure 2.2 should be applied to seat test setup. Time to reach to the maximum g-load is limited by t_1 and t_2, which are 0.081 and 0.127 secs. In addition, maximum acceptable g-load is limited by G_{min} and G_{max}, which are 22 g's and 27 g's. For this test scenario, the calculated change in the velocity should be 50 ft/sec.

During the helicopter crashes, prior to the initiation of seat energy absorbers, fuselage and landing gears plastically deformed and some portion of the crash energy was absorbed. Deformation of fuselage causes cabin and cockpit floor warpage before the seat energy absorbers activate. In order to simulate this floor pre-deformation, MIL-S-85510 demands that the seat track should be deformed initially before sled tests as given in Figure 2.4 [13].

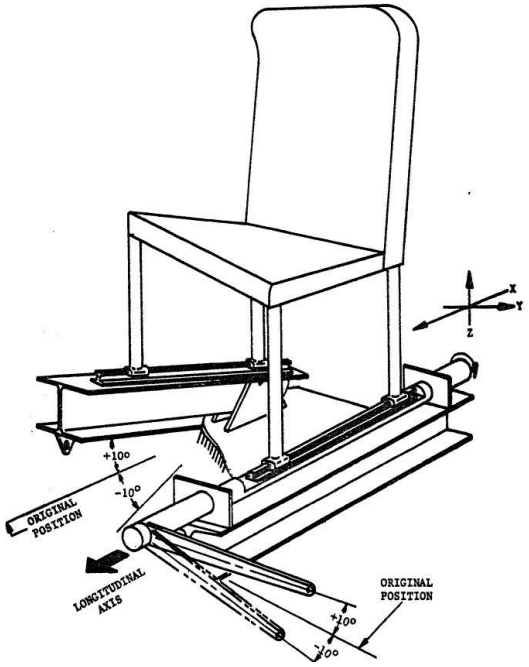

Figure 2.4. Seat floor deformation conditions [13]

Injury and Pass-Fail Criteria

During the qualification testing, seat and its critical subcomponents, such as safety belts, should not lose their structural integrities. Test dummy shall be retained within the confines of the safety belt during the tests. Furthermore, any failure of a primary load-carrying member or of a restraint system is unacceptable.

During Test-1 and Test-2, seat pan accelerations should be measured and these accelerations should stay within the acceptable pulse duration region of Figure 2.5 and Figure 2.6, respectively.

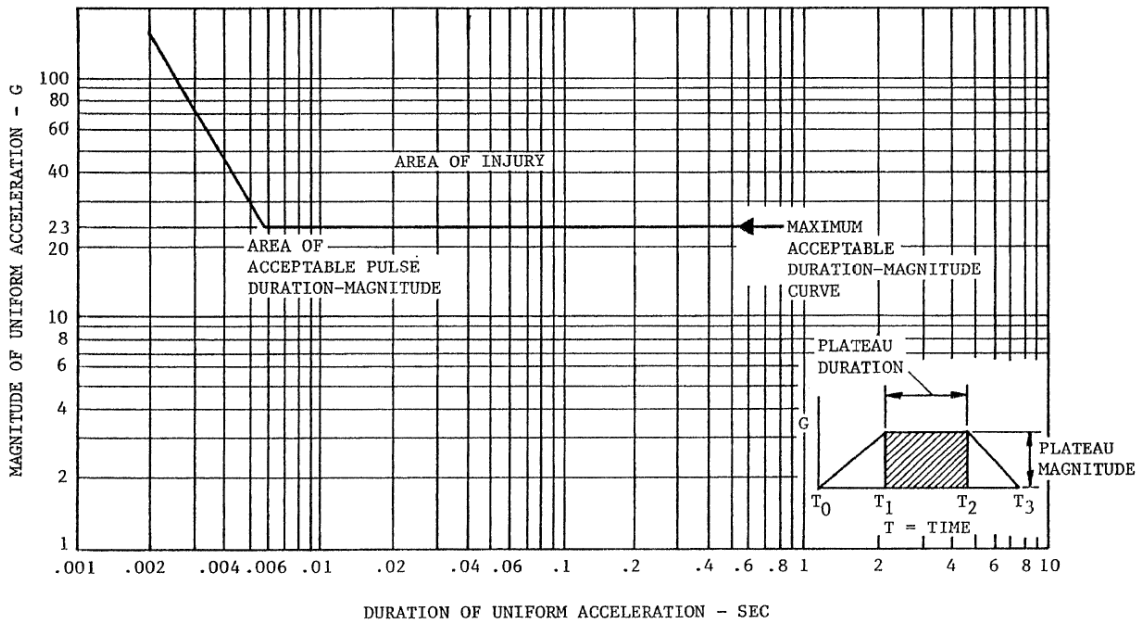

Figure 2.5. Maximum acceptable vertical pulse acceleration and duration [13]

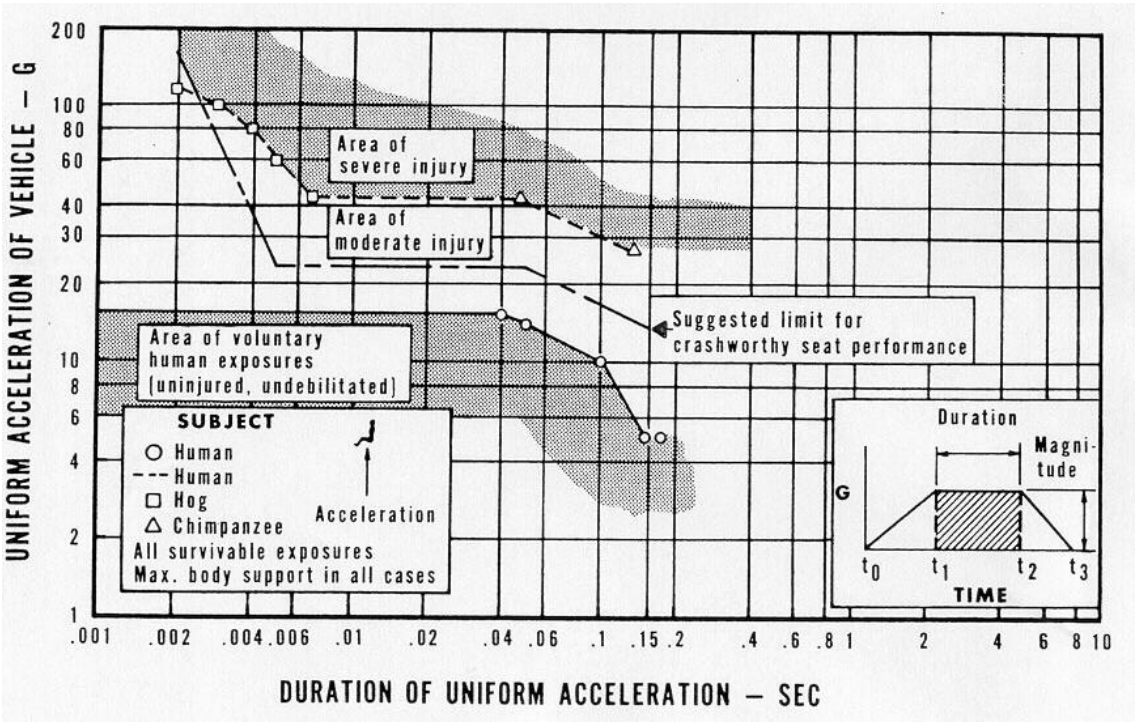

Figure 2.6. Maximum acceptable longitudinal pulse acceleration and duration [14]

The vertical pulse acceleration curve defines a 5.5 millisecond time duration at the 23 g level as recommended g level for crashworthy seat performance. However, this evaluation is based on early studies by Geertz on seat catapults in 1944 [14]. Later studies are based on the experience gained during the Black Hawk crew-seat

development activities, in which the time duration is extended to 25 milliseconds, confirmed by cadaver testing [14].

In addition to the dynamic test requirements, to demonstrate the performance of the energy absorber itself, a static test should be performed. Depending on the knowledge of human tolerance, designer should choose a maximum stroke force of 14.5 g for the seat. Subsequent studies with the crashes of the Black Hawk and the human cadaver testing have proven that 14.5 g was the optimum to prevent spinal injury in the most severe survivable impacts for the whole range of aviator population [14]. In order to prove that the seat absorbers are tuned to stroke at 14.5 g, a downward static test should be performed and the seat downward deflection-force curve obtained from the test should fit into the allowable area in Figure 2.7.

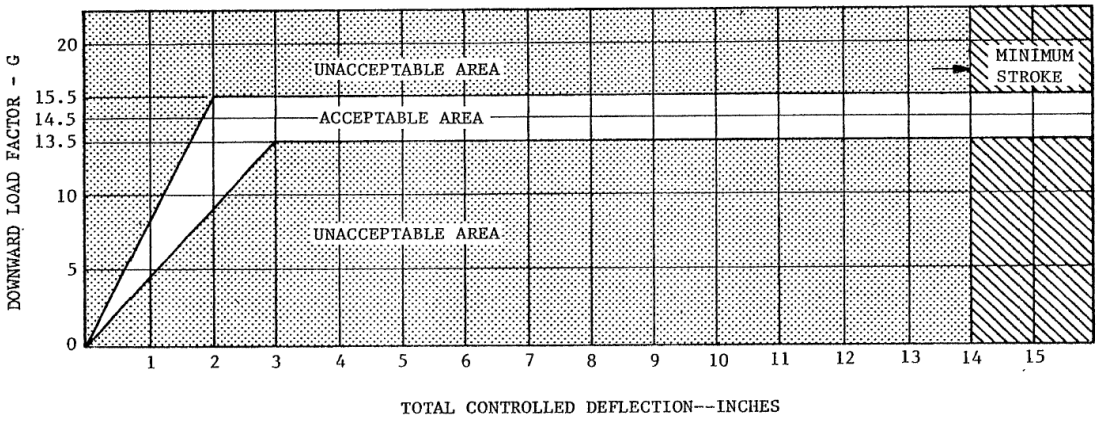

Figure 2.7. Seat downward load and deflection requirements

2.1.2. Civilian Regulations

Using the experience gained by U.S. Army in military seat development projects, FAA initiated a research program to define civilian criteria. Outcome of the research indicated that the design and testing procedures for the civilian seats are very similar to the military seats. The major differences are the g profiles of dynamic tests and the acceptance criteria. If the military testing conditions were applied for civilian platform, it would be a much conservative approach, which could yield weight and cost penalty [20]. For the civil and the transport category rotorcrafts, seat requirements are given under CS 27.562 and CS 29.562 [18, 16].

In this study, requirements for transport category helicopters CS-29 are considered only for comparison purpose. Analyses and design activities are performed for military troop seats.

Dynamic Test Conditions

In order to guarantee the performance of the rotorcraft seat and the restraint system, two main dynamic tests are required by CS-29 Section 562-1[21]. These tests are similar to the tests given by MIL-S-85510 standard.

In Test 1, which mainly evaluates the performance of the seat in vertical direction, predominant load component is aligned vertically with a horizontal component. Therefore, energy absorption to prevent spinal injuries becomes important and it may be vital to have energy absorption system to decrease the loads transferred to the occupants.

Alignment of the test setup and the inertial force of the dummy is represented in Figure 2.8. The seat should be oriented in a way that the principal axis of the seat is directed with an angle of 60° with respect to the impact velocity vector, and that the helicopter's lateral axis is perpendicular to a vertical plane which contains the impact velocity vector and the platform's longitudinal axis. In this test a triangular pulse with a peak acceleration of 30 g and with a rise time equal to or less than 0.031 sec should be applied to test setup. The minimum change in velocity for this test is 30 ft/sec [17].

Test 2 evaluates the protection performance in an impact where main load component is in the longitudinal direction with a lateral component. In this test, assessment of head injury protection is necessary since the head of the dummy could interfere with the interiors or the seat in front. Chest loads and spinal injury due to the upper torso motion are also evaluated.

Alignment of Test 2 setup and inertial force of the dummy is represented in Figure 2.8. The seat should be oriented in a way that longitudinal axis of the seat is yawed 10° sideward with respect to the impact velocity vector, and that the lateral axis of the rotorcraft is perpendicular to a vertical plane containing the impact velocity vector and the rotorcraft's longitudinal axis. In this test, a triangular pulse with a peak acceleration of 18.4 g and with a rise time equal to or less than 0.071 sec should be applied to the test setup. The minimum change in velocity for this test is 42 ft/sec [17].

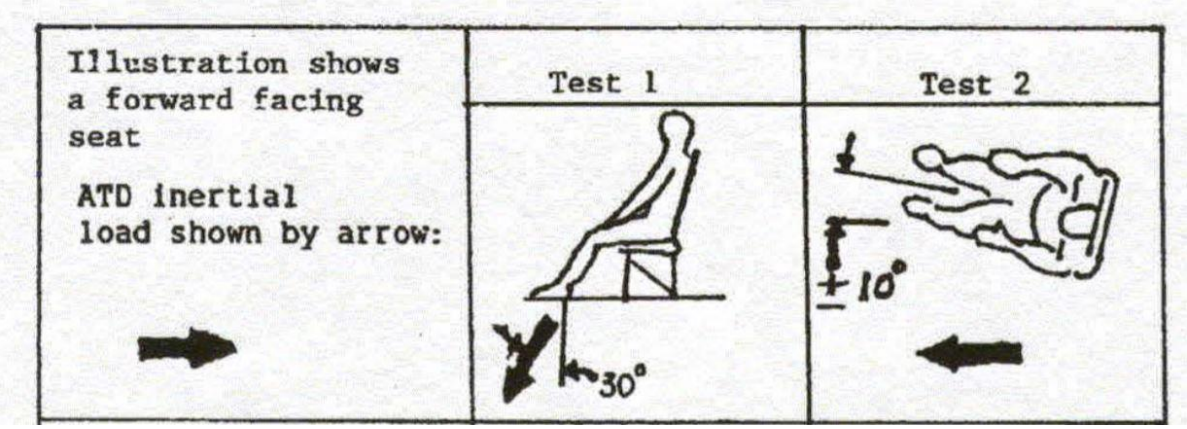

Figure 2.8. Seat restraint system dynamic test conditions given in CS-29 [21]

For both tests, attachment interfaces shall be misaligned with respect to each other by at least 10° in vertical and by at least 10° in lateral roll to simulate actual floor deformations prior to the dynamic tests.

Injury and Pass Fail Criteria

For both the dynamic tests which are demanded by CS-29 [16], compliance with the following must be presented:

1. The seat should stay intact after the dynamic tests.
2. The shoulder harness strap of ATD should remain in place during the impact.
3. The safety belt should stay on the pelvis of ATD during impact.
4. If the head of ATD contacts with any portion of the seat and the compartment, the head injury criteria (HIC) should not exceed 1000 as determined by

$$HIC = (t_2 - t_1)\left[\frac{1}{(t_2 - t_1)}\int_{t1}^{t2} a(t)dt\right]^{2.5}$$

where a(t) is the acceleration of the center of gravity of the head and t2-t1 is the impact duration in seconds. This duration is limited by a maximum duration of 0.05 seconds.

5. Loads in each shoulder harness should not exceed 1750 lbs. If dual straps exist, the total strap harness load should not exceed 2000 lbs.

6. The maximum allowable compressive load measured between the pelvis and the lumbar column of the ATD should be lower than 2000 lbs.

Dynamic test requirements for civilian regulations and military standards are summarized in Table 2.1.

Table 2.1. Dynamic test conditions for civilian and military regulations

	Civilian Regulations				Military Regulations	
Dynamic Test Requirements	FAR Part 23, CS 23 Normal & Commuter	FAR Part 25, CS 25 Transport Fixed Wing	FAR Part 27 CS 27 Normal Rotorcraft	FAR Part 29 CS 29 Transport Rotorcraft	MIL-S-58095	MIL-S-85510
TEST 1						
Test Velocity (ft/sec)	31	35	30	30	50	50
Seat Pitch Angle (degrees)	60	30	60	60	60	60
Seat Roll Angle (degrees)	10	10	10	10	10	10
Seat Yaw Angle (degrees)	0	0	0	0	0	0
Peek Deceleration (G's)	19/15	14	30	30	46-51	32-37
Time to Peak (seconds)	0.05/0.06	0.08	0.031	0.031	0.043-0.061	0.059-0.087
Floor Deformation (degrees)	None	None	10 Pitch / 10 Roll	10 Pitch / 10 Roll	10 Pitch / 10 Roll	10 Pitch / 10 Roll
TEST 2						
Test Velocity (ft/sec)	42	44	42	42	50	50
Seat Pitch Angle (degrees)	0	0	0	0	0	0
Seat Roll Angle (degrees)	10	10	10	10	10	10
Seat Yaw Angle (degrees)	10	10	10	10	30	30
Peek Deceleration (G's)	28/21	16	18.4	18.4	28-33	22-27
Time to Peak (seconds)	0.05/0.06	0.09	0.071	0.071	0.066-0.100	0.081-0.127
Floor Deformation (degrees)	10 Pitch / 10 Roll	10 Pitch / 10 Roll	10 Pitch / 10 Roll	10 Pitch / 10 Roll	10 Pitch / 10 Roll	10 Pitch / 10 Roll

2.2. Seat Energy Absorption Mechanisms

After detailed analyses of helicopter crashes and human crash tolerance, it was concluded that deceleration limit should be 14.5 g [16]. Therefore, seat energy absorbers, which will be used for military helicopter seats, should be optimized for a deceleration limit of 14.5 g, which means the weight of the 50th % occupant and effective weight of seat itself are multiplied by 14.5 g [22]. The vertical effective weight is defined as the sum of the 80% of the occupants' weight, 80% of the weight of the passenger not involving boots, and 100% of the weight of any items completely located above the knee level [13]. Optimized energy absorbers should be activated at 14.5 g and

should provide constant load throughout the whole crash pulse. Later studies performed on cadaveric testing and analysis verified the limit load factor G_L of 14.5 g [40]. The limit load which is L_L can be calculates as;

$$L_L = 14.5g \times W_{eff}$$

Where W_{eff} is the seat effective weight including effective weight of the occupant, which is approximately 80% of 50th percentile male occupant plus effective portion of the seat.

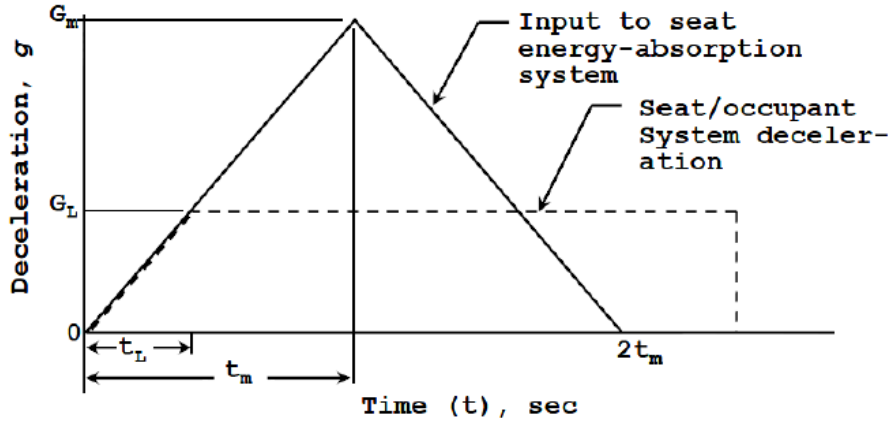

Figure 2.9. Seat setup triangular pulse and seat-occupant deceleration level [22]

According to MIL-S-85510 standard G_m which is seat test setup maximum acceleration input should be taken as 32-37 g's, tm which called as time to reach peak value should be taken as 0.059-0.087 sec with a velocity change of 50 ft/s for military troop seats.

In crash situation, loads that are experienced by the structures and sub systems are due to a sudden loading are called as impact. Unlike static loading conditions in impact case there is not an equilibrium point. The objects involved in crash exposed to elastic and plastic deformations. Throughout the crash, some energy is stored by elastic strain whereas most of the energy is dissipated by plastic deformation, stress wave propagation, material damping or other phenomenon such as sound and heat [15]. Considering the limited available space under the seats, the most effective way of limiting the crash load is to dissipate crash energy via plastic deformation process rather than storing it via elastic deformation [23].

In order to cover different human percentiles and to optimize the use of available stroke distance different energy absorber concepts are designed. These concepts are explained in the following chapters.

2.2.1. Fixed Load Energy Absorbers (FLEA)

Fixed load energy absorbers are arranged and optimized according to 50th percentile occupant weight and they provide a approximately constant load during the available stroking distances. Since the maximum limit load (L_L) is calculated by 14.5 g criteria, the maximum energy absorbed by the device becomes the stroke distance times the limit load value obtained via 14.5 g criteria. Therefore, typical load displacement curve of the energy absorber becomes as indicated in Figure 2.10.

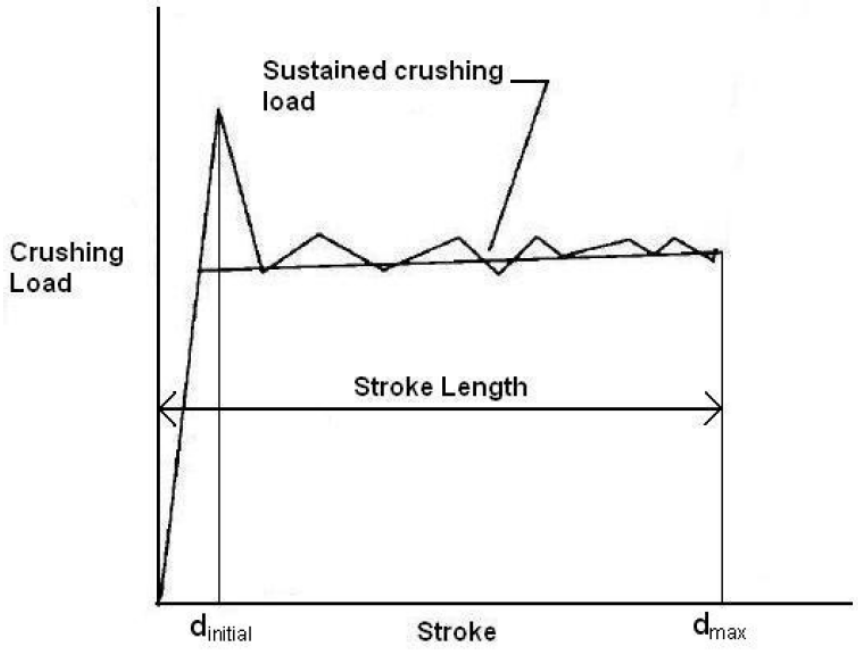

Figure 2.10. Typical load-stroke curve for a fixed load energy absorber [7]

In these FLEA concepts, lighter occupants such as 5th percentile female could receive higher g-loads whereas heavier occupants such as 95th percentile occupants could use all available stroke at lower load levels and the seat bottoms out at the end. However, since fixed load energy absorbers are easy to design and implement and since they are designed for the optimum 50th percentile they are highly preferred by the seat companies. Furthermore, authorities like EASA and FAA demands certification tests to be performed by 50th percentile ATD's only.

2.2.2. Variable Load Energy Absorbers (VLEA)

The variable energy absorbers are designed to adjust the limit load according to the occupant's weight input. The weight input is done manually by the occupant before boarding and the limit load of the energy absorber is adjusted accordingly.

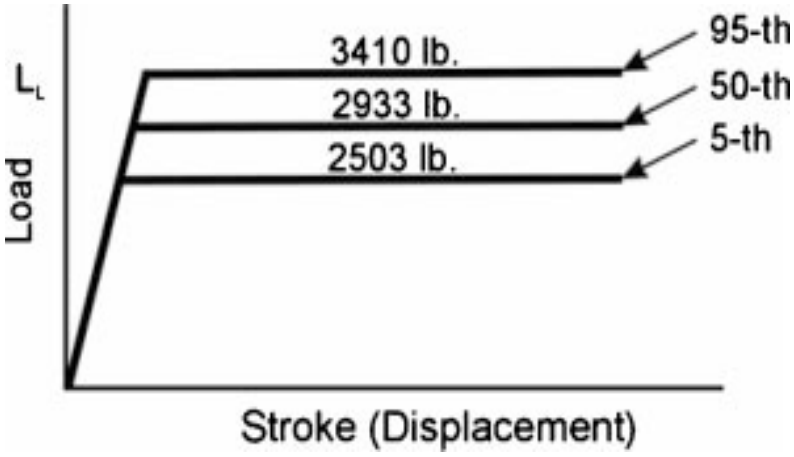

Figure 2.11. Variable load energy absorber adjustment range [23]

2.2.3. Fixed Profile Energy Absorbers (FPEA)

In variable load profile energy absorber, the occupant needs to adjust the absorber weight setting manually before boarding. To eliminate this step and to maximize the energy absorbed throughout the whole stroke while still covering 5th to 95th percentile occupants fixed profile energy absorber concepts are developed. In fixed profile energy absorbers, load is not constant at a specific value along the whole stroke, it varies with stroke. At the beginning, the limit load which is the actuation load of the absorber could be set to the optimum value for the 50th percentile occupant. After some percentage of the available stroke is used at that load setting, energy absorber could start deforming at a higher load level as in Figure 2.12.

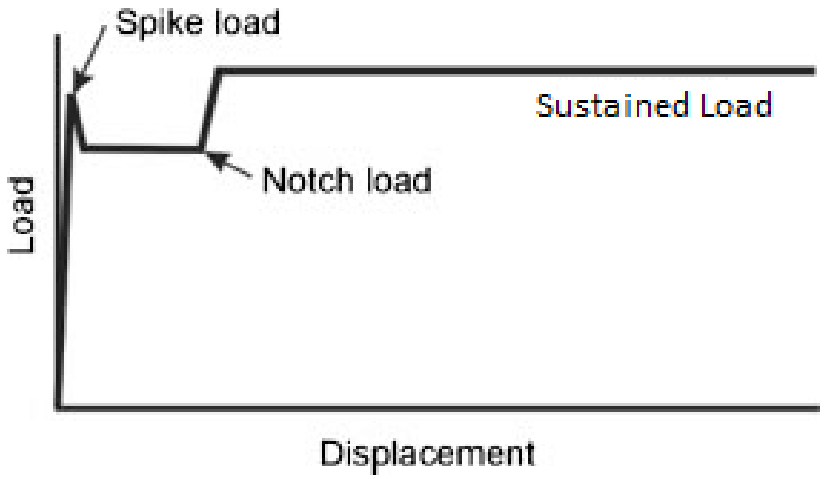

Figure 2.12. Load and displacement curve for fixed profile energy absorber [23]

2.2.4. Variable Profile Energy Absorbers (VPEA)

Variable profile energy absorbers are combination of FPEA and VLEA type energy absorbers. In variable profile energy absorption, sustained load value varies with the stroke and limit load can be manually adjusted before boarding.

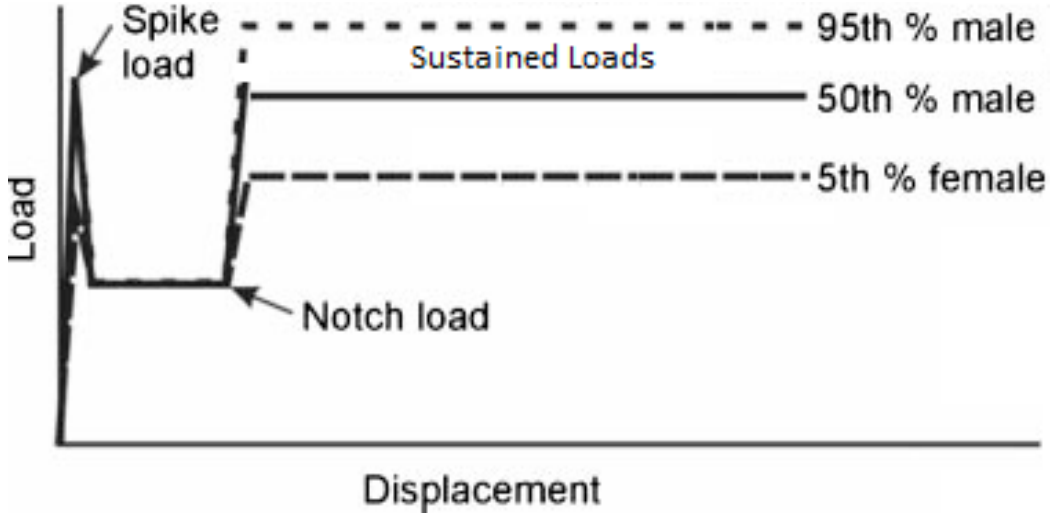

Figure 2.13. Variable profile energy absorber load-displacement curve

2.2.5. Advanced Energy Absorbers (AEA)

Advance energy absorbers combine all of the desirable features of the FPEA, VLEA and VPEA absorbers. They sense occupant weight and prevent the possibility of human error in weight setting. These systems are rather complex which may prevent its use or development in the close future. In addition, cost and producibility analysis needs to be performed on the concepts and specific applications.

Semi active and active energy absorbers could be evaluated as advanced energy absorbers. Fixed and variable load energy absorbers are passive type absorbers meaning that they cannot adapt their energy absorption force or load-displacement profile automatically by sensing passenger weight or any other measurements such as shock and vibration level etc. However, active energy absorber concepts use electronically changeable energy absorber that can alter load-displacement profile with respect to the real time input [24].

Magnetorheological energy absorbers (MREAs) provide a new solution technique to control the energy absorber loads via feedback control system. MREAs are expected to provide best combination of stroke and load level combination for a specific occupant [24].

In this reference study tube-roller type, fixed load energy absorber (FLEA) is analyzed and tested. Test is performed to check if analyses results are consistent or not. After the energy absorber is evaluated by itself, it will be implemented to a troop seat and dynamic explicit analysis will be performed. By using analysis tools time to optimize the absorber is decreased and new concepts could be evaluated much more rapidly.

D. Y. Hu et al. [6] conducted full-size drop test for a crashworthy helicopter pilot seat to check the crash performance of a fixed load type inversion tube energy absorber. To understand the physics behind numerical simulation performed by using Mathematical Dynamical Model (MADYMO) and nonlinear finite element code (LS-DYNA). Before full-size vertical crash testing a tensile test is conducted to get the characteristics of the energy absorber.

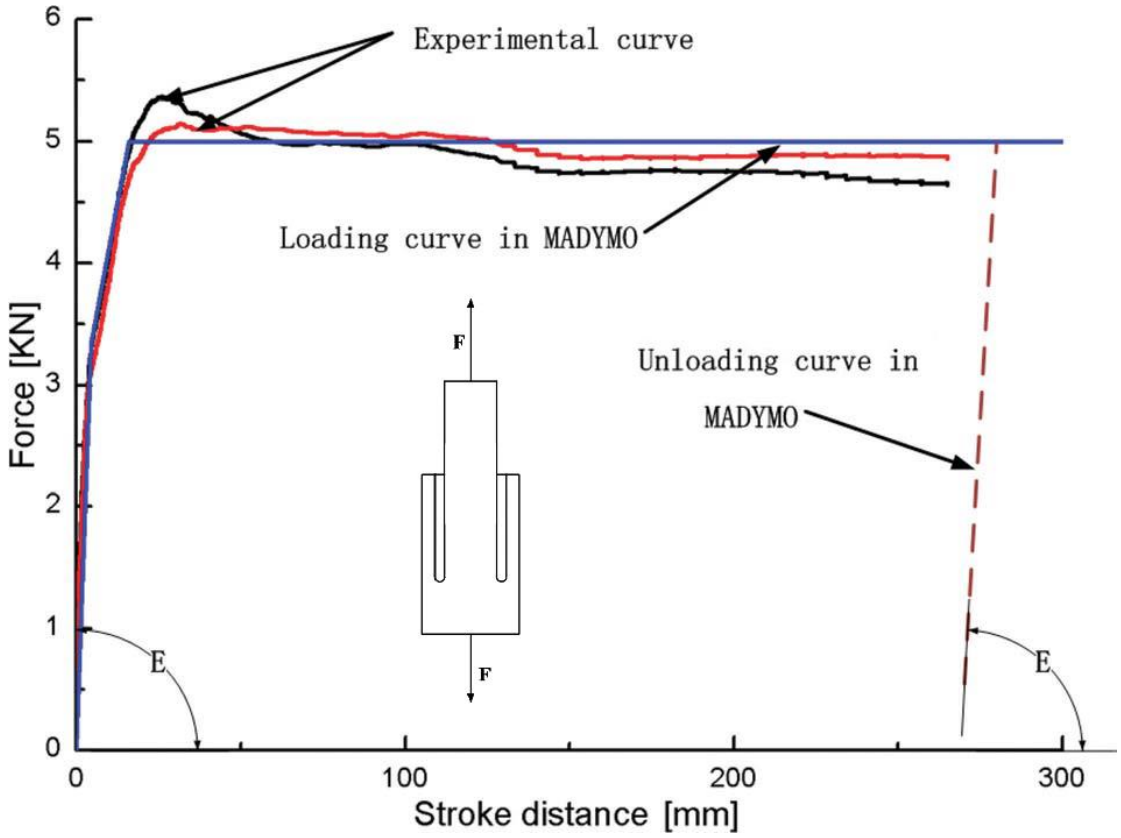

Figure 2.14. Inversion tube energy absorber and force-displacement curve [6]

Tong Yan et al. [25] performed design, testing and analysis of fixed load ultra-light composite energy absorber for helicopters. The energy absorber concept made of woven carbon fiber in cylindrical thin-walled tube form and the trigger as seen in Figure 2.15.

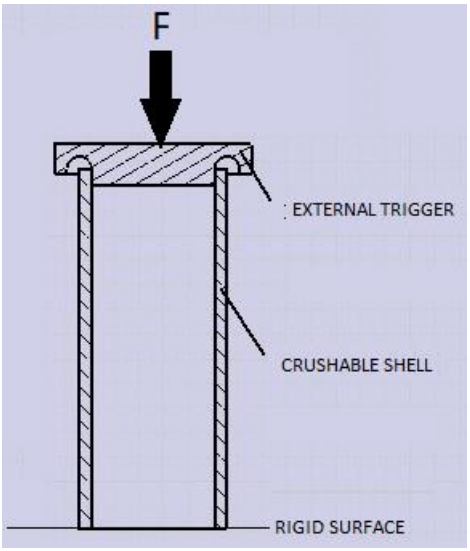

Figure 2.15. Structure of the composite energy absorber component [25]

The energy absorber component tested and dynamic explicit analysis performed on this concept. Related load-displacement (time) graph for an example test and analysis given in Figure 2.16.

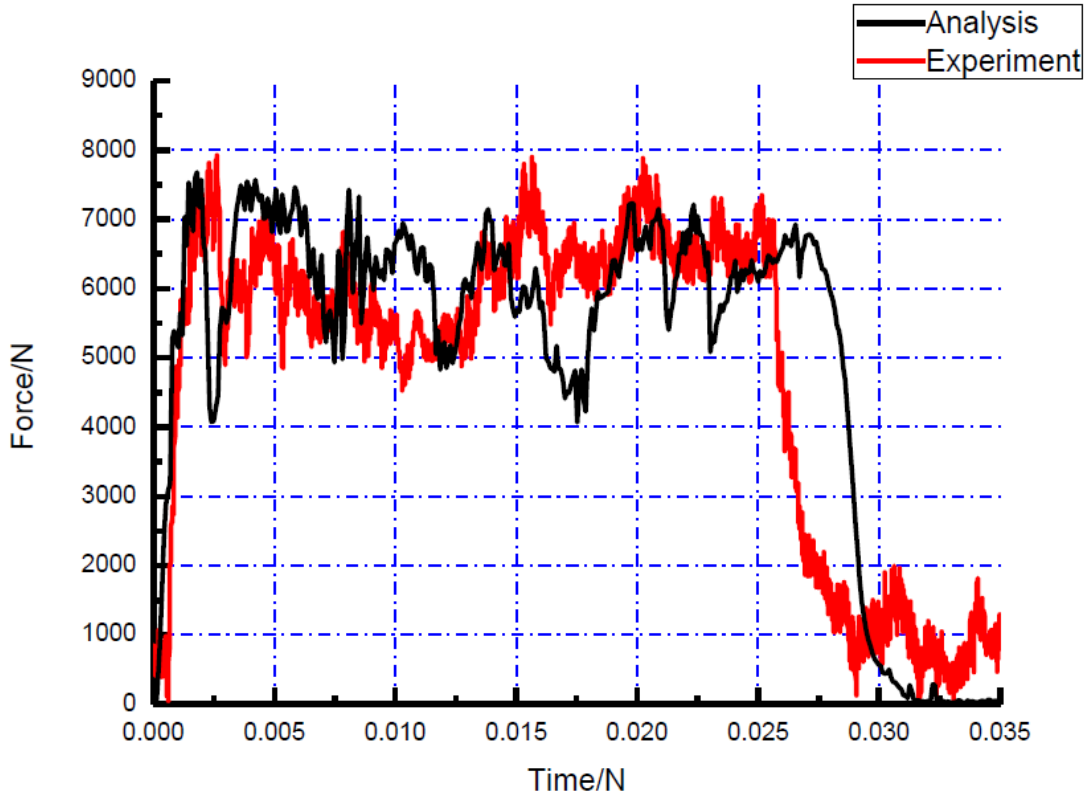

Figure 2.16. Load-displacement curve for composite absorber [25]

Jian Li et al. [26] studies the load limiting performance of shrink hollow tube which is exposed quasi-static loading throughout experiments and analysis. Energy is absorbed via plastic bending and compression of tubular material with the help of the friction between cone and the tube. Jian Li et al. obtained constant load and deformation curve during the shrink tube experiments as in Figure 2.17.

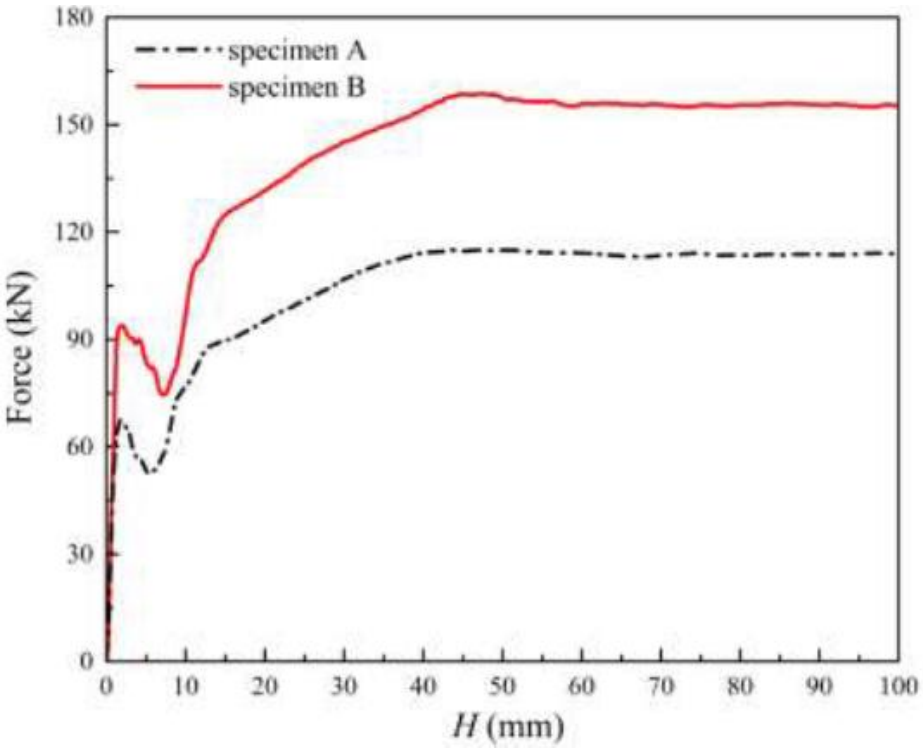

Figure 2.17. Reaction force – stroke distances for shrink tube energy absorbers [26]

Gupta et al. [27] also studied deformation of circular tube of metallic materials by a conical die experimentally and numerically as shown in Figure 2.18. It is concluded that main mechanisms which create energy absorption is the plastic deformation and frictional slide. The energy absorption performance highly depended on physical parameters (thickness, diameter) and material properties. The energy absorber shows fixed load type behavior through the whole stroke as in Figure 2.19.

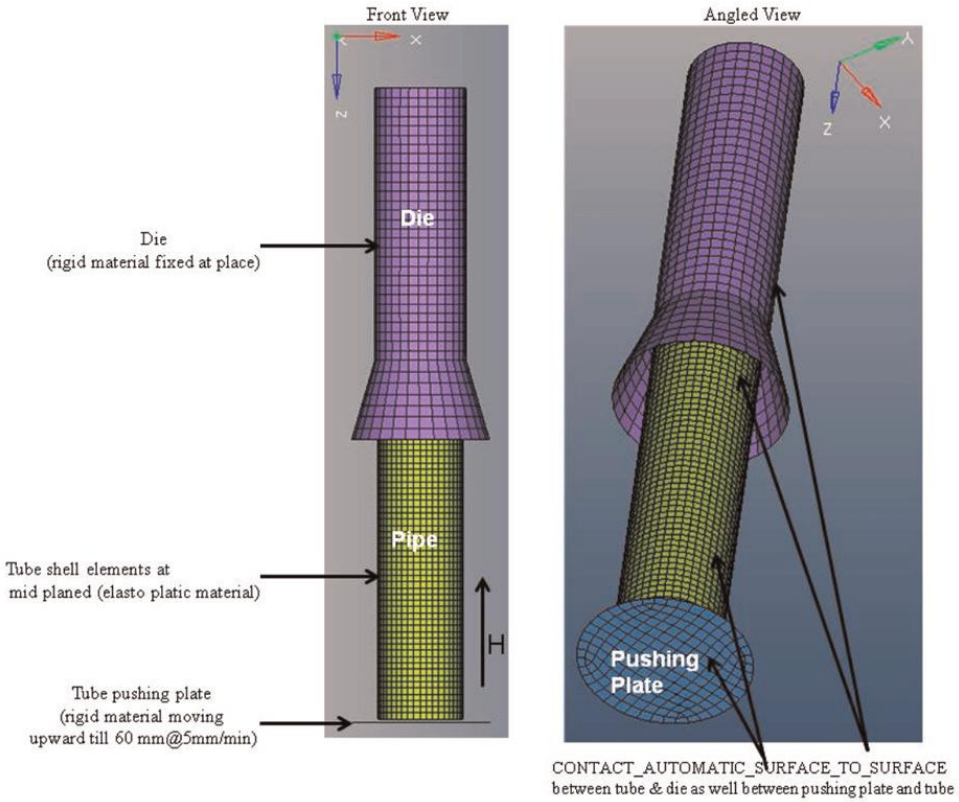

Figure 2.18. Finite element model of the absorber

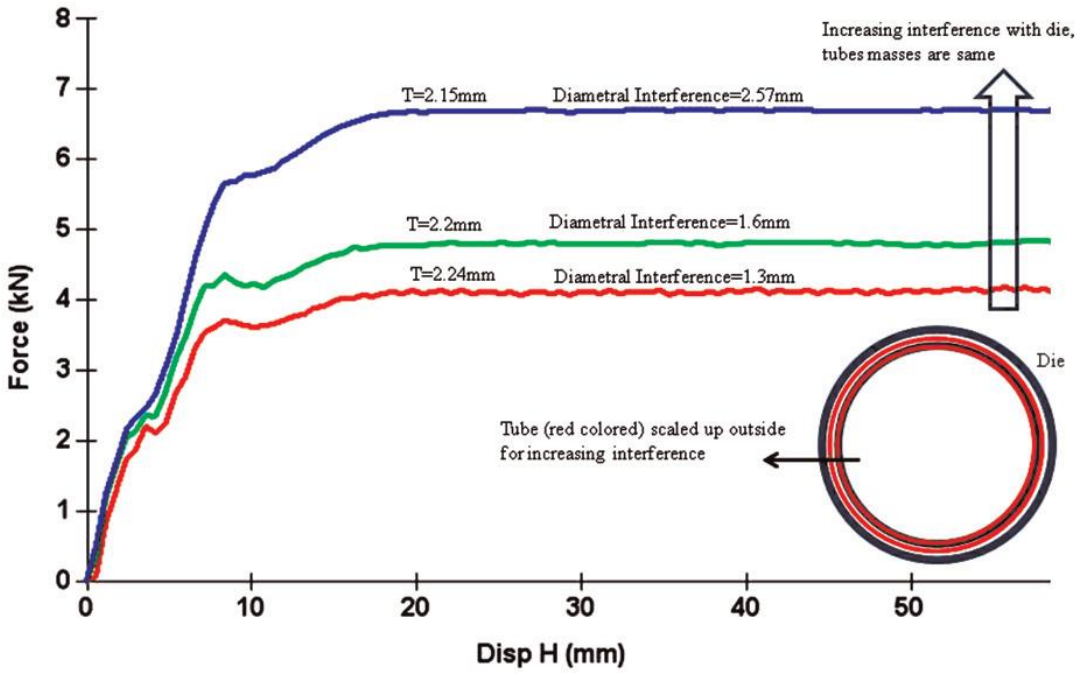

Figure 2.19. Force graph with different deformations for same tube mass and die [27]

3. EXPERIMENTS AND ANALYSES

3.1. Energy Absorption Methodology and Test Specimen Manufacturing

3.1.1. Energy Absorber Methodology

In this study fixed load type tube-stud type energy absorber subjected to the design and analysis with respect to the MIL-S-85510 requirements. The energy absorption is performed by deforming hollow tubes radially by two studs as shown in Figure 3.1. The decrease in the diameter of the hollow tube creates a constant loading during the deformation process and causes energy absorption.

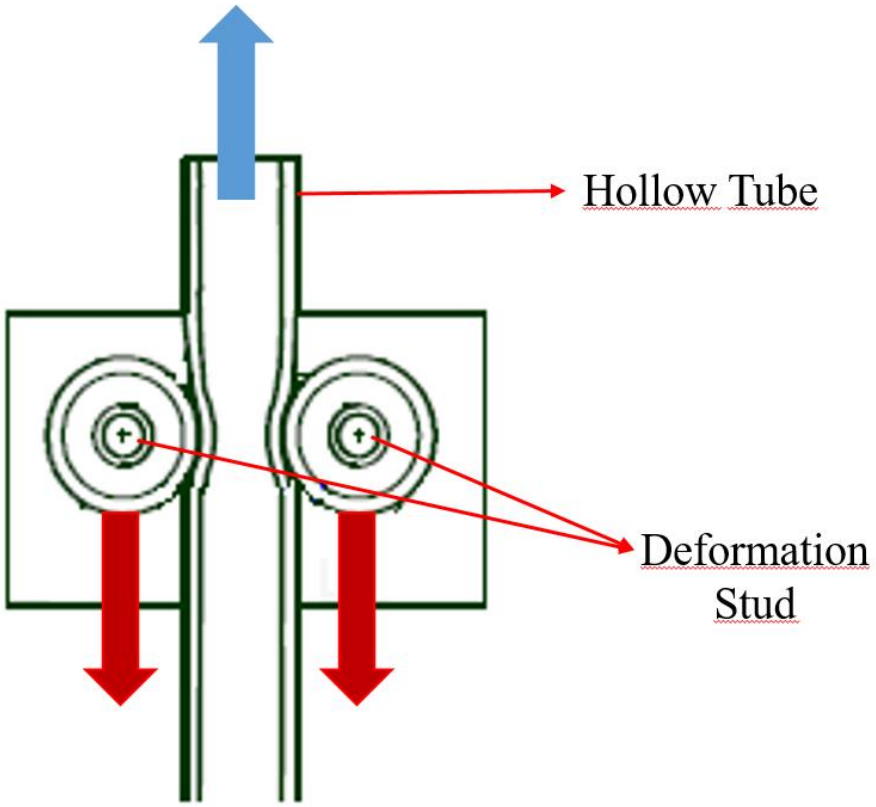

Figure 3.1. Energy absorber concept

The tube-stud type energy absorbers are easy to design and integrate to a troop seat system. Since they do not require occupant adjustment, they reduce the risk and training requirement. Furthermore, this type of energy absorber concepts can be adjusted to civilian platforms considering civilian certification requirements such as CS-29. Since the system starts to stroke at a specific load value by itself, there is no need for a fuse system such as a shear pin. The system components are simple, lightweight and they can be found as commercial off-the-shelf (COTS) items.

In this study, the energy absorber concept is designed by considering different tube diameters, tube materials, tube wall thickness and amount of deformation. Furthermore, the energy absorber system is tested at different rates to evaluate the deformation rate effects on energy absorption.

As mentioned in the previous chapter, for a crashworthy helicopter seat the energy absorber should be optimized for 50th percentile male occupant and should operate at a limit load of 14.5 g. According to the Table IV of MIL-S-85510, the vertical effective weight for a 50th percentile male occupant is 160.7 lbs. Multiplying it with 14.5 g yields a limit load of 2230 lbs which is equal to 10364 N in SI Units. Therefore, each energy absorber should provide a constant load value around 5182 N.

Item	95th percentile wt-lb	50th percentile wt-lb	5th percentile wt-lb
Troop weight	201.9	156.3	126.3
Clothing (less boots)	3.0	3.0	3.0
Boots	4.0	4.0	4.0
Equipment	33.3	33.3	33.3
Total weight	242.2	196.6	166.6
Vertical effective weight clothed	163.9	127.4	103.4
Vertical effective weight equipped	197.2	160.7	136.7

1/ Refer to US Army Natick Research and Development Laboratories Technical Report TR 72-51.

Figure 3.2. Occupant weight tables according to MIL-S-85510 [13]

3.1.2. Design and Manufacturing of Energy Absorber Test Adapter Assembly

Simple tension tests are done in order to check energy absorber concept and evaluate the behaviors of the absorber under different conditions. Therefore, a test adaptor assembly as in Figure 3.3 is designed and manufactured in order to simulate the deformation concept during the tension test. The adapter assembly is also needed to create interface surface between test machine and the samples.

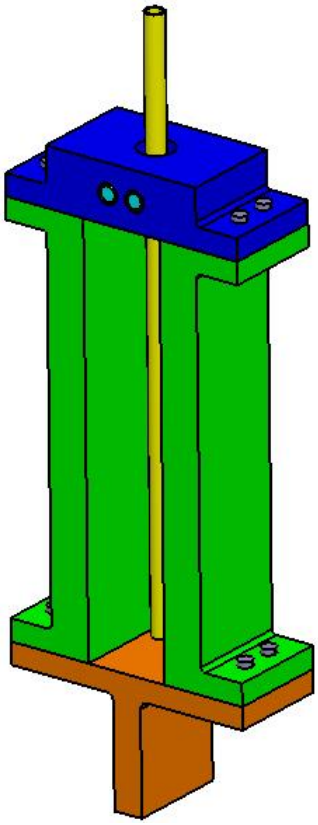

Figure 3.3. Test Adaptor Assembly

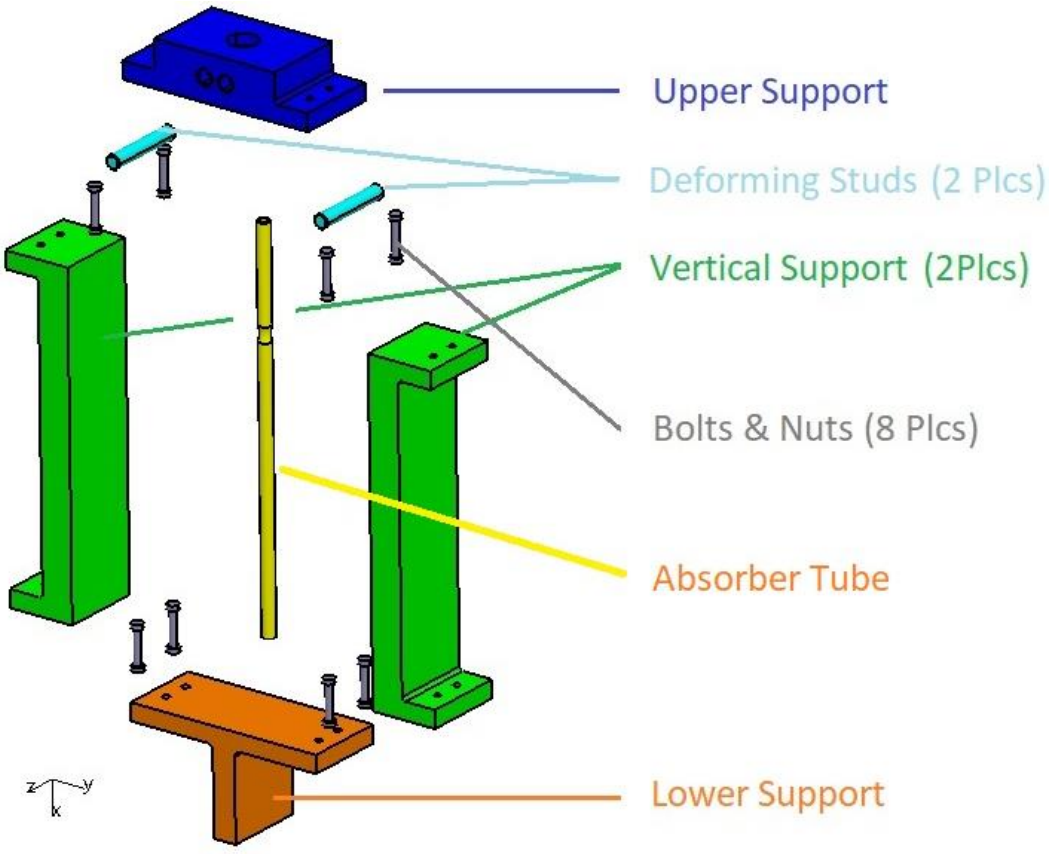

Figure 3.4. Exploded view of test adaptor assembly

The test adapter assembly designed by CATIA V5 3D design software and the detail parts are manufactured at Turkish Aerospace except the deforming studs and absorber tubes. Deforming studs are standard dowel pins of Technifast Company [28] and absorber tubes are selected among commercially available options.

The energy absorber test adapter assembly designed without any weight restriction. Since some of the parts would be used more than once during the tension tests the test adaptor assembly designed as bulky as possible. Dimensional considerations are related to the interface requirements, which are provided by the test center.

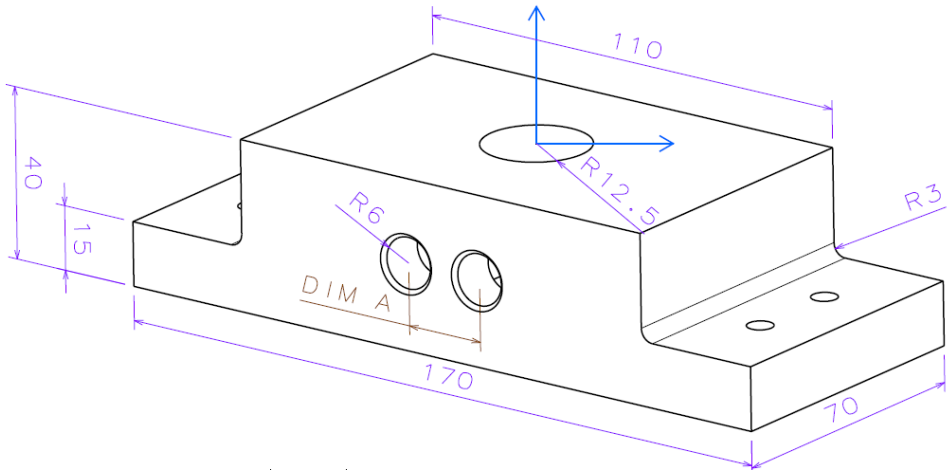

Figure 3.5. Upper support dimensions

Two different upper support part manufactured for different values of DIM A. DIM A is the center-to-center distance between the deforming studs as shown in Figure 3.5. By having different DIM A values during test and analysis energy absorbers at different diameters could be deformed at a different amount which yield different reaction forces. DIM A values are shown in Table 3.1.

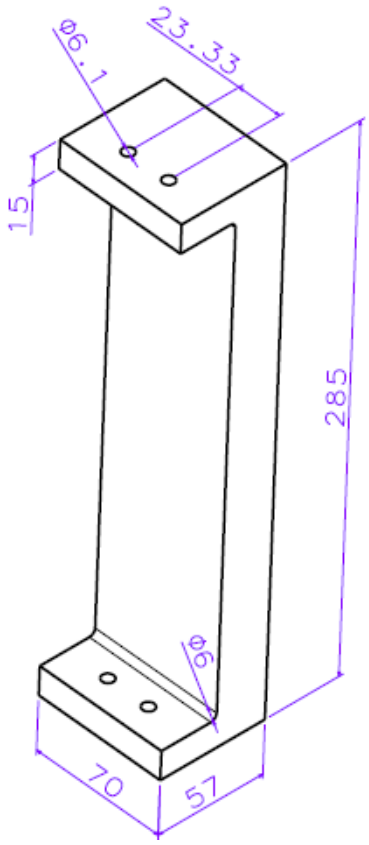

Figure 3.6. Vertical Support Dimensions

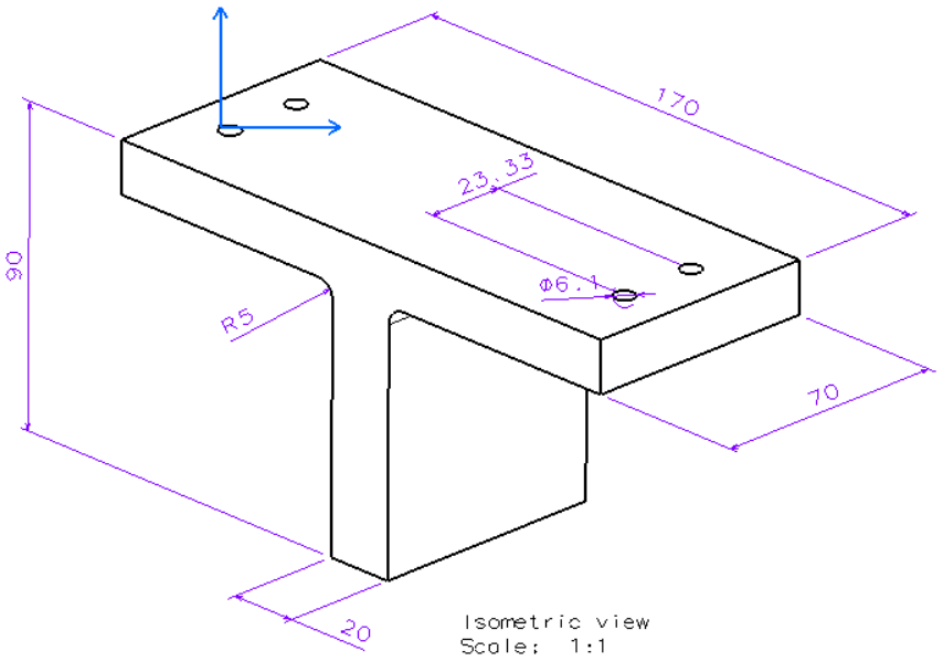

Figure 3.7. Lower Support Dimensions

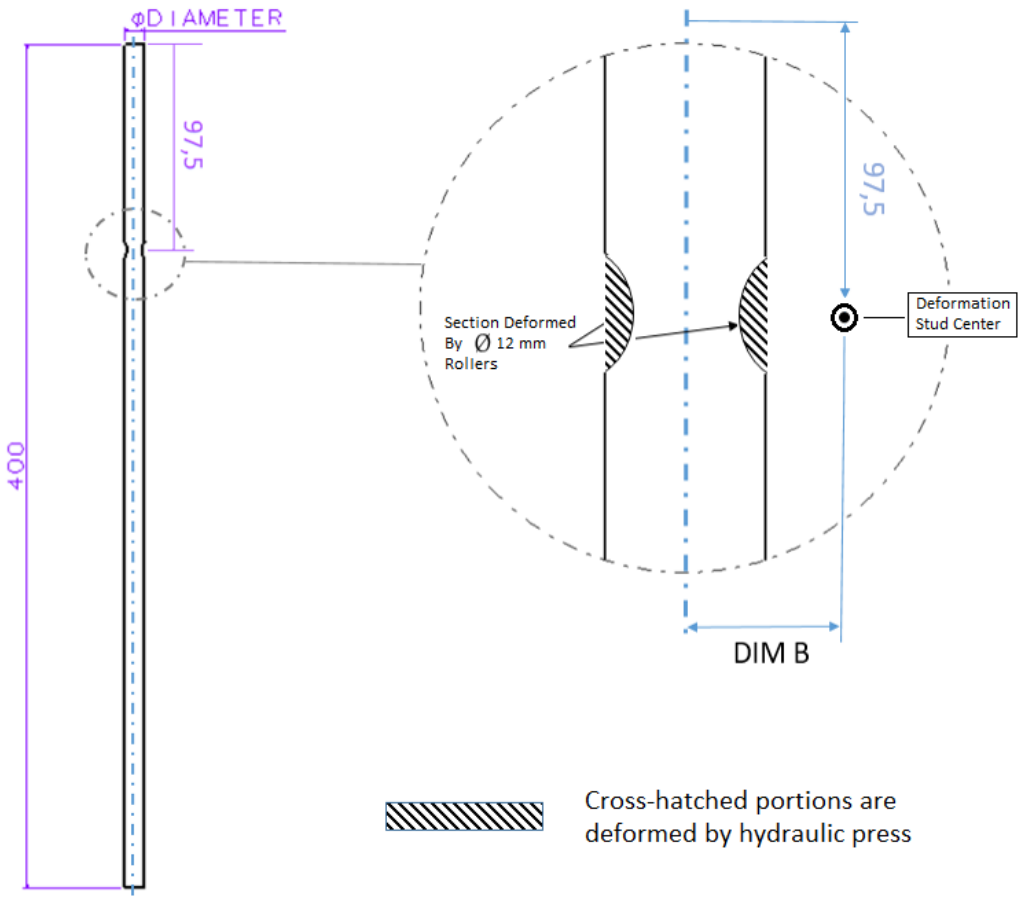

Figure 3.8. Absorber Dimensions

DIM B shown in Figure 3.8 is the distance between the center of the deforming studs and absorber tube centerline. DIM B is the half of the DIM A basically.

Table 3.1. DIM A and DIM B

	Upper Support -1	Upper Support -2
DIM A	19.5 mm	21 mm
DIM B	7.5 mm	9 mm

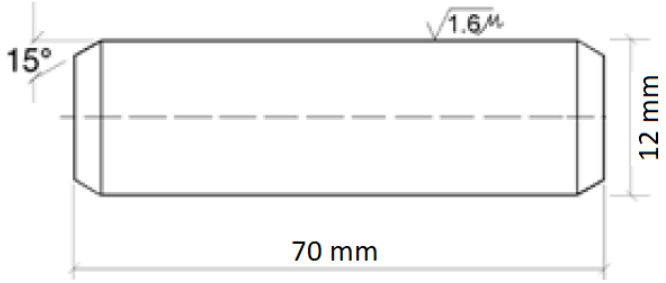

Figure 3.9. Dimensions of deformation stud [28]

3.2. General Considerations about Finite Element Analysis

Finite Element Analysis (FEA) aims to represent real life loadings, boundary conditions, material properties in order to estimate the behavior of a part or assembly under the conditions in real usage. FEA is a critical tool since it is a way of validation of the design rapidly and it decreases the amount of test to be performed and therefore testing costs.

In this study, depending on the loading rate two types of analyses are performed which are named “quasi-static” and “dynamic” FEA. For Quasi-static analysis strain rates are close to zero, generally around 10^{-4}/s to 10^{-2}/s [29]. In order to check the behavior of the energy absorber only and to correlate the tension test results with the analysis, dynamic approach is considered at low strain rates. However, in real crash scenarios loading rates range in between 10^{-2}/s to 10^{2}/s. Therefore, troop seat crash analysis performed by considering dynamic explicit approach.

Considering the solution methods of the system of equations there are two approaches named as “implicit” and “explicit”. Nonlinear equation sets must be solved at each time increment. Therefore, implicit solvers provide stable results for the solution of the nonlinear set of equations but they require many computational resources. The explicit procedure is inexpensive compared to the implicit methods since there is no solution for a set of simultaneous equations with respect to time. However, error may propagate rapidly due to error accumulation [30].

In this thesis study ABAQUS® 6.14 Workbench is used as FEA tool since it is widely used in aerospace and automotive industries. ABAQUS® /Explicit sub tools are used for the analyses. ABAQUS®/Explicit is efficient for dynamic analysis of complex assemblies containing interactions since it can handle complex interaction problems by a simple contact definition [30].

The personal computer used in that study that has Intel İ7-7700HQ CPU @2.80 Ghz, 8 cores, 16 GB RAM, NVIDIA GeForce GTX 1050Ti. FEA analysis times could change if computer configurations change.

In order to obtain reasonable results during Finite Element Analysis the input data should be implemented correctly into the FEA tool. Preparation of geometries, mesh types, assembly module, step module, definition of the interactions, boundary conditions and material properties play an important role in FEA. After importing the

3D model of the detail parts, modelling of the analysis performed in ABAQUS®. Modeling steps are defined as,

- Material definitions such as densities, young modulus, yield stress values, stress-strain diagrams for plastic behaviors and Poisson's ratios
- Meshing of detail parts which consists of selection of mesh element types, mesh sizes
- Step module definition which means analysis time definition, mass scaling definition
- Output module definitions
- Constraints definitions
- Interaction definitions
- Boundary conditions and initial condition definitions

During the analysis, ABAQUS® users should pay attention to use consistent units. In this study, units are considered as in Table 3.2.

Table 3.2. ABAQUS® input units

Measure	**Unit**
Time	s
Length	mm
Velocity	mm/s
Acceleration	mm/s^2
Weight	tonne
Energy	N.mm
Stress	Mpa

3.3. Finite Element Analysis of Energy Absorber and Test Apparatus

CATIA V5 3D design tool is used to design the absorber test setup assembly and detail parts and the geometry imported to ABAQUS® as step file. Whole detail parts except absorber tube are considered as 3D deformable bodies. Mesh element size of the absorber tube is small compared to the other parts. Therefore, the absorber tube modeled as shell element in order not to increase the computation time too much. Furthermore, since thickness and diameter of the samples varies it becomes easy to implement these changes for shell element by only changing shell thickness and diameter.

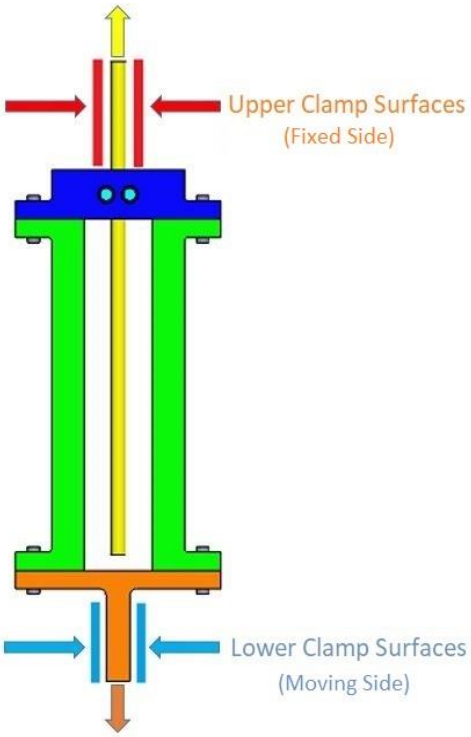

Figure 3.10. Absorber adapter assembly and test machine interface

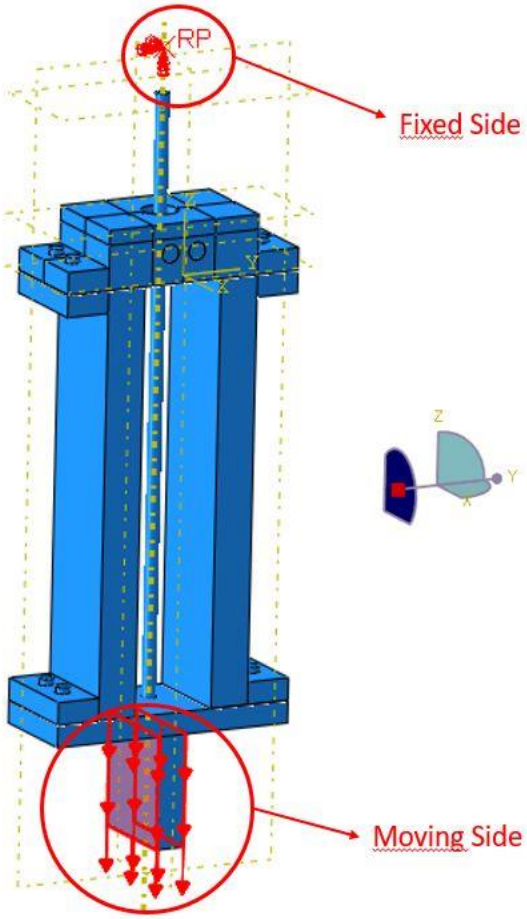

Figure 3.11. Absorber test adapter assembly analysis model

3.3.1. Geometry Preparation

The 3D design of the detailed parts and assembly procedures made in CATIA V5 are starting points for the analysis and manufacturing. The CAD part that is designed in CATIA V5 must be the same with the part to be manufactured in every detail. However, for FEA, the geometry of the part must be modified in order to reduce the time of computation, time of modelling and meshing. In addition, modification of the real part could decrease the errors obtained during FEA. Eliminating fillets and radii could simplify the FEA model and decrease the overall computation and modelling time. The part that is used for manufacturing and part that is simplified for analysis are exemplified in Figure 3.12.

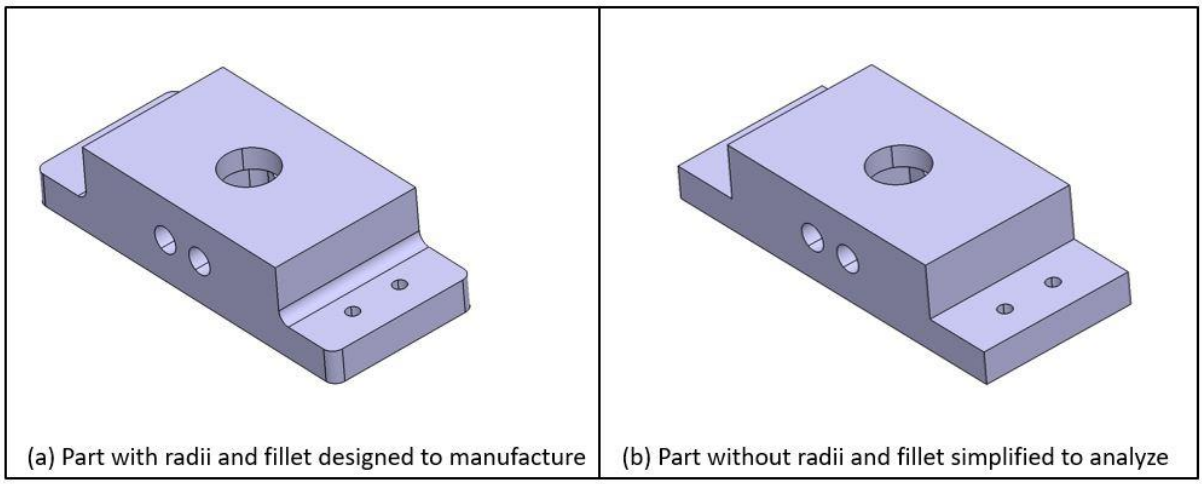

Figure 3.12. Comparison of geometries for manufacturing and analysis

Fasteners used in test adaptor assembly are bolts, washers and nuts. These fasteners are also simplified during the analyses as indicated in Figure 3.13. Threads of bolts and nuts are not modelled. They are modeled as cylindrical single parts carrying tension loads. The only evaluation related to the bolts are to check if they fail during the tension test or not beforehand. Detailed structural behaviors of bolts are not in the scope of this study.

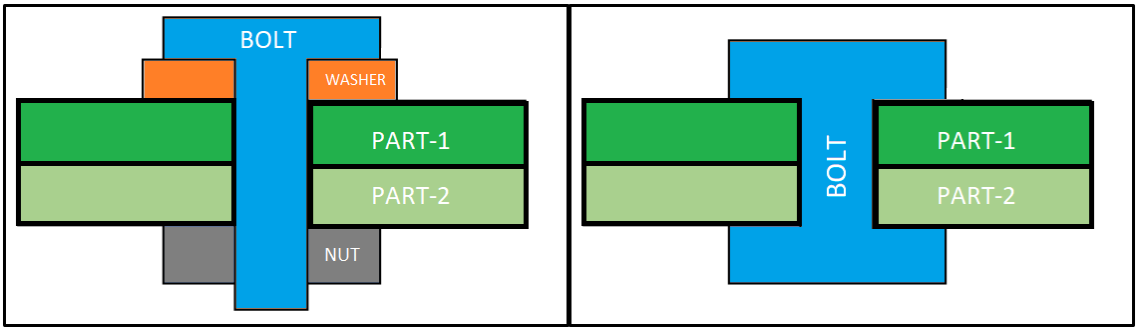

Figure 3.13. Bolt simplification

3.3.2. Material Properties

The materials used in the test setup assembly are either steel alloy or aluminum alloy. Selection of the materials are based on not only mechanical properties but also availabilities of the materials. Especially test setup assembly detail parts are manufactured from scrap material to decrease the manufacturing cost.

All detail parts of the test setup assembly except deformation studs are selected as Al 7075 T651 since they are available as scrap material and their mechanical properties are superior. Al 7075 type aluminum alloy is the strongest among the aluminum alloys and light in weight. Also, during manufacturing Al 7075 material provides high crack resistance and has low micro surface cracks due to machining process. Therefore, Al 7075 selected for test adaptor assembly detail parts.

Fasteners used in the test adaptor assembly are bolts and nuts made of 8.8 Grade Steel which are highly available in the market. Metric 6 bolts and nuts are used in the assembly.

The deformation studs are selected as from AISI 303 stainless steel dowel pins of Technifast Company [28] since they are available in the market.

For all materials strain rate effects are neglected for both quasi-static and dynamic crash analysis. Some important properties that are created from existing references [31] are tabulated in Table 3.3.

Table 3.3. Mechanical properties of materials used during analyses

Material	Al 7075-T651	AISI 303 Stainless Steel	8.8 Grade Steel
Density [kg/m^3]	2810	8000	7850
Poisson's Ratio [m/m]	0,33	0,25	0,29
Modulus of Elasticity [GPa]	71,7	193	200
True Yield Strength [MPa]	462	240	543,9
True Ultimate Tensile Strength [MPa]	572	620	800
Elongation at Failure [%]	10	50	12

The first aspect of an energy absorber material is collapsing due to impact in order to absorb the crash energy as much as possible. Second aspect of the material is providing structural integrity during crash. Features such as the ultimate strength, yield strength, and percentage of the elongation at failure point become critical for energy absorbers. Therefore, aluminum and steel materials become candidates for energy absorption. However, for aerospace applications weight and easiness of manufacturability are other critical parameters to consider. Therefore, aluminum materials, which have superior weights and manufacturability, are generally used in energy absorber. Aluminum alloys with series 2024 are selected since they are highly used in aerospace applications and the absorber tubes could be found commercially. In addition, the material data of 2024 series aluminum, which is given in Table 3.4 is well known and available on the literature [31].

Table 3.4. Absorber tube material properties [31]

Material	Al 2024-T3
Density [kg/m^3]	2780
Poisson's Ratio [m/m]	0,33
Modulus of Elasticity [GPa]	71,7
True Yield Strength [MPa]	290
True Ultimate Tensile Strength [MPa]	483
Elongation at Failure [%]	11

3.3.3. Mesh Definition and Mesh Size Refinement

Depending on the type of mesh and element size used during analysis the result may be obtained properly or analysis could yield inappropriate results. Therefore, meshing has a vital role in analysis.

In FEA, aim of meshing is to divide the model into smaller elements where the equation sets are solved with respect to the geometry. If these elements are made too small, solution will approximate the true solution. However, it is critical to find an appropriate element size which gives proper results because as the element size are made smaller and smaller, the computation time increases significantly.

The selection of mesh element is also vital for the accuracy of the analysis. The elements employed for the analysis are linear, hexahedral elements of type C3D8R and quadratic, hexahedral elements of type C3D20R. Both elements have three degrees of freedom [32]. For ABAQUS® element coding explained in Figure 3.14.

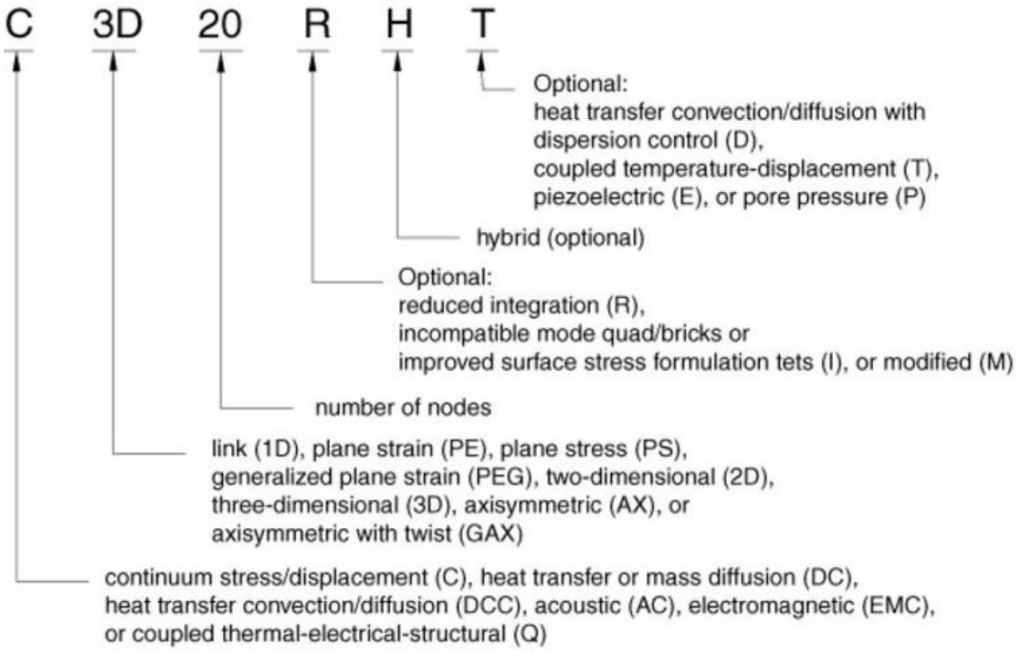

Figure 3.14. Finite Elements Coding Rules in ABAQUS® [32]

For dynamic explicit analysis C3D20R type of element are not supported by ABAQUS®/Explicit. Therefore, C3D8R type elements are selected for whole parts in this study. C3D8R coding refers to;

- Continuum element;
- Three-dimensional element;
- Eight nodes;
- Reduced integration.

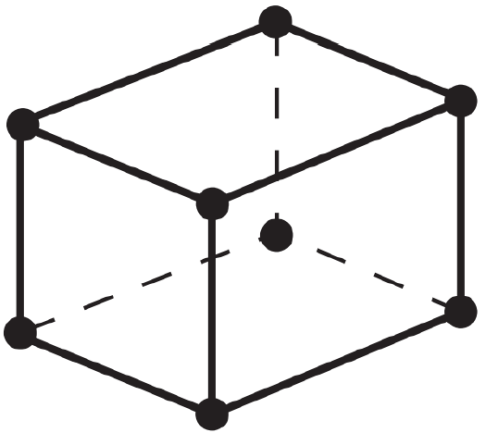

Figure 3.15. General C3D8R type element

Overall meshing of the energy absorber test assembly and meshed views of the detail parts are provided in Figure 3.16 to Figure 3.21 below.

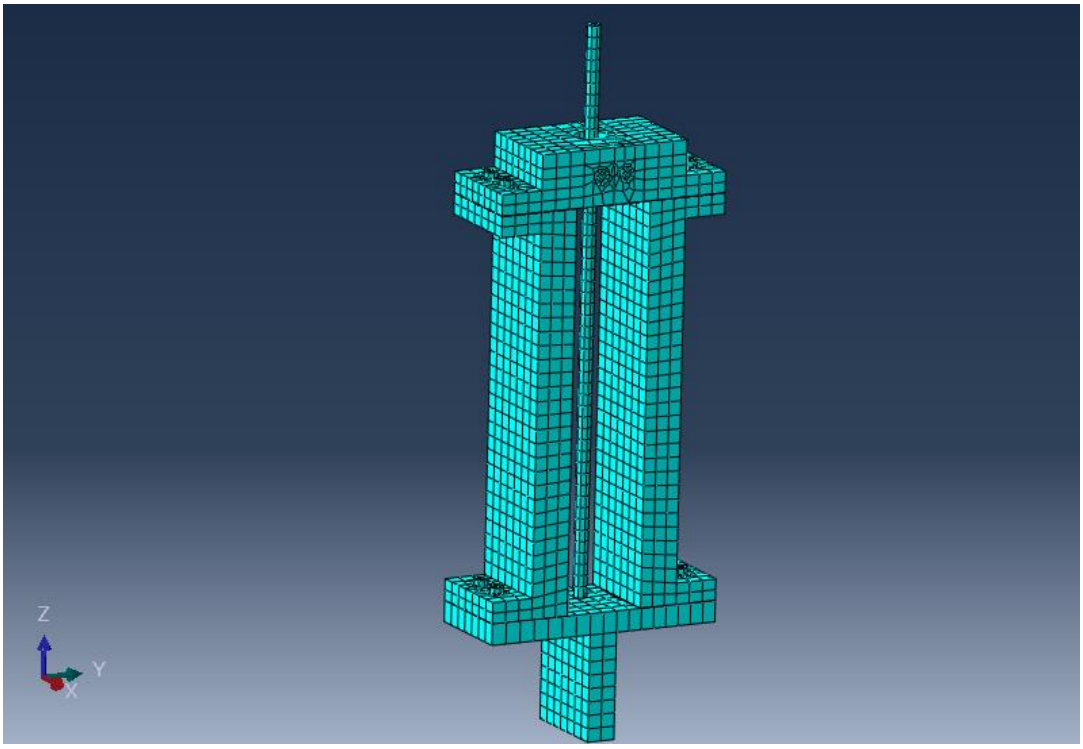

Figure 3.16. Energy absorber test adapter assembly meshing

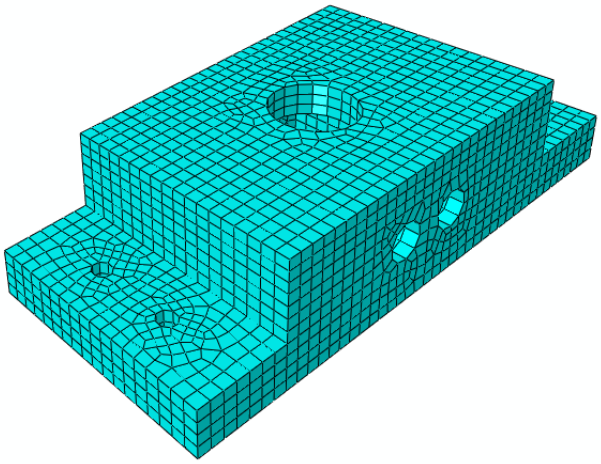

Figure 3.17. Upper support example meshing

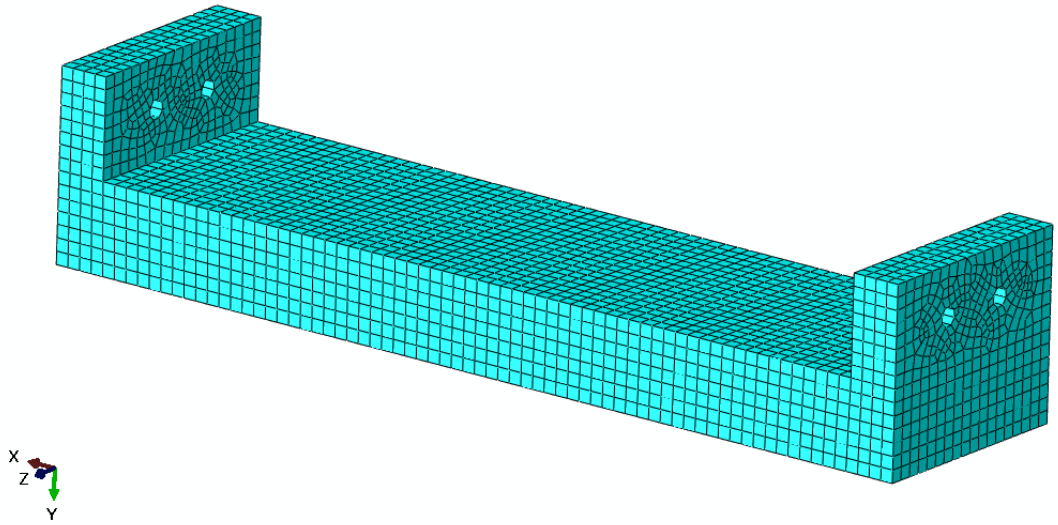

Figure 3.18. Vertical support example meshing

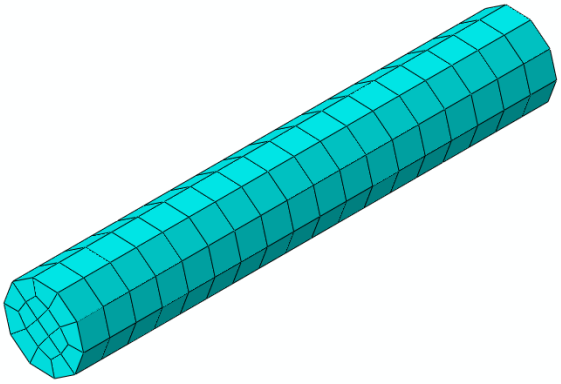

Figure 3.19. Deformation stud example meshing

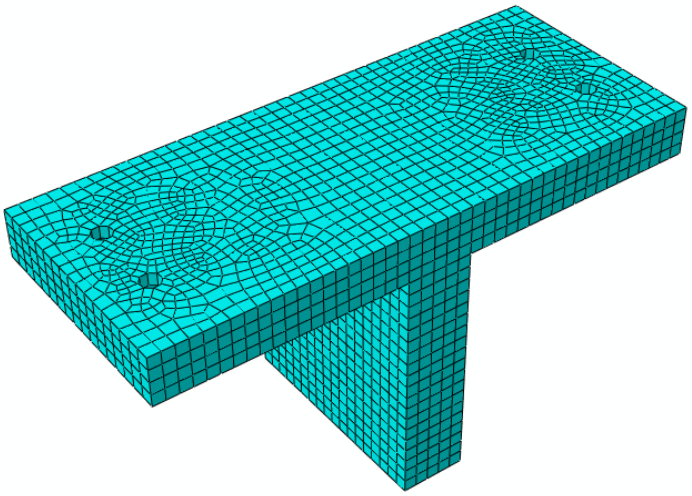

Figure 3.20. Lower support example meshing

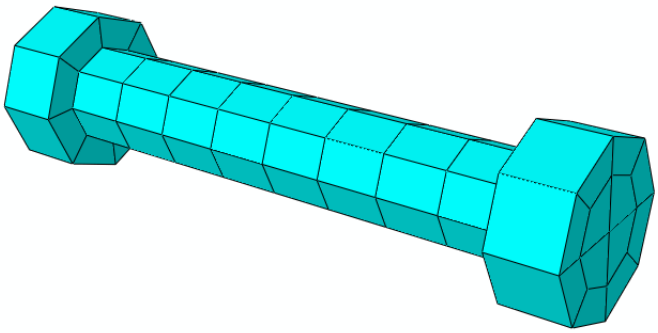

Figure 3.21. M6 bolt example meshing

In order to perform mesh refinement, the analysis performed with different element sizes. Initially only the element size of the absorber and deformation stud is changed between 1 mm to 4 mm while other parts element sizes are kept constant at 4 mm as indicated in Table 3.5. Local meshing is applied to the absorber deformed section as indicated in Figure 3.22, because initial interaction of the absorber and the deformation studs appears in this section. As an initial guess, the local mesh size is selected as 0.5 mm which gives minimum 2 elements along the thickness. According to this evaluation maximum element size which does not affect reaction force results is selected for absorber meshing. The reaction force results are evaluated for each element sizes whether solution converges or not.

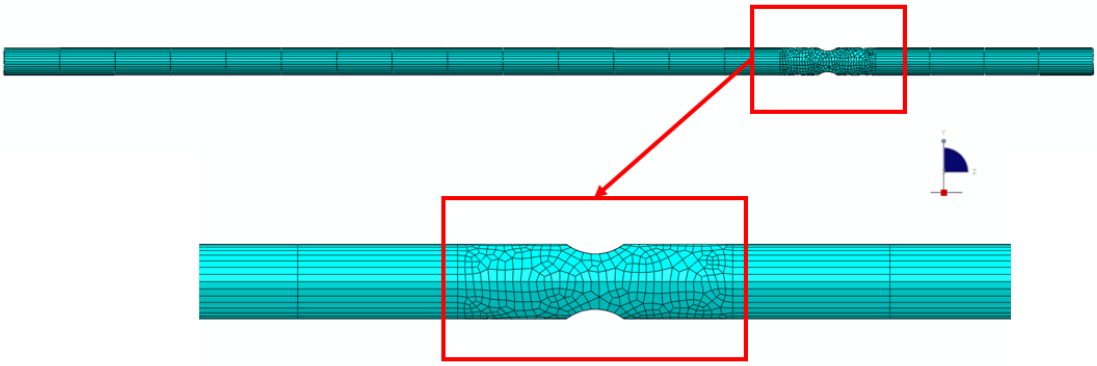

Figure 3.22. Local meshing location on absorber

Table 3.5. Mesh element size evaluation for absorber

	Global Mesh Size for Absorber and Deformation Stud [mm]	Global Mesh Size for Rest of the Assembly [mm]	Local Mesh Size [mm]
Trial 1	1	4	0.5
Trial 2	2	4	0.5
Trial 3	4	4	0.5
Trial 4	6	4	0.5

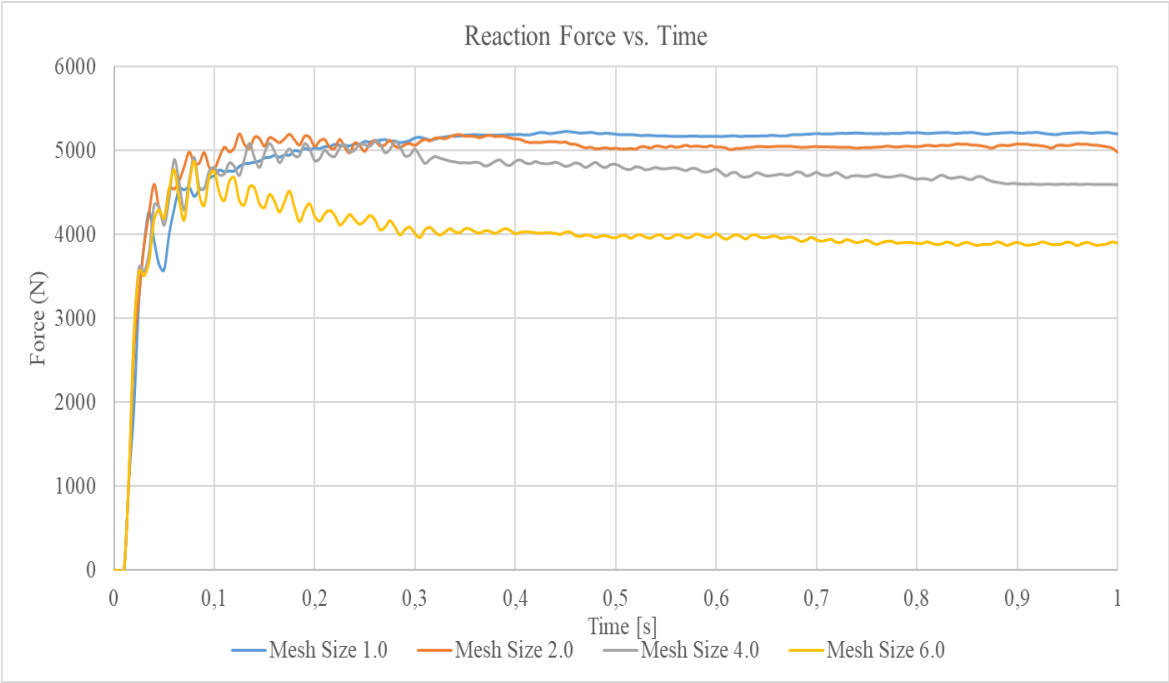

Figure 3.23. Filtered Reaction force vs time graphs for different mesh sizes

As seen on Figure 3.23 as element size gets smaller reaction force approximates to 5.2 kN for plateau region of the reaction force-time graphs. Considering 5.2 kN as exact value, analysis results of 2 mm approximates it within 10%. Therefore, in the first part

of the mesh optimization study for energy absorber and deformation studs, the optimum value for mesh size of the absorber tube and deformation stud is selected as 2.0 mm. Local mesh size on the absorber is also selected as 0.5 mm.

The energy absorber element size, which is selected in the first part of the mesh optimization, is used as the mesh size of the absorber during optimization of the mesh size of the rest of the assembly. In the second part, while the element size of the absorber kept constant, the element sizes of the other parts changed between 2 mm to 6 mm as indicated in Table 3.6. The reaction force results are evaluated for each element sizes whether solution converges or not.

Table 3.6. Mesh element size evaluation for whole model except energy absorber

	Global Mesh Size for Assembly [mm]	Global Mesh Size for Absorber and Deformation Stud [mm]	Local Mesh Size for Absorber [mm]
Trial 1	2	2	0.5
Trial 2	4	2	0.5
Trial 3	6	2	0.5

During mesh optimization of the other parts of the absorber test adapter assembly the mesh sizes are taken as in Table 3.6. Evaluating the reaction force results given in Figure 3.24, it is concluded that as the element size gets smaller the reaction forces converges to a specific value. As a result of the mesh optimization study of the second part, energy absorber test adapter parts mesh sizes are selected as 4 mm.

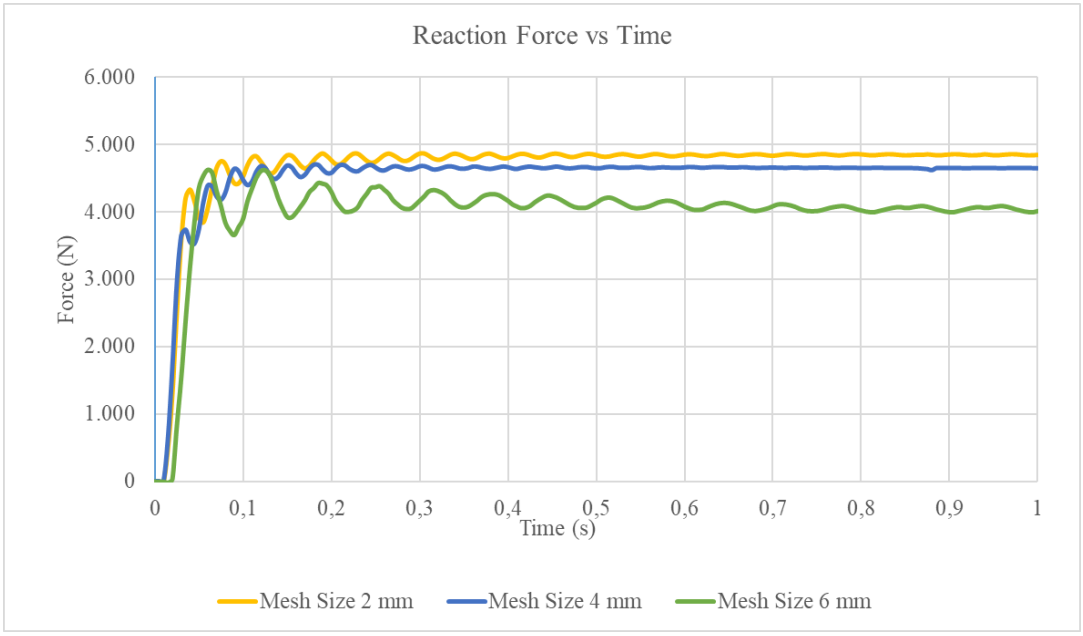

Figure 3.24. Force results for different mesh size of the test adapter assembly

3.3.4. Load and Boundary Conditions

In order to simulate the real testing scenarios, one side of the energy absorber test adapter held fixed and the other side is displaced along the real loading direction. While simulating the test scenario, a reference point (RP) is created in the space and absorber end surface is linked to this point via Multi Point Constraint (MPC) of ABAQUS®. On the RP encastre type boundary condition is applied. Beam type MPC constraint is defined between the end surface of the absorber and the RP because MPC beam provides a rigid connection between two points to limit the rotation and displacement of the first node to the rotation and displacement of the second node. In this way, the reaction forces generated on absorber along z direction are easily obtained during the analysis through RP.

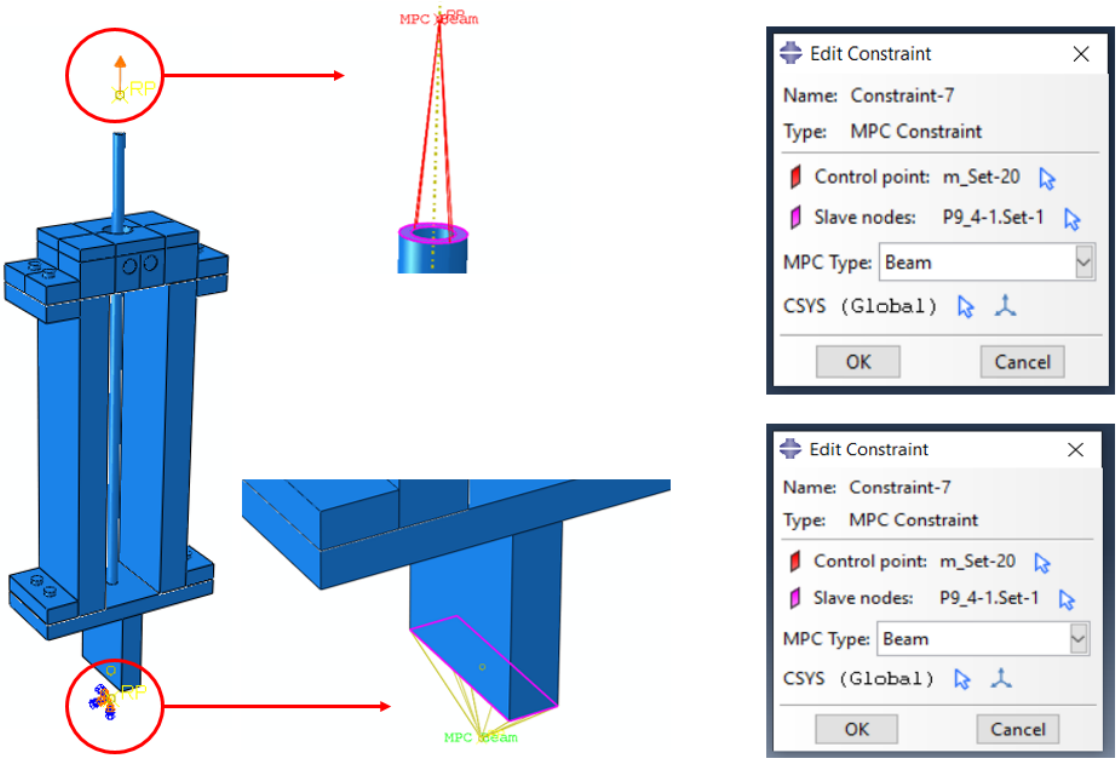

Figure 3.25. Boundary condition and constraint definition

The lower section of the energy absorber test adapter part is displaced 350 mm along z axis to simulate the test setup stroke.

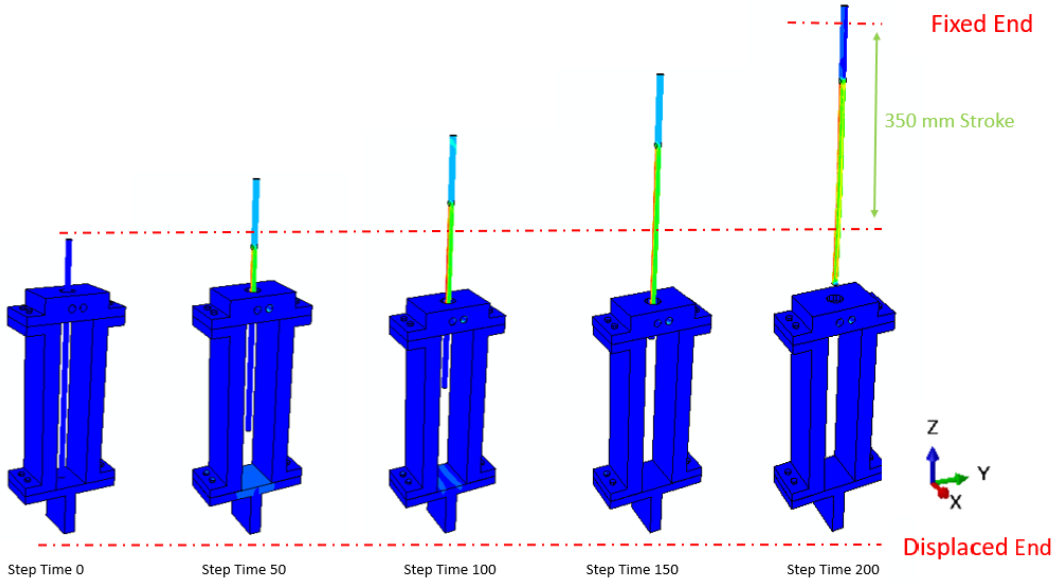

Figure 3.26. Test setup stroking

3.3.5. Analysis of Energy Absorber Assembly and Force Results

In this study except mesh optimization section, 18 samples are analyzed and 8 of the samples are tested in order to perform test and analysis correlation activities. These samples are numbered at Table 3.7 and test items are highlighted in green.

Table 3.7. Test and analysis matrix to be performed

Absorber Diameter		**9.525 mm**			**11.11 mm**			**12.7 mm**		
Wall Thickness		0.028	0.049	0.065	0.028	0.049	0.065	0.028	0.049	0.065
Deformed to	**7.5 mm**	1	2	3	4	5	6	7	8	9
	9.0 mm	10	11	12	13	14	15	16	17	18

Absorber Diameter		**9.525 mm**		
Wall Thickness		0.028	0.049	0.065
Deformed to	**7.5 mm**	1	2	3
	9.0 mm	10	11	12

Samples are extruded tubular materials, which are available as COTS item and highly used in aerospace applications. In this study, tubes with outer diameters (OD) of 9.525 mm, 11.11 mm and 12.7 mm, which are made of Al2024-T3 material are considered.

Samples are initially deformed to 7.5 mm, which yield a decrease in diameter around 2 mm. Secondly, by using a different upper support part samples are deformed to 9.0 mm which yield a decrease in diameter around 0.5 mm. In this way, it is aimed to evaluate the effect of deformation amount on reaction forces. In addition, effect of wall thickness

on reaction force could be evaluated by testing samples that have different wall thickness values.

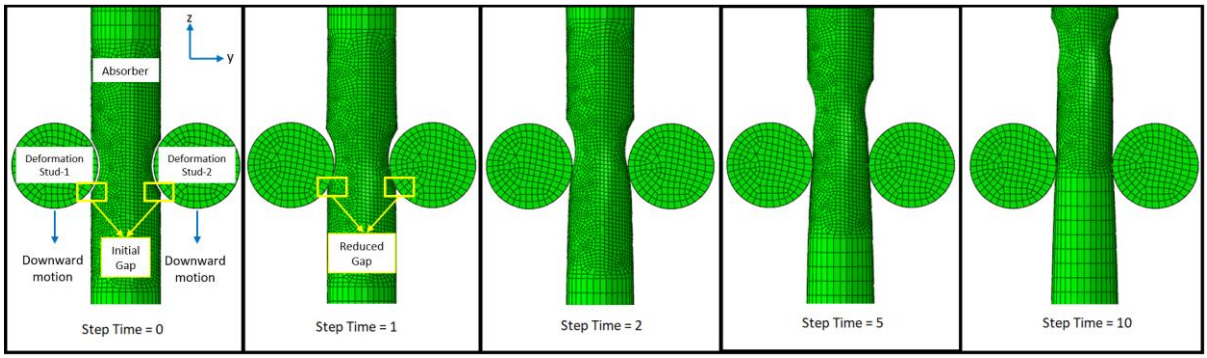

Figure 3.27. Detailed view of energy absorber deformations at various time steps

Figure 3.27 shows how an absorber tube is deformed by deformations studs during energy absorption stroke. At the initial step of the analysis, there is a very small gap between deformation studs and undeformed energy absorber tube. As top part and deformation studs move downward initial contact is performed between tube and deformation studs. After step time=2 deformation studs deform energy absorber tube in a way that diameter of the tube is decreased at a constant force level.

Analysis results for the tubes with 9.525 mm OD which are deformed to 7.5 mm and 9.0 mm are given by Figure 3.28.

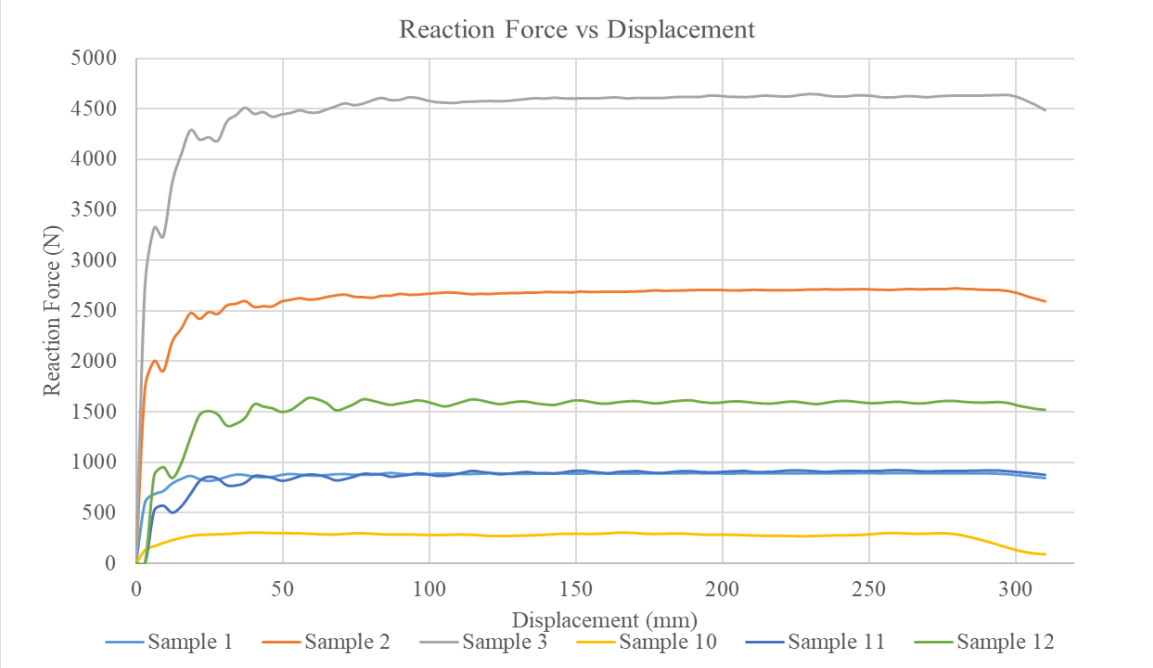

Figure 3.28. Force results for tubes 9.525 mm OD (Samples [1-3] and [10-12])

Analysis results for the tubes with 11.11 mm OD which are deformed to 7.5 mm and 9.0 mm are given by Figure 3.29.

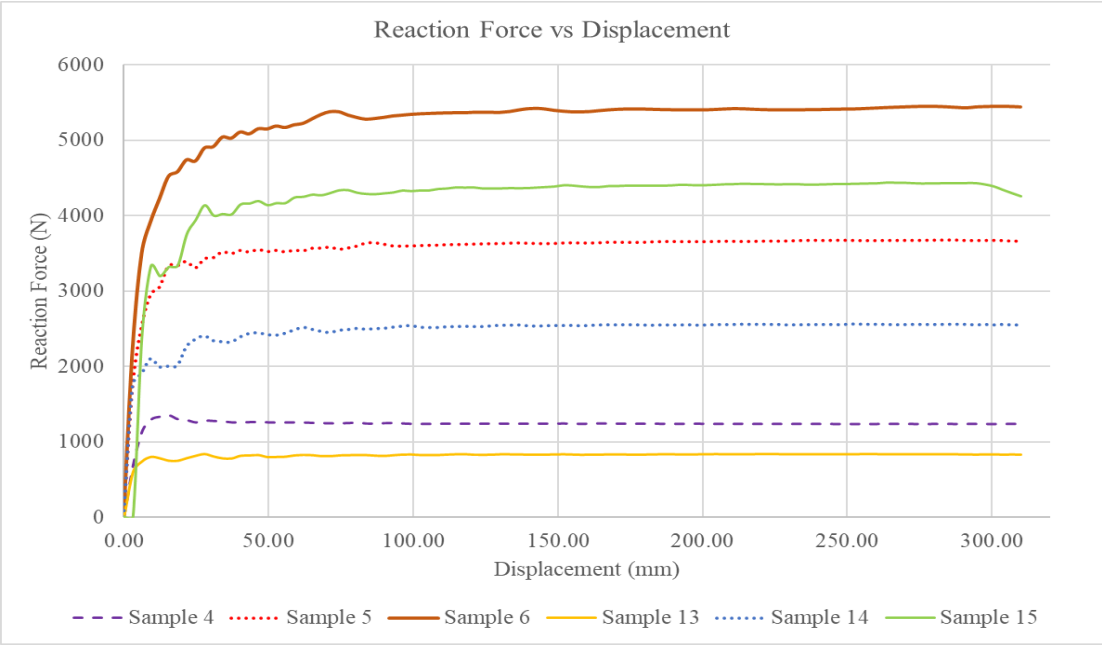

Figure 3.29. Force results for tubes 11.11 mm OD (Samples [4-6] and [13-15])

Analysis results for the tubes with 12.7 mm OD which are deformed to 7.5 mm and 9.0 mm are given by Figure 3.30.

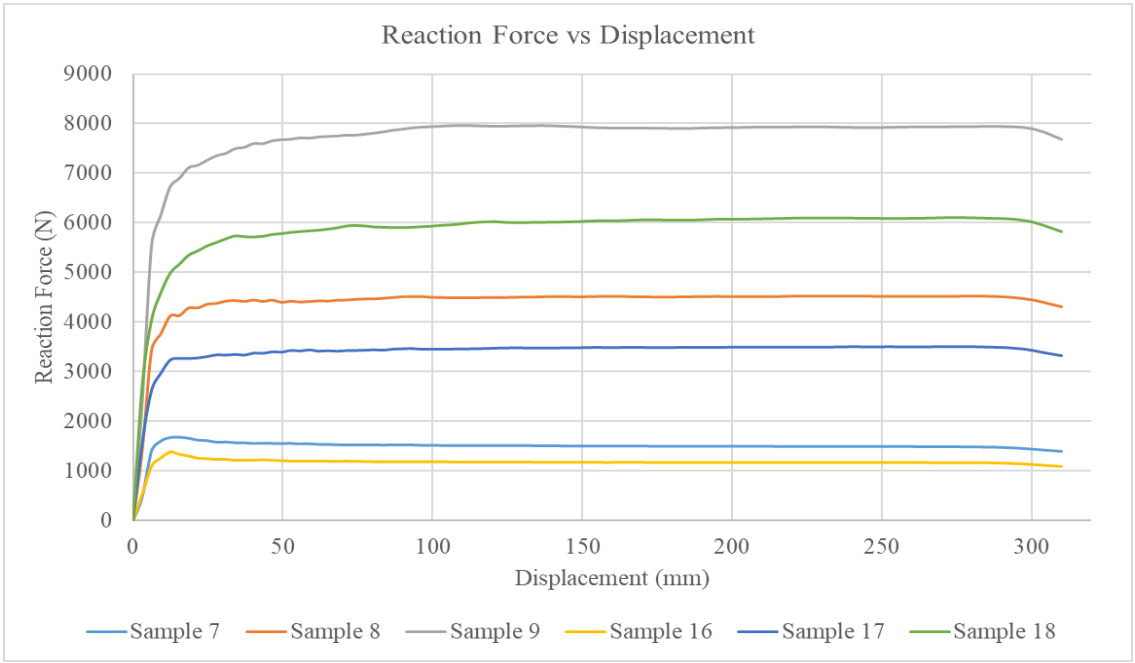

Figure 3.30. Force results for tubes 12.7 mm OD (Samples [7-9] and [15-18])

3.3.6. Energy Absorber Assembly Test Results and Analysis Correlation

The current study focused on correlation of low-speed force and displacement results of test and analysis, which are performed at 50 mm/min where quasi-static analysis is applicable [33,34]. Therefore, experiments are performed in quasi-static loading. Before the experiment test adaptor is placed between lower and upper clamps of Zwick Roell Z250 material testing machine as in Figure 3.32. The displacement control testing is performed via movable lower clamp of the testing machine while upper clamp kept fixed.

Figure 3.31. Testing Machine Zwick Roell Z250

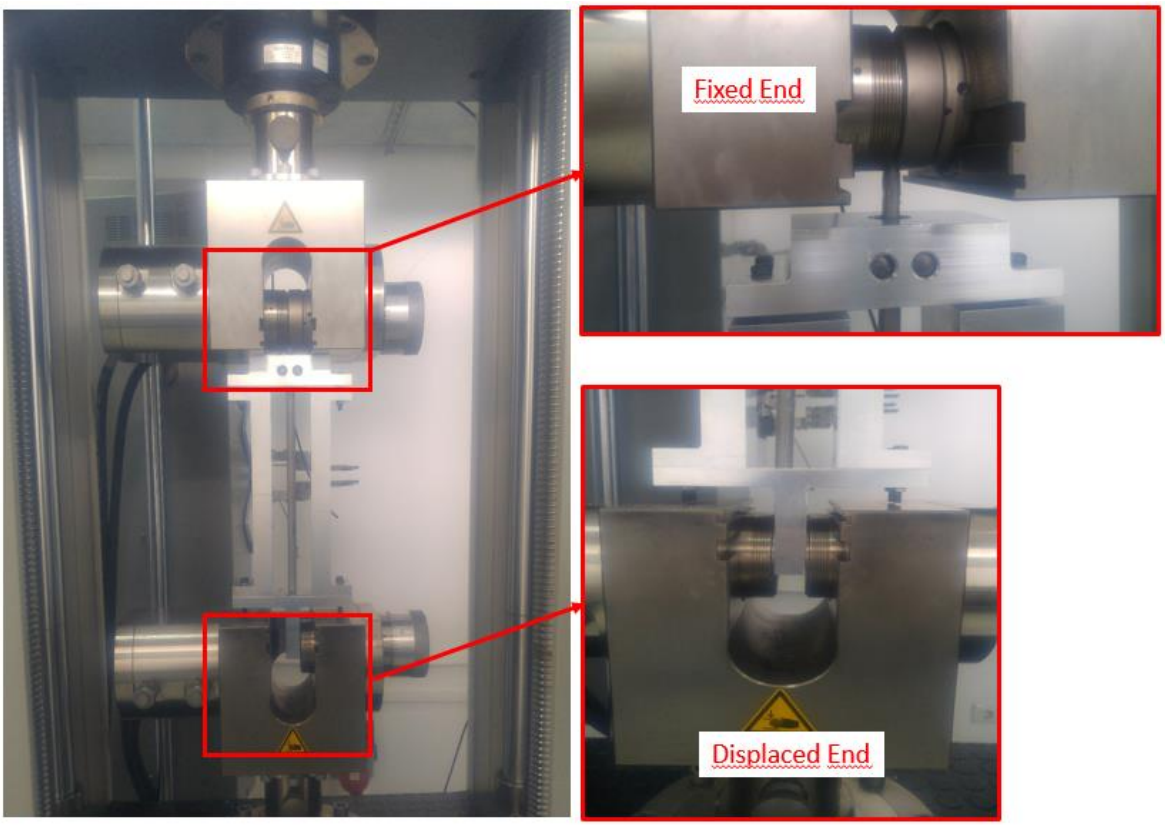

Figure 3.32. Test adapter assembly installed to tensile testing machine

Displacement controlled testing is performed for each sample highlighted at Table 3.8 and reaction force-displacement curves are obtained along vertical axis.

Table 3.8. Absorber samples

Absorber Diameter		**9.525 mm**			**11.11 mm**			**12.7 mm**		
Wall Thickness		0.028	0.049	0.065	0.028	0.049	0.065	0.028	0.049	0.065
Deformed to	**7.5 mm**	1	2	3	4	5	6	7	8	9
	9.0 mm	10	11	12	13	14	15	16	17	18

Initially Samples 1,4,5,6 and 7 are tested by using Upper Support-1, which decreases absorbers' diameters to 7.5 mm. Secondly Samples 10,13 and 16 are tested by using Upper Support-2, which decreases absorbers' diameters to 9.0 mm. Related force-displacement curves for these samples that are obtained from test and analysis are provided in below figures.

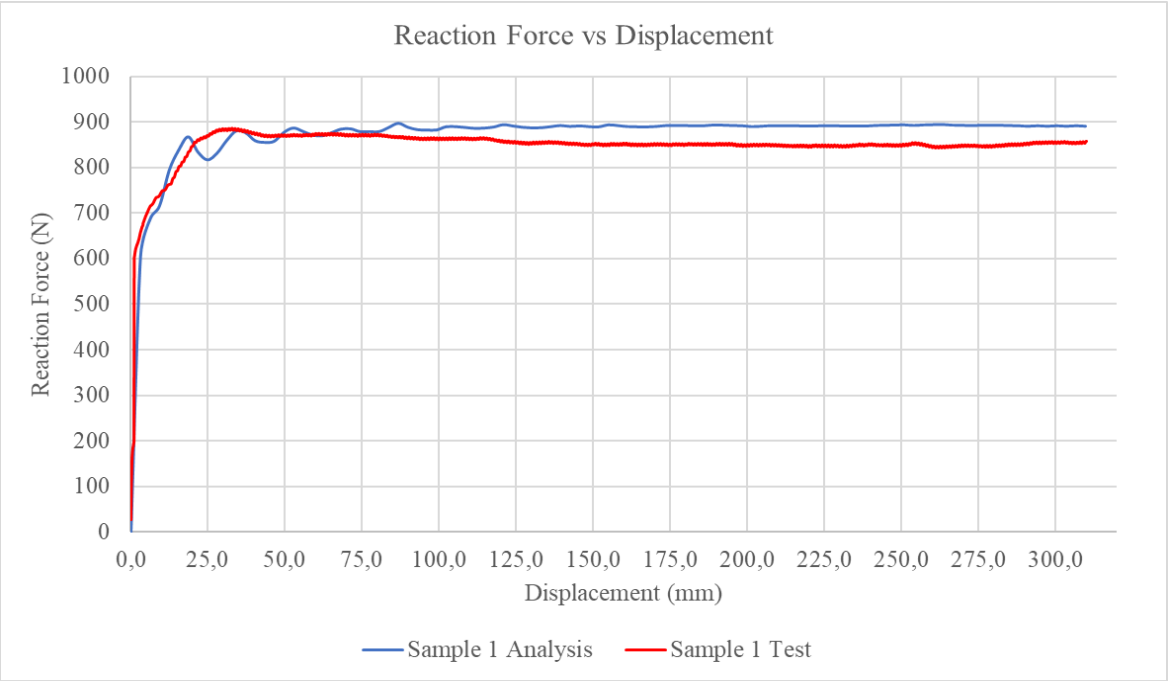

Figure 3.33. Reaction force results for Sample 1

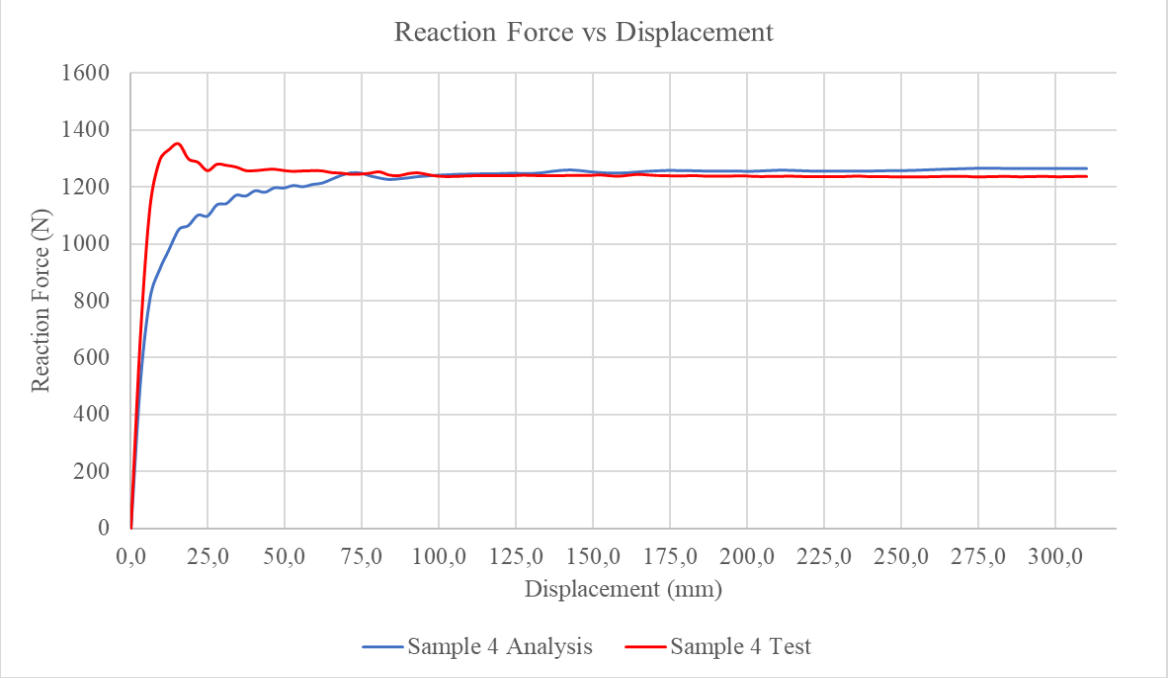

Figure 3.34. Reaction force results for Sample 4

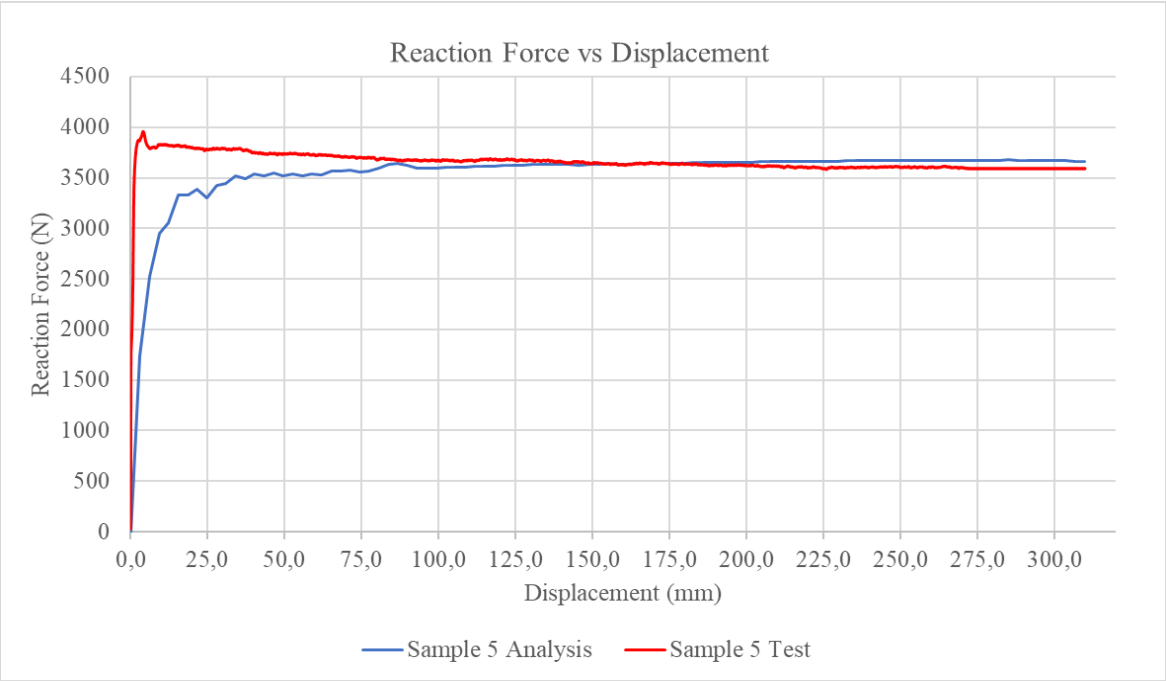

Figure 3.35. Reaction force results for Sample 5

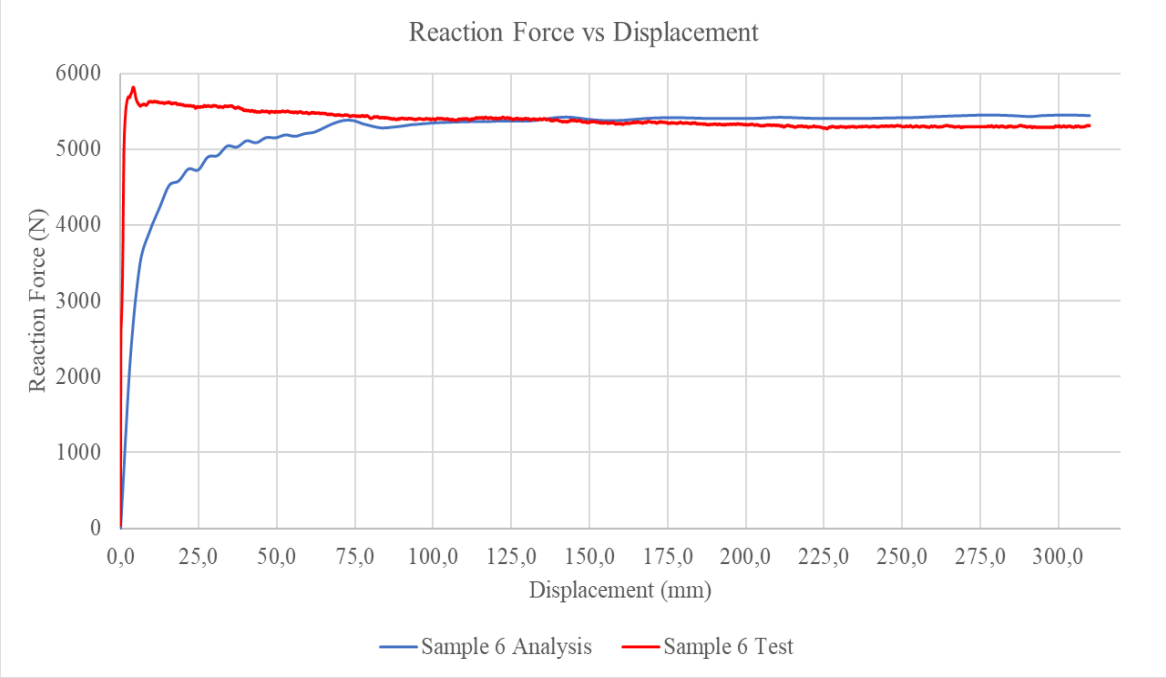

Figure 3.36. Reaction force results for Sample 6

Figure 3.37. Reaction force results for Sample 7

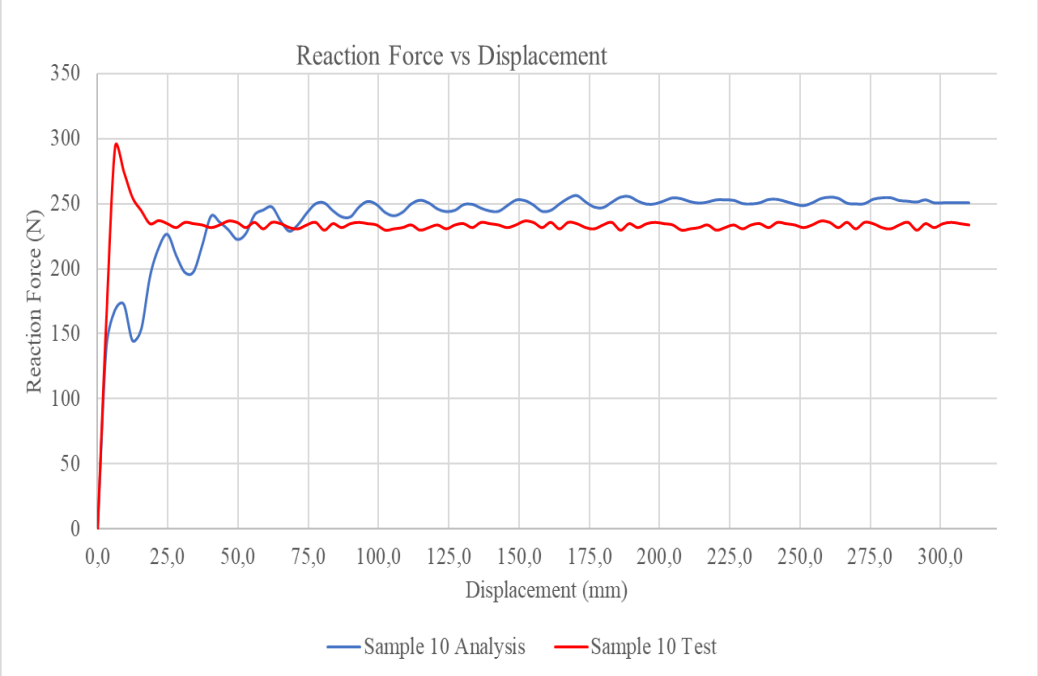

Figure 3.38. Reaction force results for Sample 10

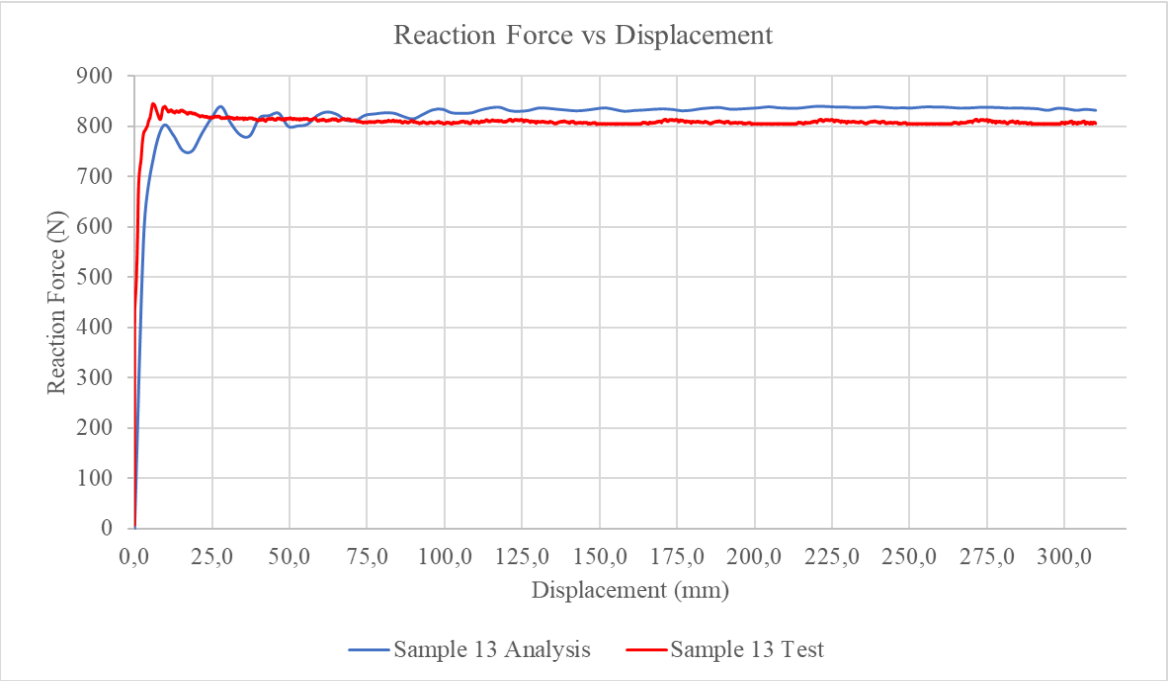

Figure 3.39. Reaction force results for Sample 13

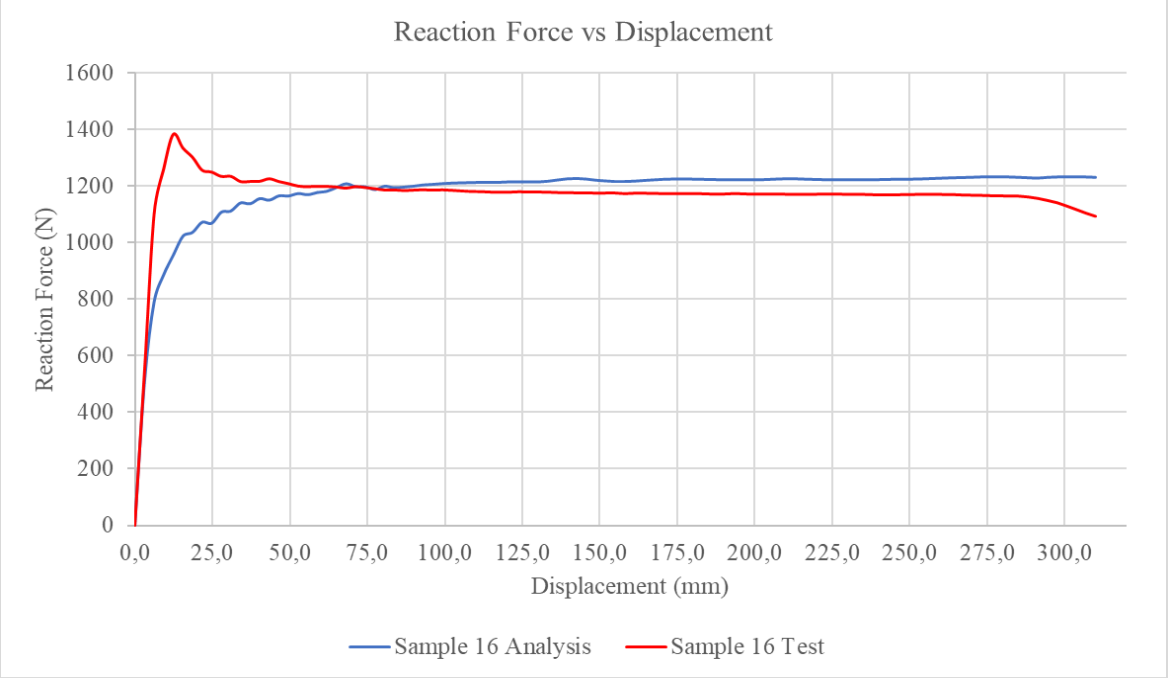

Figure 3.40. Reaction force results for Sample 16

3.4. Implementation of Energy Absorber to a Troop Seat Assembly and Finite Element Analysis of Troop Seat Assembly with Energy Absorber

In this part of the thesis study, a troop seat system with a tube-stud type energy absorber which is deformed under military crash load is analyzed. Tube-stud type energy absorber parameters are selected according to the load and displacement results

obtained during the energy absorber quasi-static test results and 14.5 g limit load requirement given by MIL-STD-85510 standard. The required average force value for a 50th percentile male occupant is around is 10.4 kN. Since Sample 6 provides a constant force value of 5.2 kN approximately, it becomes appropriate to use two Sample 6 energy absorbers as a candidate for a crashworthy troop seat system.

Seat model consist of 3 main components which are 2 seat poles, seat bucket and 2 energy absorbers as indicated in Figure 3.41. Tube-stud type energy absorbers are aligned parallel to the vertical load axis of the troop seat in order to alleviate the vertical crash loads transferred to the occupant.

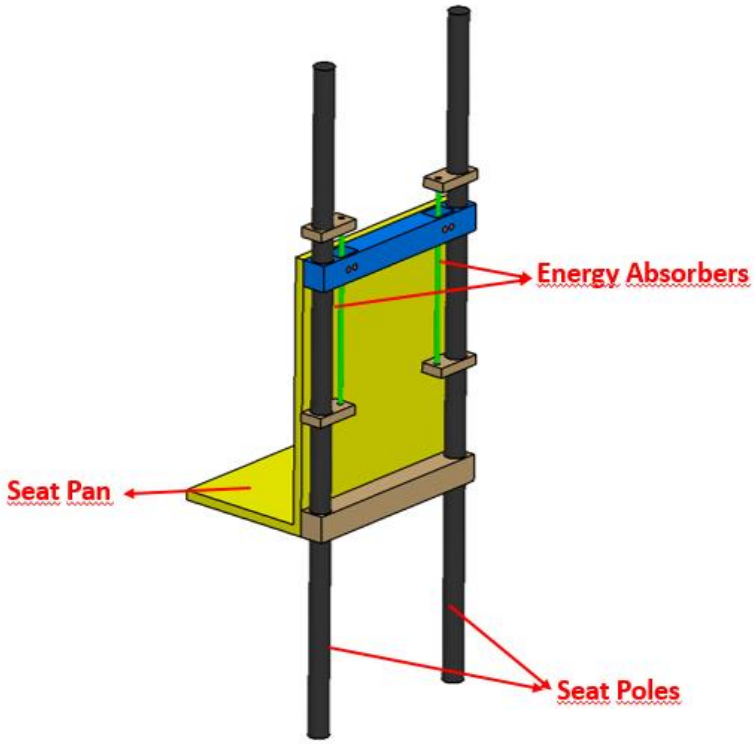

Figure 3.41. Troop seat model

Detailed view of tube-stud type energy absorber is given in Figure 3.42. Working principle of the tube-stud type energy absorber is provided in Section 3.1.1 Energy Absorber Methodology.

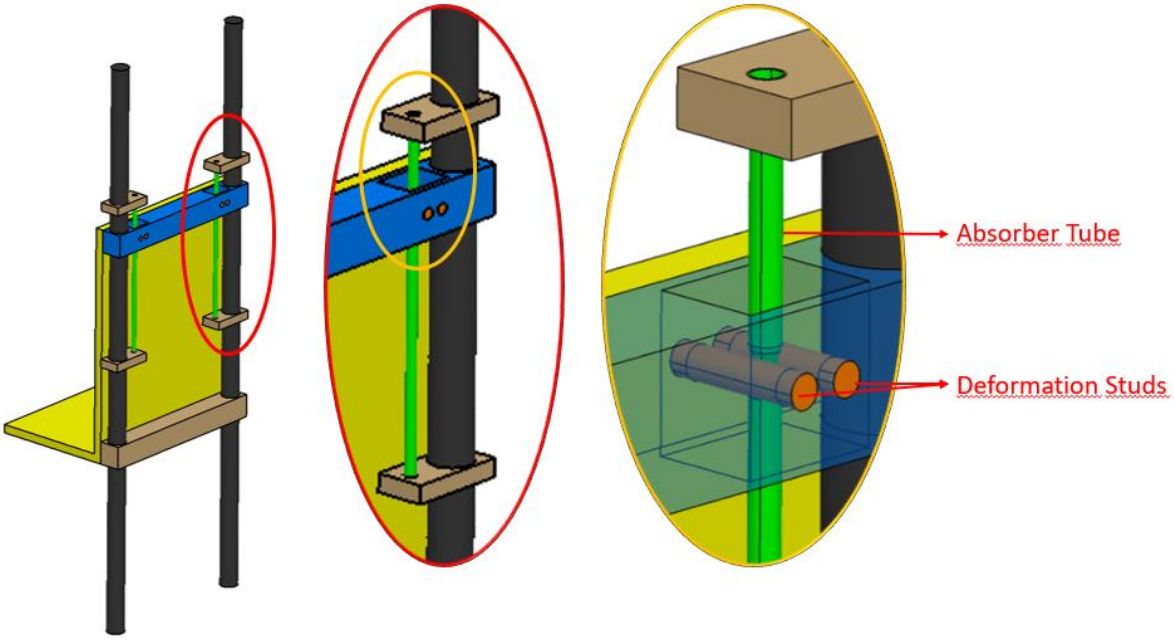

Figure 3.42. Troop seat energy absorber detail view

Main Dimensions of the troop seat are given in Figure 3.43.

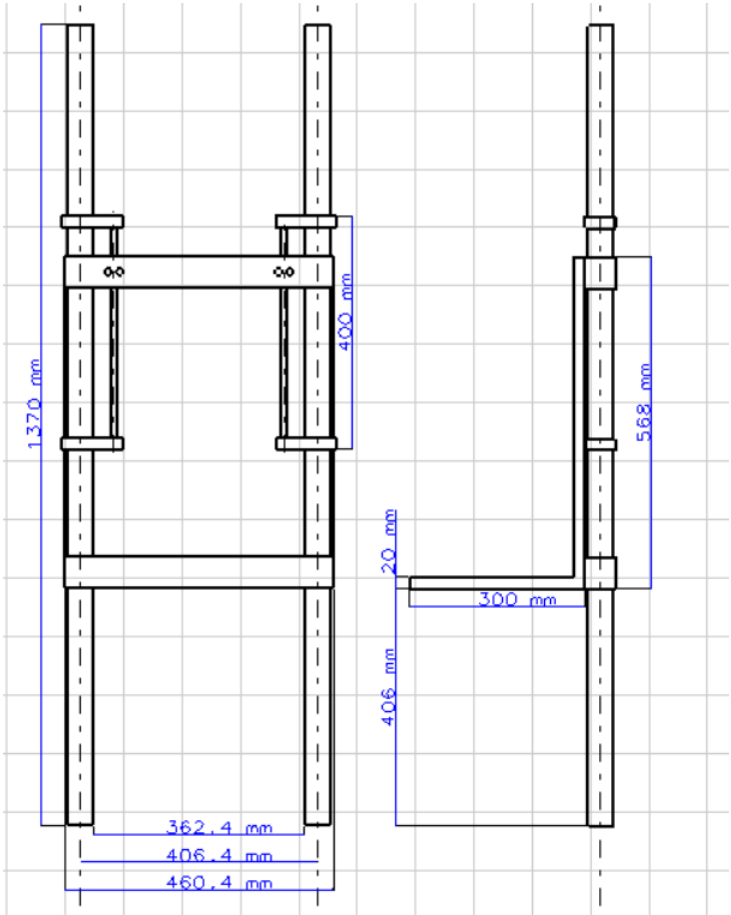

Figure 3.43. Back view and right view of troop seat with main dimensions

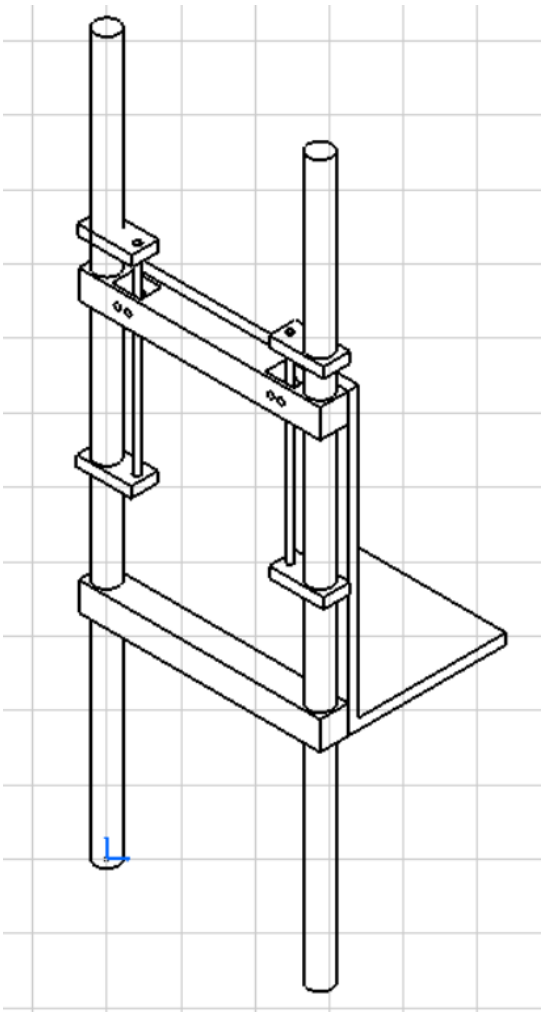

Figure 3.44. Isometric view of troop seat

3.4.1. Geometry Preparation

CATIA V5 3D design tool is used to design the crashworthy troop seat and the geometry imported to ABAQUS® as step file to perform analysis. Whole detail parts except absorber tube are considered as 3D deformable bodies as in the case of previous sections. Mesh element size of the absorber tube is small compared to the other parts. Therefore, the absorber tube modeled as shell element in order not to increase the computation time too much.

Crashworthy helicopter troop seats are attached to helicopter platform by both ceiling and floor sides. Considering the general installation concepts, ceiling side attachments carries vertical loads while floor side attachments are used to carry horizontal loads. The loads due to crash are transmitted from ceiling and floor via these attachments. Therefore, during crash simulation upper and lower planes are included in the analysis

as shown in Figure 3.46 and acceleration test pulses are applied to the seat via these ceiling and floor simulating planes.

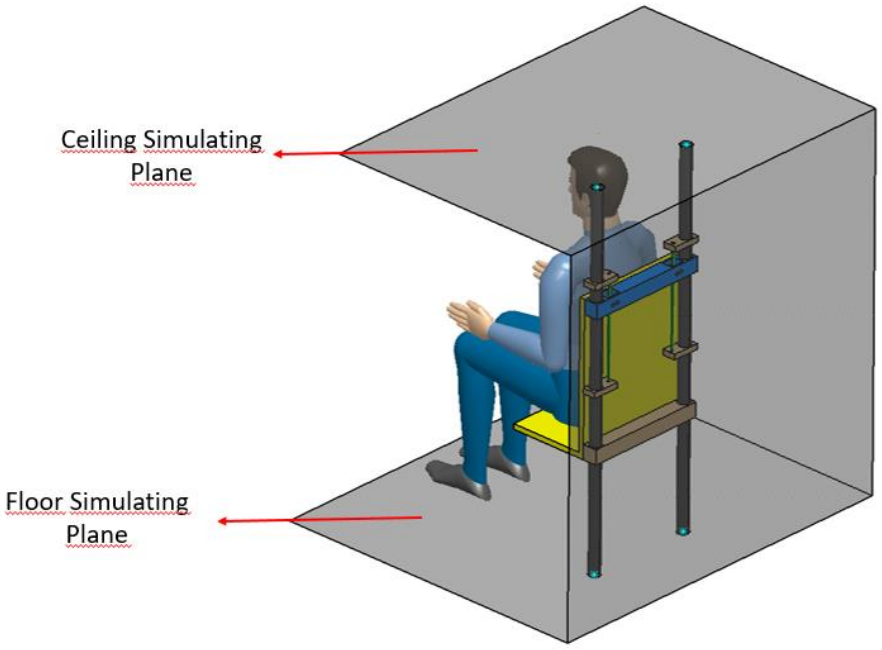

Figure 3.45. Analysis seat setup model

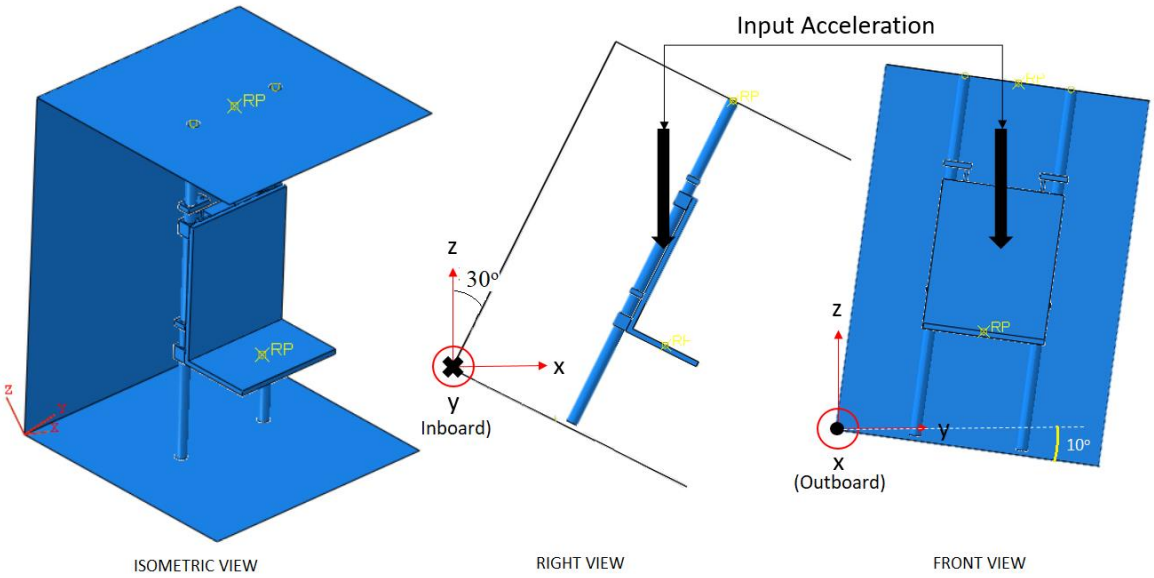

Figure 3.46. Seat analysis scenario

3.4.2. Material Properties

The parts used in the crashworthy seat assembly are mainly 7075 T651 series aluminum except for energy absorber, deformation studs and seat pan. Energy absorber material is 2024 T3 series aluminum and deformation studs are AISI 303 type steel material. For

military troop seats generally, foldable seat pans are used. However, to decrease simulation time and simplify crash analysis non-foldable seat pan that has a material property of 7075 T651 series aluminum is considered. The related material properties are provided in Table 3.3. Ceiling and floor simulating surfaces are modelled as rigid surfaces since they are only used for load application and their deformations are not in the scope of this thesis study.

3.4.3. Mesh Definition and Mesh Refinement

Since type of the mesh that is used during analysis has a major impact on analysis results and convergence a mesh optimization study is performed for troop seat assembly model.

In order to find and appropriate size of meshing seat assembly parts mesh sizes are changed while holding absorber and deformation stud mesh sizes at a constant value. Energy absorber tube and deformation studs are meshed 1 mm as found in energy absorber analysis studies and other parts are mesh sizes are changed as 2, 4 and 6 mm.

In order to check the quality of the model and suitability of the mesh sizes artificial strain energies are evaluated. The artificial strain energy contains energy values due to hourglass stiffness and transverse shear in shell and beam elements. High values of artificial strain energy are indicative of low quality of the applied meshes and requires mesh refinement. Therefore, to find appropriate mesh sizes, artificial strain energies are plotted for different mesh sizes as seen in Figure 3.47.

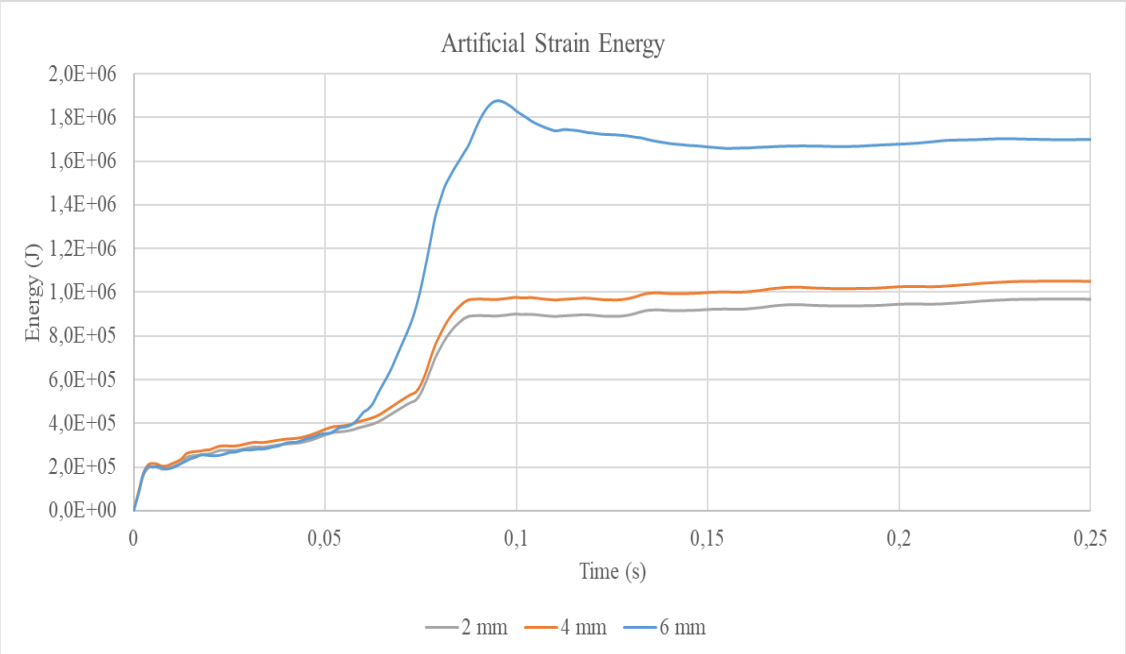

Figure 3.47. Artificial strain energies for various mesh sizes

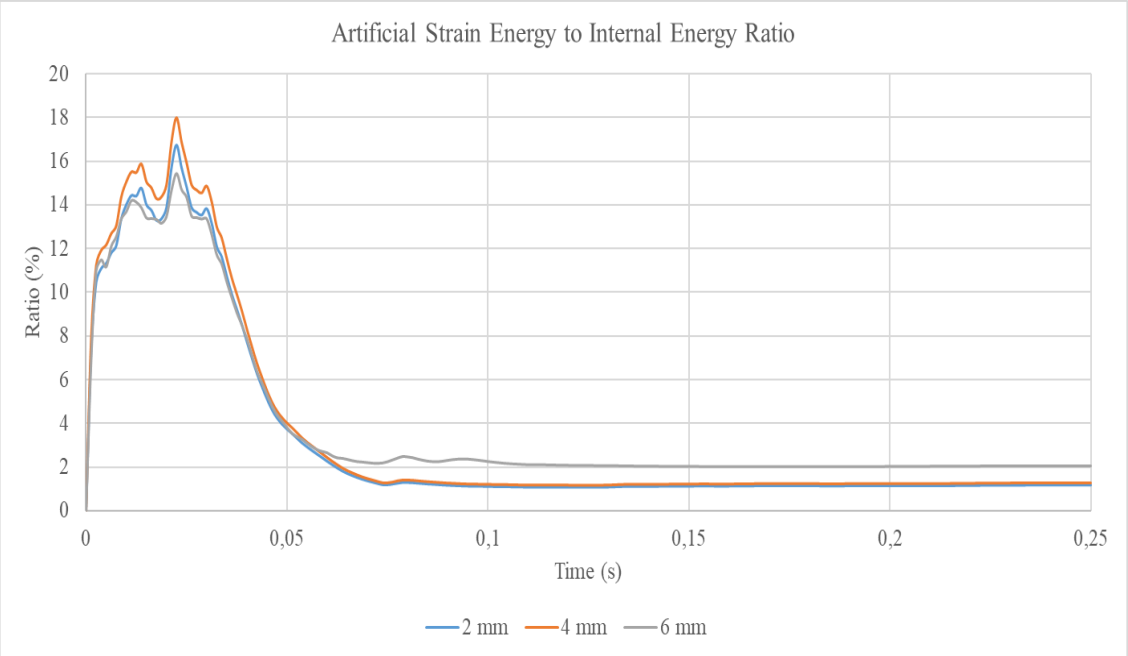

Figure 3.48. Artificial strain energy to internal energy ratios for different mesh sizes

Considering Figure 3.47, it is revealed that as we use finer meshes, which means smaller mesh sizes during analysis, artificial strain energy decreases. Figure 3.48 shows that the artificial strain energy to internal energy ratio reaches maximum of 18% for mesh sizes of 4 mm at the very beginning of the analysis. Later on, the ratio of the artificial strain energy to internal energy decreases down to 2-4%. Generally, the upper limit for artificial strain energy to internal energy is generally considered to be 15% during analysis. As a result, mesh sizes of 2-6 mm could be used for this study. Considering time of analysis and available CPU mesh sizes are taken as 4 mm for general mesh size for seat assembly parts [47].

3.4.4. Load and Boundary Conditions

In this study, it is aimed to simulate the testing conditions provided by MIL-S-85110 by applying correct boundary conditions, initial conditions, constraints and loads.

Considering the general attachment concepts of troop seats, main poles are tied from ceiling side whereas floor side attachments are free to move along z axis. Tie constraints also applied to energy absorber to absorber support connections and seat pan to upper and lower support connections.

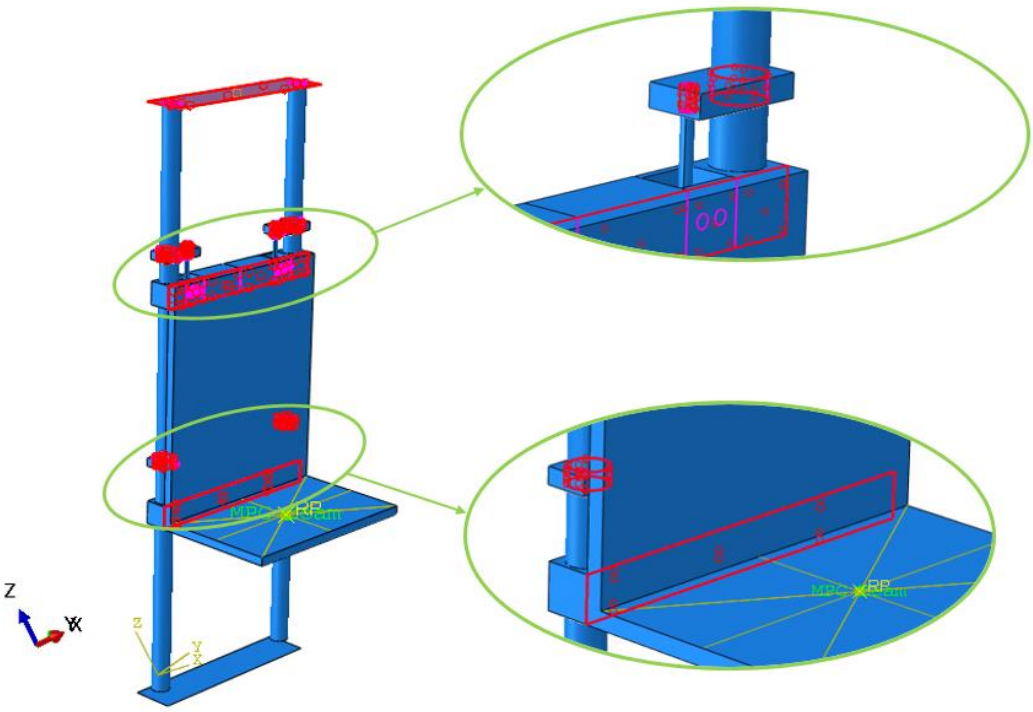

Figure 3.49. Tie constraint locations

Considering the occupant vertical effective weight which is provided by MIL-S-85510 as 73 kg including clothes etc. a simple point mass is applied to the seat bottom as indicated in Figure 3.50.

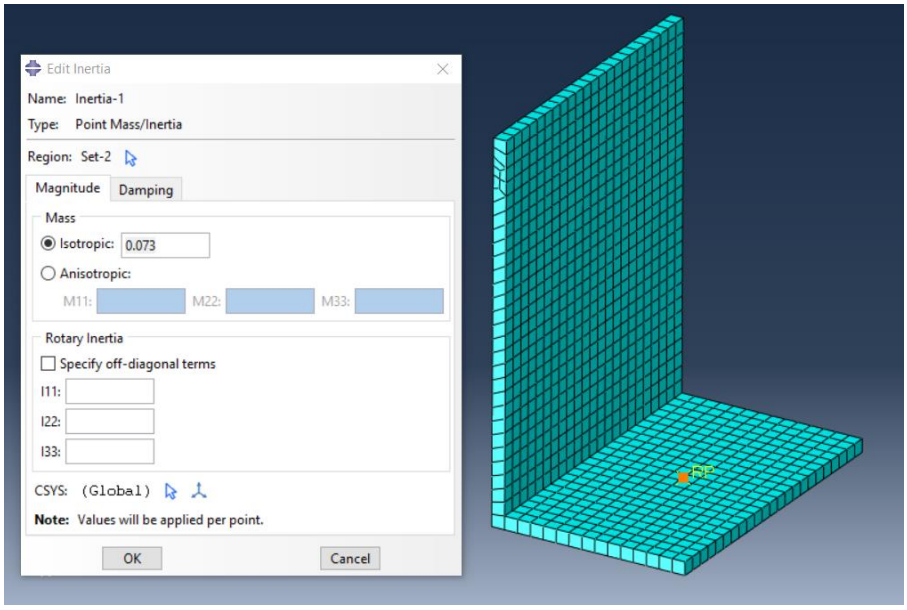

Figure 3.50 Point mass application which simulates vertical effective weight

According to the combined test requirements of MIL-S-85510, calculated velocity change should be 50 ft/sec and seat should be decelerated by a triangular deceleration pulse. Therefore, an initial velocity input of 15.2 m/s, which corresponds to 50 ft /sec that is given by MIL-S-85510 could be applied to all parts under the seat assembly. However, in this study seat is accelerated from stationary situation in a similar way to obtain 15.2 m/s velocity change.

Seat assembly is accelerated by applying a triangular pulse which reaches up to 32 g as shown by Figure 3.51. Total duration of the triangular pulse is taken as 0.096 secs as defined by MIL-S-85510.

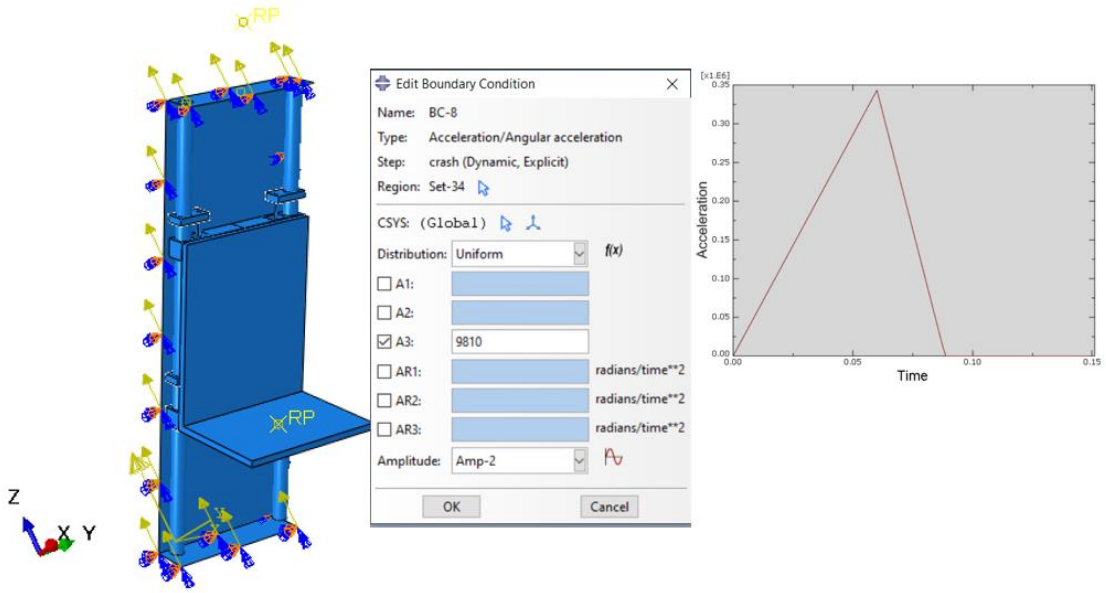

Figure 3.51. Deceleration boundary conditions applied to seat setup

3.4.5. Finite Element Analysis of Crashworthy Troop Seat

In this study, dynamic explicit analysis of troop seat is performed to simulate crash test behavior of the designed energy absorber under the loading conditions provided by MIL-S-85510. Dynamic explicit analysis requires time step, which is the duration of the analysis and frequency for data collecting sequence. In this study, the seat pan and the test setup acceleration, velocity and displacement histories collected as analysis data at the indicted locations in Figure 3.52.

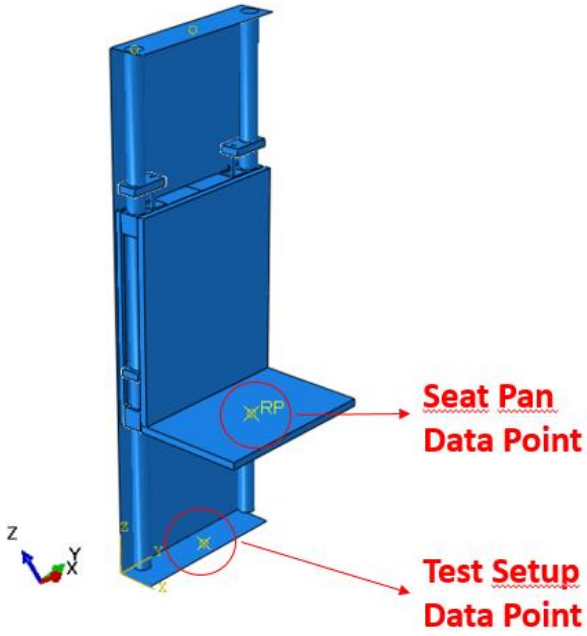

Figure 3.52. Data points for seat pan and test setup

Seat pan acceleration histories are recorded because the indicated location on the seat pan is critical since it is the closest point to occupant's pelvis and acceleration of this point has a direct effect on loads transferred to the occupant.

In dynamic explicit analysis, mass scaling phenomenon is used in order to decrease the analysis duration and to have a cost-efficient solution. In explicit finite element analysis, solution time step is governed by the smallest elements in the model. By mass scaling analysis program adds artificial masses to the elements, which have smaller time steps. In this study, stable time increment is taken as 10^{-7} seconds.

During dynamic explicit analysis, step time of the simulation is taken as 0.15 seconds. A triangular pulse, which lasts 0.96 seconds and reaches at 32 g's, is applied as shown in Figure 3.51 starting from the beginning of the analysis. In order to collect acceleration, velocity and displacement data the analysis step time is divided into 200 evenly spaced time intervals.

Figure 3.53 show the undeformed seat structure at the beginning of the analysis at t=0.0 seconds and behavior of the troop seat structure throughout the analysis.

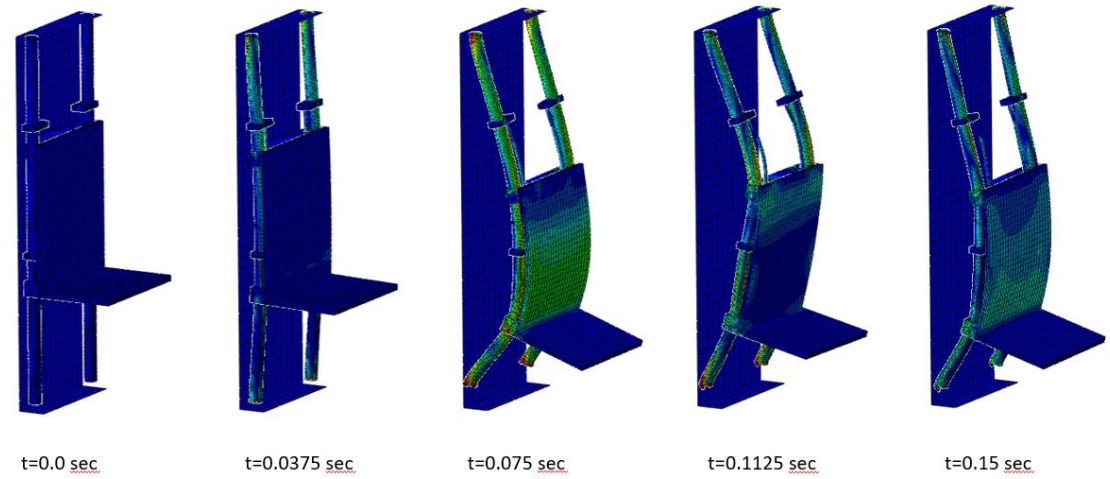

Figure 3.53. Seat behavior during crash analysis

Figure 3.54 shows energy absorber initiation during the early stages of the analysis as acceleration levels and crash loads increase. As acceleration applied to the setup increases, the deformation studs deform the energy absorber tubes as expected. By this way the seat pan accelerations and the loads transferred to the occupants are limited at a safe level.

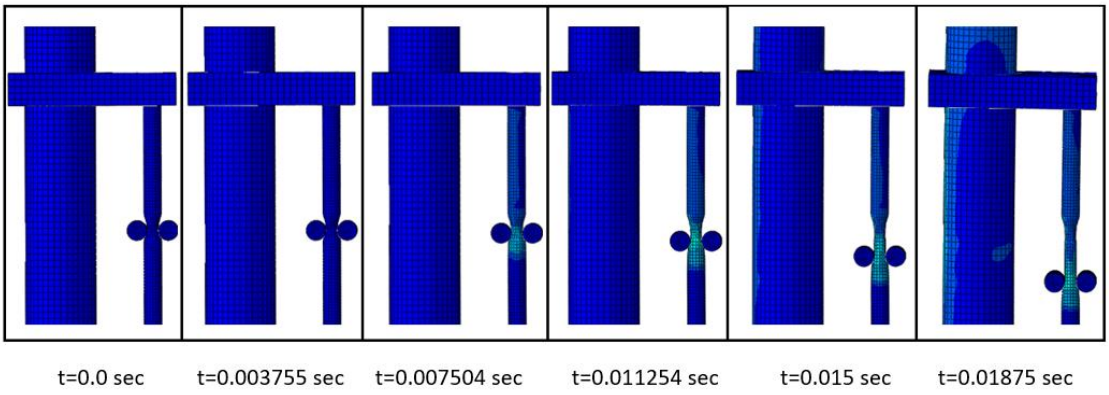

Figure 3.54. Energy absorber initiation during analysis

Acceleration result of the seat pan and test setup is given in Figure 3.55. Seat setup acceleration graph fits the triangular pulse given by MIL-S-85510 standard as expected since it is a user-defined parameter. Initially, the acceleration vs time graph of the seat pan follows the setup accelerations up to 15.6 g's. Then the accelerations vary around 14.1 g level up to 0.122 secs. The acceleration of the occupant is limited to 14.1 g's, which is an acceptable level to eliminate the spinal cord injuries.

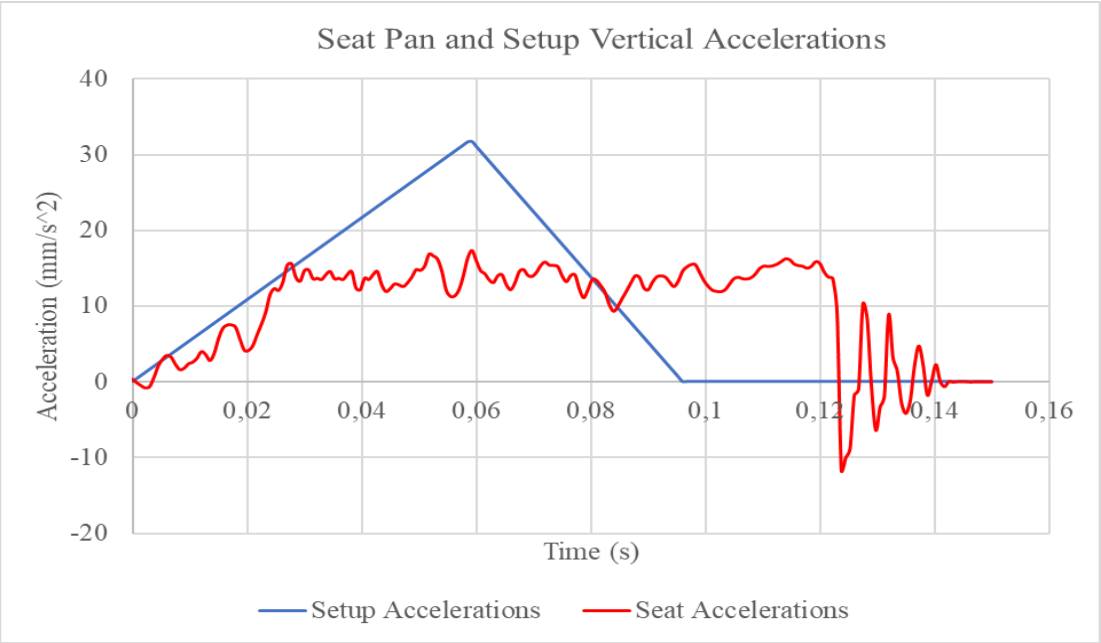

Figure 3.55. Seat pan and seat setup vertical accelerations

Velocity vs time graphs of the seat pan and the seat setup are given in Figure 3.56. The figure indicates that the seat setup has a velocity change of 15.2 m/s as defined by MIL-S-85510 requirements. The seat pan velocity vs time graph shows that the total velocity change of the seat pan is also 15.2 m/s however the duration of this change is longer compared to the seat setup velocity change.

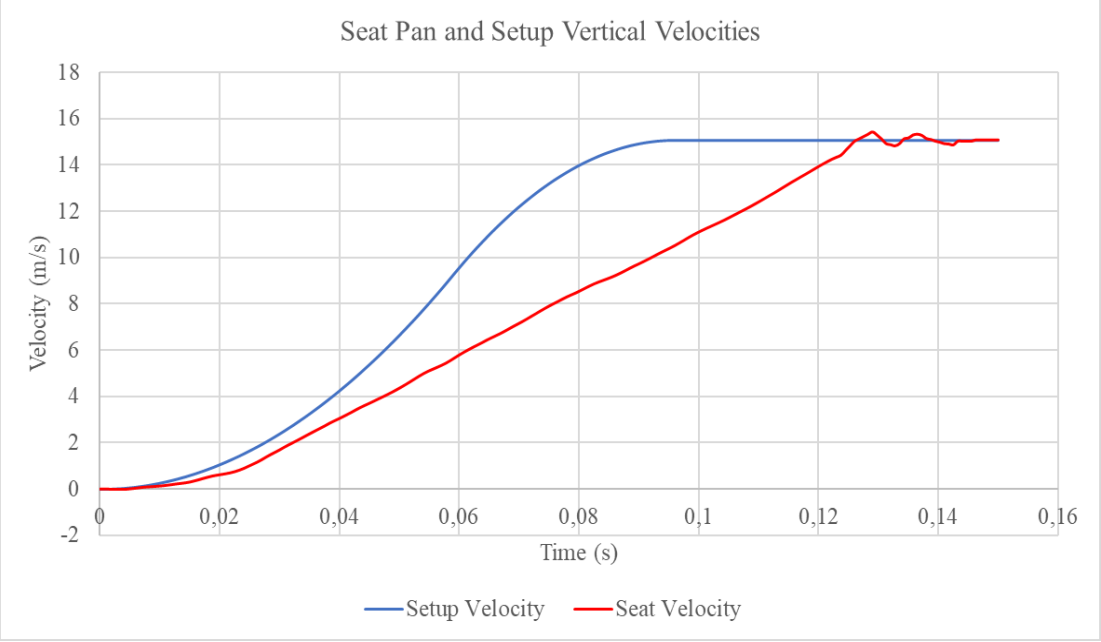

Figure 3.56. Seat Pan and Seat Setup Velocities

Displacement vs time graphs of the seat pan and the setup are given in Figure 3.57. The graph shows the displacement of the seat pan, which is the displacement of the occupant, and the floor displacement of the helicopter in a crash condition. The relative displacement between seat pan and helicopter floor given in Figure 3.58 gives the stroke distance of the energy absorbers as 0.32 m. In other words, this stroke distance of 0.32 m gives the amount of displacement of the occupant through the floor plane in a crash. Therefore, helicopter and seat manufacturer should pay attention to leave the volume under the seat pan free, in order not to prevent seat stroking during crash.

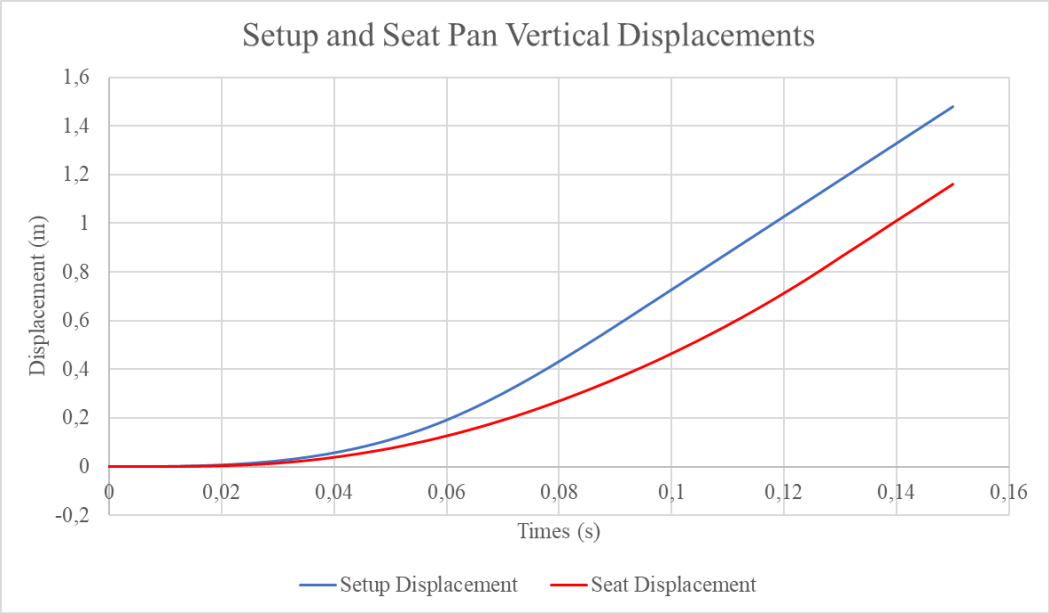

Figure 3.57. Seat Pan and Seat Setup Displacements

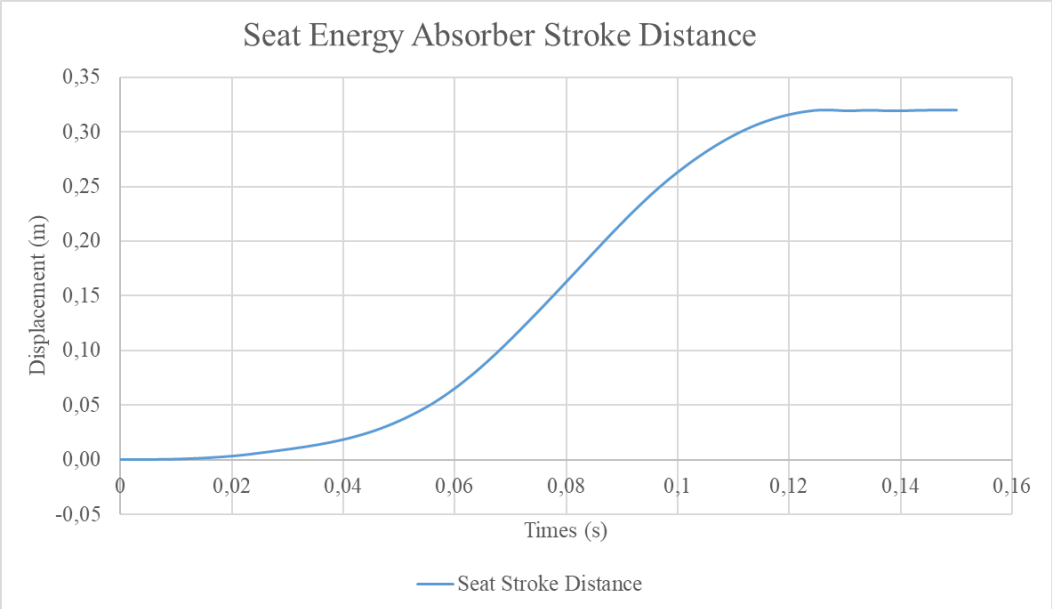

Figure 3.58. Seat Energy Absorber Stroke Distance

4. RESULTS AND DISCUSSION

The main objectives of this thesis study were designing and implementation of a tube and roller type energy absorber for a troop seat system according to the MIL-S-85510 crash test requirements which is indicated again in Figure 4.1.

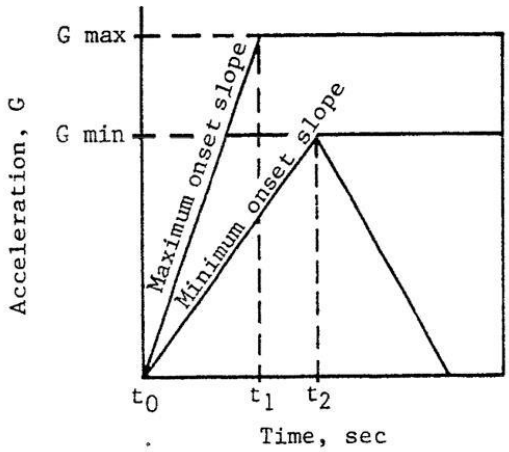

Parameter	Cabin seats	
	Qualification	R&D
t_1 sec	0.059	0.034
t_2 sec	0.087	0.087
G min	32	32
G max	37	37
△v min, ft/sec	50	50

Test	Configuration 1/
1	Dummy inertial load, 30°, 10°

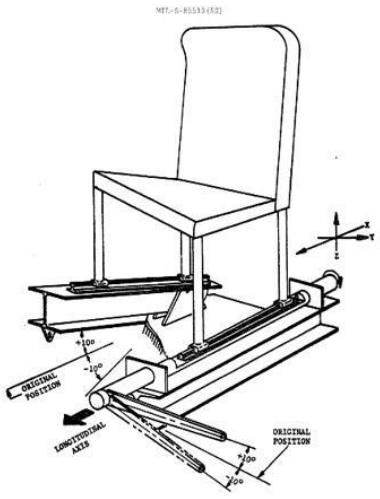

Figure 4.1. MIL-S-85510 crash test conditions [27]

Initially stand-alone design and testing activity of energy absorber was completed. Considering the reaction force results obtained during test and analysis studies, sustained force displacement curves are obtained through the analysis and test studies. Considering the oscillations in the analysis results of Sample 10, it can be concluded that mesh size of the model could decrease the initial oscillations. Effective energy absorber parameters are decided and candidate energy absorber was selected for troop seat implementation.

Dimensions and reaction force results of the samples are given in Table 4.1. Considering the test and analysis results of energy absorbers and 14.5 g limit load requirement of MIL-S-85510, Sample 6 is selected as candidate energy absorber. Dimensions of the Sample 6 energy absorber is highlighted in Table 4.1.

Table 4.1. Energy absorber dimensions

Sample Number	Sample Outer Diameter (mm)	Sample Thickness (mm)	Diamater of Deformed Sample (mm)	Amount of Deformation (mm)	Average Reaction Forces via Analysis (mm)	Average Reaction Forces via Test (mm)	Percent Error (%)
1	9.5	0.7	7.5	2.0	880	851	3
2	9.5	1.2	7.5	2.0	2660	N/A	N/A
3	9.5	1.7	7.5	2.0	4620	N/A	N/A
4	11.1	0.7	7.5	3.6	1237	1225	1
5	11.1	1.2	7.5	3.6	3670	3636	1
6	11.1	1.7	7.5	3.6	5253	5238	1
7	12.7	0.7	7.5	5.2	1489	1470	1
8	12.7	1.2	7.5	5.2	4534	N/A	N/A
9	12.7	1.7	7.5	5.2	7921	N/A	N/A
10	9.5	0.7	9.0	0.5	251	233	8
11	9.5	1.2	9.0	0.5	912	N/A	N/A
12	9.5	1.7	9.0	0.5	1589	N/A	N/A
13	11.1	0.7	9.0	2.1	834	803	4
14	11.1	1.2	9.0	2.1	2553	N/A	N/A
15	11.1	1.7	9.0	2.1	4413	N/A	N/A
16	12.7	0.7	9.0	3.7	1211	1192	2
17	12.7	1.2	9.0	3.7	3474	N/A	N/A
18	12.7	1.7	9.0	3.7	6066	N/A	N/A

The stand-alone analysis and tests of energy absorbers revealed that wall thickness and amount of deformation of the tube diameters have major effects on reaction force results.

Keeping tube diameter, wall thickness constant and changing the deformation amount changes the reaction force results. For each tube diameters 9.525 mm, 11.11 mm and 12.7 mm if the deformation amount is changed while the wall thickness kept constant the reaction force results increase.

Considering the effect of wall thickness at the same tube diameter and same amount of deformation levels, it is concluded that increasing the wall thickness increases the absorber reaction force always.

In order to evaluate effects of tube diameter on reaction force values, wall thickness and deformation amount values kept at the same levels. Table 4.2 indicates that increasing

tube diameter does not affect reaction force since at the same amount of deformation, even if tube radius increased, the ratio of deformation amount to tube radius decreased.

Table 4.2. Effect of tube diameter on reaction force

Sample Number	Sample Outer Diameter	Sample Thickness	Diamater of Deformed Sample	Amount of Deformation	Average Reaction Forces
1	9,5	0,7	7,5	2,0	880,0
13	11,1	0,7	9,0	2,1	834,0
2	9,5	1,2	7,5	2,0	2660,0
14	11,1	1,2	9,0	2,1	2553,0
3	9,5	1,7	7,5	2,0	4620,0
15	11,1	1,7	9,0	2,1	4413,0

Secondly the energy absorber Sample 6 which is designed in a stand-alone approach was implemented to a basic troop seat system to protect the occupant in a crash condition. Then the troop seat system was analyzed explicitly considering the crash test conditions provided by MIL-S-85510 standard. It is shown that crash g-loads which are transferred to the occupant in a crash condition could be decreased to 14.1 g levels which is acceptable by the applicable standard. Difference between quasi static and dynamic explicit analysis is around 3 %. Acceleration results are compared with Department of Defense Joint Service Specification Guide: Crew Systems Crash Protection Handbook [14] suggestions and with similar studies.

Figure 4.2, Figure 4.3 and Figure 4.4 shows the acceleration, velocity, displacement time histories of a reference study which is performed on a similar military troop seat that is analyzed according to the dynamic test requirements of MIL-S-85510 standard [7].

Acceleration vs. time graphs of the aircraft floor and occupant given in Figure 4.2 indicates that deceleration of the troop seat is limited to 13.125 g's. Therefore, in this reference study it is concluded that the designed energy absorber works properly and prevents the possible spinal and lumber column injuries of the occupants. In current thesis, acceleration vs time graph of the occupant, which is shown in Figure 3.55, limited at 14.1 g's during the crash event. Considering 14.5 g's limit load requirement by MIL-S-85510 it could be concluded that energy absorber limits the occupant acceleration below the specified threshold of 14.5 g's by MIL-S-85510.

The displacement vs time graphs in Figure 3.58, shows the displacement of the seat pan and aircraft floor in a crash event. The maximum displacement of the energy absorber is 0.32 m. Therefore, the stroke distance of the energy absorber which is the relative

displacement between seat pan and aircraft floor, is found as 0.32 m. In the calculation of the stroke distance elastic spring back effects are neglected. In comparison, the stroke distance of the energy absorber is found as 0.225 m in the reference study. Stroke distance of the energy absorber is lower in the reference study since energy absorber is tuned to a higher limit load which is 14.5 g.

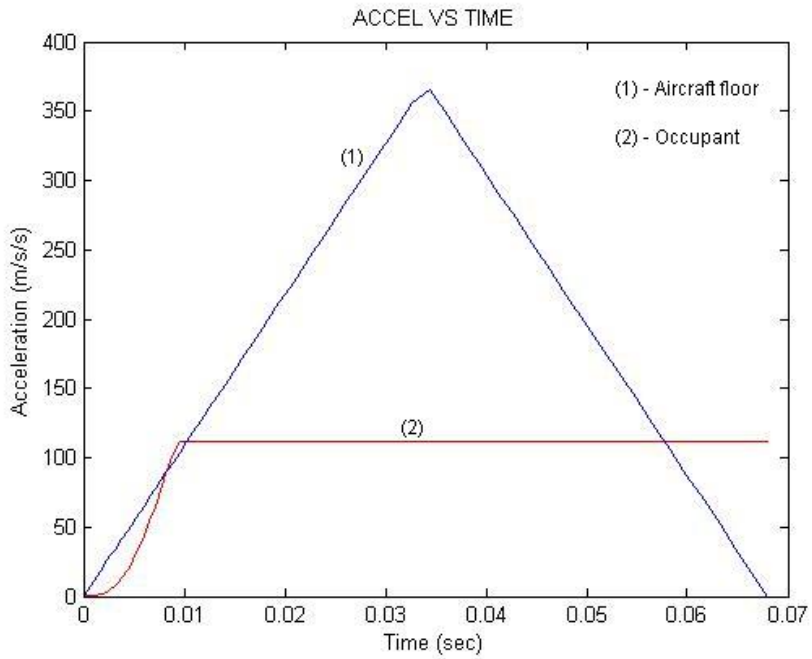

Figure 4.2. Acceleration vs time graph of a troop seat pan and aircraft floor [7]

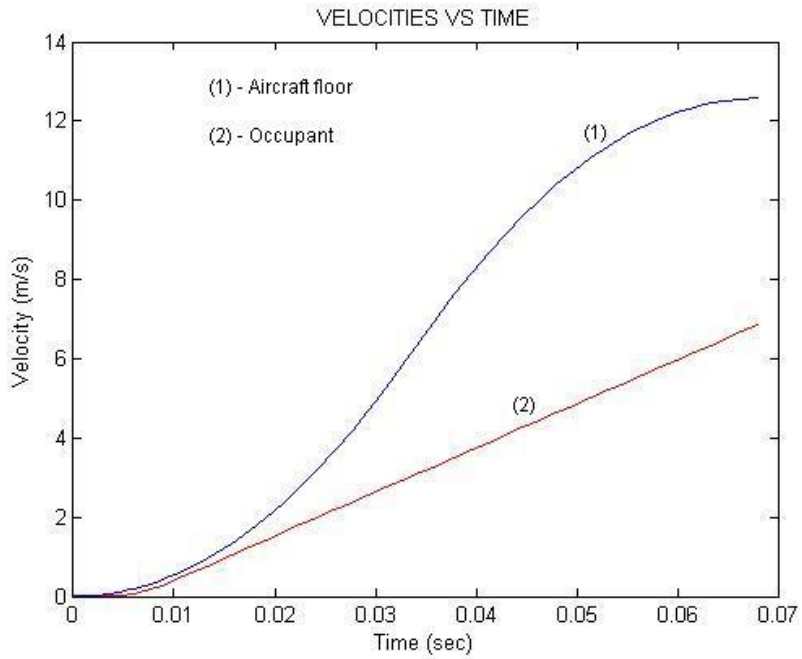

Figure 4.3. Velocity vs time graph of a troop seat pan and aircraft floor [7]

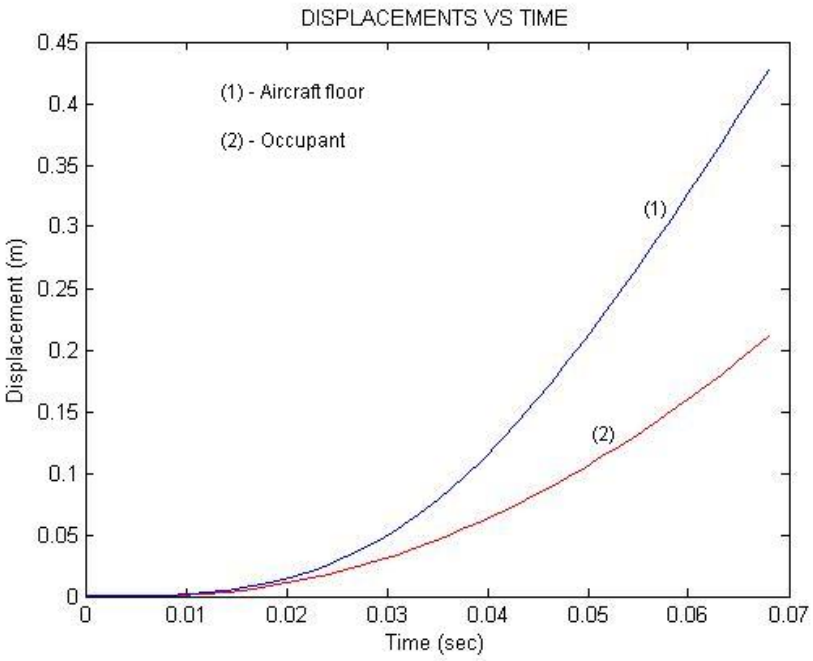

Figure 4.4. Displacement vs time graph of a troop seat pan and aircraft floor [7]

5. CONCLUSIONS AND FUTURE WORKS

5.1. Conclusions

Helicopter troop seat crash test requirements, which are provided by MIL-S-85510 standard, are evaluated in a comprehensive way thought this thesis study. The fundamental inputs to the analysis are derived from MIL-S-85510 standard and they are outlined in the analyses sections. The inputs such as geometry, material data, mesh type, mesh size and boundary conditions are critical since the have important effect on analyses results.

Stand-alone analysis and test studies performed on energy absorber candidates in order to find the suitable energy absorber for a military troop seat. Simple test adapter assembly designed and manufactured in order to use during tensile tests of the energy absorbers. Test adaptor design was also important since it could affect the force results of the tensile tests. Analyses and test studies enlightened the relations between reaction force vs tube design parameters such as tube diameter, deformation amount and tube wall thickness.

Energy absorbers are implemented into a basic military troop seat and explicitly analyzed by using ABAQUS®. According to the analyses results tube-stud type concept energy absorbers could be used for crash load attenuation purposes for military helicopter troop seats. This analysis enlightens the relative behavior of helicopter floor and crashworthy troop seats under the given crash conditions. Effect of energy absorption system on acceleration levels and velocity graphs are evaluated considering the helicopter floor and seat pan acceleration and velocity graphs.

5.2. Future Works

As future studies below topics could be evaluated;

- In order to cover a wide range of occupant weights a closed loop controlled energy absorber can be designed as shown in Figure 5.1. By controlling the deformation stud position actively amount of deformation of the tubes could be changed. In this way, different crash loads could be generated for different weighted occupants. A sample controller diagram could be as indicated in Figure 5.2.

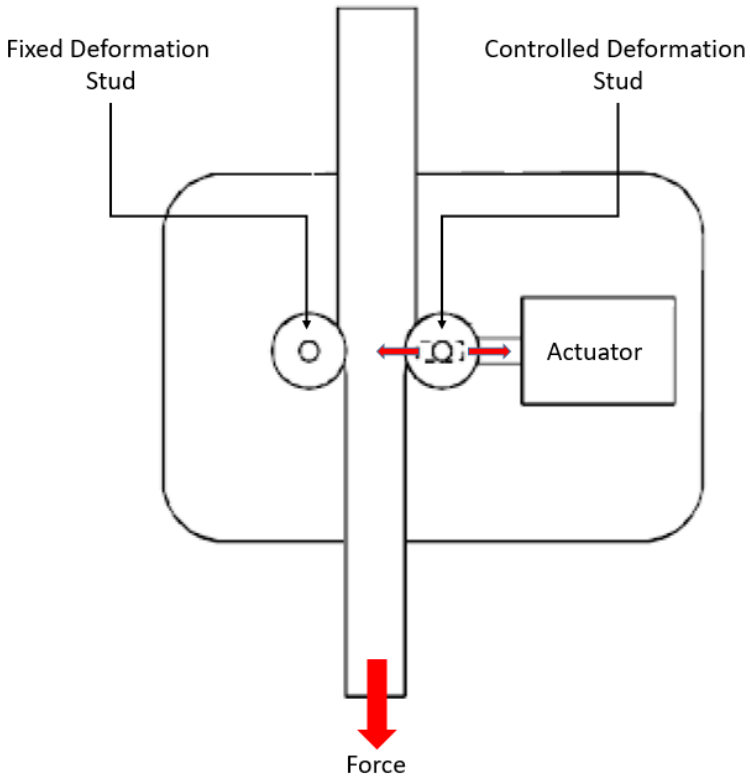

Figure 5.1 Controlled tube-stud type energy absorber

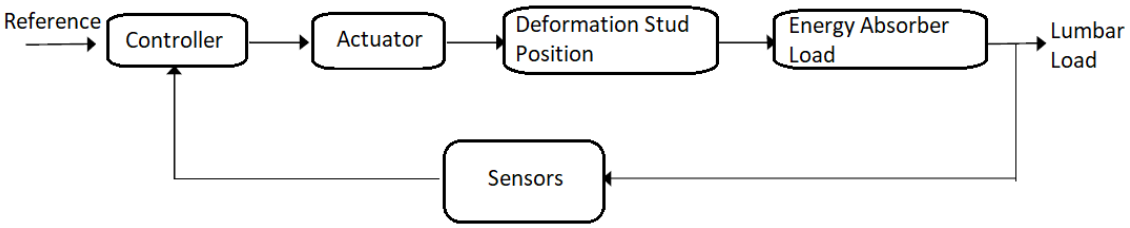

Figure 5.2 Sample closed loop-controlled tube-stud energy absorber diagram

- An anthropometric dummy (ATD) can be used in the crash analysis parts to see occupant lumbar loads, occupant kinematic behaviors.
- A simple troop seat system which has tube-stud type energy absorber can be manufactured and can be tested dynamically to check real performance of the concept energy absorber.
- Same energy absorber concept can be evaluated for military pilot seats requirements.
- Same energy absorber concept can be used for civil certified passenger and pilot seats.

REFERENCES

[1] Bois, P. D., Chou, C. C., Fileta, B. B., Khalil, T. B., King, A. I., Mahmood, H. F., Mertz, H. J., & Wismans, J. (2004). Vehicle Crashworthiness and Occupant Protection. American Iron and Steel Institute.

[2] Ambrosio, J. A. C. (Eds.). (2001). Crashworthiness: Energy Management and Occupant Protection. Springer-Verlag Wien GmbH.

[3] Annett, M. S., & Horta, L. G. (2011). Comparison of Test and Finite Element Analysis for Two Full-Scale Helicopter Crash Tests. American Institute of Aeronautics and Astronautics. 52nd AIAA/ASME/ASCE/AHS/ASC Structures, Structural Dynamics and Materials Conference.

[4] Joseph, L. & Haley, Jr. Helicopter Structural Design for Impact Survival. Journal of American Helicopter Society. Octorber.1971. 9-18

[5] US Army Aviation Systems Command (1989). Aircraft Crash Survival Design Guide Volume I – Design Criteria and Checklist.

[6] Hu, D. Y., Yang, J. L. & Hu, M. H. (2009). Full-scale vertical drop test and numerical simulation of a crashworthy helicopter seat/occupant system, International Journal of Crashworthiness, 14:6, 565-583.

[7] Mhaskar, N. H. A. L. (2008). Analysis and Optimization of A Crashworthy Helicopter Seat.

[8] Hughes, M. (2009). Martin-Baker Aircraft Co Ltd: Evolution of MBA Crashworthy Seating. SAFE Europe.

[9] Raymond, W. M. (2002). “Crashworthy Aircraft Seat”, United States Patent US 6,394,393 B1.

[10] Sieveka, E. & Kitis, L. (2005). An Investigation of Troop Seat Testing Methodology Using Madymo Models. 20.

[11] Fischer-Seats (date accessed: 2020, January 7). Retrieved from: www.fischer-seats.com/solutions/0718-passenger-seat-170-260-h160/

[12] T-Kalıp (date accessed: 2020, January 15). Retrieved from: www.t-kalip.com/tr/dusey-carpmaya-karsi-korumali-koltuklar/

[13] Department of Defense of the USA (1981). MIL-S-85510 (AS) Military Specification Seats, Helicopter Cabin, Crashworthy, General Specification for.

[14] Department of Defense of USA (1998). Crew Systems Crash Protection Handbook. Joint Service Specification Guide.

[15] Moradi R., Beheshti H.K., Lankarani H.M. (2012). Lumber Load Attenuation for Rotorcraft Occupants Using a Design Methodology for the Seat Impact Energy-Absorbing System. Central European Journal of Engineering, Volume 2, pp. 562-577.

[16] Desjardins, S. P. (2003). The Evolution of Energy Absorption Systems for Crashworthy Helicopter Seats, PRESIDENT SAFE, INC TEMPE, ARIZONA

[17] European Aviation Safety Agency (2012). Certification Specifications CS-29: Large Rotorcrafts, December 2012.

[18] European Aviation Safety Agency (2018). Certification Specifications CS-27: Large Small Rotorcrafts, Amendment 6.

[19] Department of Defense of the USA (1986). MIL-S-58095A (AV) Military Specification Seat System: Crash-Resistant, Non-Ejection, Aircrew, General Specification for.

[20] Wiggenraad, J. F. M. (1997). Design, Fabrication, Test and Analysis of a Crashworthy Troop Seat, European Rotorcraft Forum.

[21] European Aviation Safety Agency (2018). Advisory Circular AC 29-2C: Certification of Normal Category Rotorcraft.

[22] Murugan, M., JinHyeong Y., & Hiemenz, G. (2014). “Simulation of Adaptive Seat Energy Absorber for Military Rotorcraft Crash Safety Enhancement”, ARL Technical Report, ARL-TR-6892.

[23] Desjardins, S. P., Cannon, M. R., & Shane, S. J. (1988). “Discussion of Transport Passenger Seat Performance Characteristics,” SAE Technical Paper Series, 881378, Aerospace Technology Conference and Exposition, Anaheim, CA.

[24] Hiemenz, Gregory & Choi, Young-Tai & Wereley, Norman. (2007). SemiActive Control of Vertical Stroking Helicopter Crew Seat for Enhanced Crashworthiness. Journal of Aircraft - J AIRCRAFT. 44. 1031-1034. 10.2514/1.26492.

[25] Yan, T., Wang, J. (2014). Crashworthy Component Design of an Ultra-Light Helicopter with Energy Absorbing Composite Structure. Procedia Engineering, Volume 80, pp. 329-342.

[26] Jian Li, Guangjun Gao, Weiyuan Guan, Shuai Wang, Yao Yu, (2018). Experimental and numerical investigations on the energy absorption of shrink circular tube under quasi-static loading, International Journal of Mechanical Sciences.

[27] Gupta, P., & Sahu, R. (2013). Experimental and numerical studies on the tube contraction using a conical-cylindrical die. The Journal of Strain Analysis for Engineering Design. 48. 482-493.

[28] Technifast (2019). Standard Dowel Pins: Solid and extractable dowel pins in metric and imperial sizes.

[29] Goldsmith W. (2001). The Theory and Physical Behavior of Colliding Solids. Dover Publications.

[30] ABAQUS, ABAQUS Inc. (1978), https://www.simulia.com.

[31] Matweb (date accessed 2020, May 7). Retrieved from: www.matweb.com

[32] Dassault Systèmes Simulia, “Abaqus Analysis User’s Guide,” v. 6.14, 2015.

[33] M. Yamashita and M. Gotoh, (2005). Impact behavior of honeycomb structures with various cell specifications-numerical simulation and experiment, Int. J. Impact Eng. 32 (1-4), pp. 618-630.

[34] Zhao, H., Gary, G., (1998). Crushing behavior of aluminum honeycombs under impact loading, Int. J. Impact Eng. 21 (10), pp. 827-836.